Studies on the antidiabetic activity of co-encapsulated andrographolide and curcumin in nanostructured lipid carrier system

Thesis submitted

by

Asit Kumar De

Doctor of Philosophy (Science)

Department of Chemistry

Faculty Council of Science

Jadavpur University, Kolkata, India

2022

CERTIFICATE FROM THE SUPERVISOR(S)

This is to certify that the thesis entitled "**Studies on the antidiabetic activity of co-encapsulated andrographolide and curcumin in nanostructured lipid carrier system**" submitted by **Sri Asit Kumar De ,** who got his name registered on **20.02.2017.**For the award of Ph. D. (Science) degree of Jadavpur University, is absolutely based upon his own work under the supervision of **Prof . Tanmoy Bera, Department of Pharmaceutical Technology, Jadavpur University, Kolkata 700032, India** and that neither this thesis nor any part of it has been submitted for either any degree/diploma or any other academic award anywhere before.

25.03.22

Tanmoy Bera, M. Pharm., Ph.D.
Professor
Division of Medicinal Biochemistry
Department of Pharmaceutical Tech.
Jadavpur University, Kolkata - 700 032

(Signature of the Supervisor(s) date with official seal)

DECLARATION

I do hereby declare that the work of **"Studies on the antidiabetic activity of co-encapsulated andrographolide and curcumin in nanostructured lipid carrier system"** was carried out by me under the supervision of Prof . Tanmoy Bera, Department of Pharmaceutical Technology, Jadavpur University, Kolkata 700032, India. This work is original and has not been submitted to anywhere in any part or in full for any other degree or diploma.

Asit Kumar De

(Asit Kumar De)

Place: Kolkata

Dedicated

to

My family

ACKNOWLEDGEMENT

This thesis is the outcome of long rigorous journey in which I have been encouraged and supported by many people. It is indeed a pleasant moment to express my gratitude for them.

First I wish to convey my deep sense of gratitude to my thesis guide Prof. Tanmoy Bera, Department of Pharmaceutical Technology, Jadavpur University, for providing me the opportunity to carry out my PhD work. His immense support and ideas guided me to hit the ground running. His valuable guidance, constant inspirations and untiring effort in every aspect through the tenure enable me to complete my thesis in a very disciplined manner.

I also thank Sri Soumen Mukhopadhyay, Director (Admin), Sri C Hariharan, Director (In-charge) and Dr. Arindam Basu (HOD, Pharmaceutical Chemistry Department) of Central Drugs Laboratory for giving me all necessary official permission for allowing me to pursue my dreams.

With immense pleasure, I express my gratitude and respect full regards to Registrar, Vice chancellor, Department of Chemistry and Department of Pharmaceutical Technology of Jadavpur University, Kolkata.

My words of thanks are less for my fellow lab mates of Laboratory of Nanomedicine, Division of Pharmaceutical Biotechnology, Department of Pharmaceutical Technology, Jadavpur University for their constant technical assistance with a special mention of Dr. Santanu Ghosh, Dr. Suman Das, Dr. Nabanita Kar, Dr. Shreyasi Chakraborty, Gyamcho Tschering Bhutia and Leena Kumari.

I show my sincere respect and thanks to my family members , office colleagues and my friends for their constant motivation, encouragement and unconditional support to complete my research work.

1. List of Publications

i. **Asit Kumar De**, Tanmoy Bera. Analytical method development, validation and stability studies by RP-HPLC method for simultaneous estimation of Andrographolide and Curcumin in co-encapsulated nanostructured lipid carrier drug delivery system. International Journal of Applied Pharmaceutics. 2021; 13(5): 73-86.

ii. **Asit Kumar De**, Rajkumar Sil, Santanu Ghosh, Tanmoy Bera, Inhibitory effect of quercetin-loaded nanostructure lipid carrier on compound 48/80-induced mast cell degranulation. Global Journal of Nanomedicine, Juniper Publishers. 2017; 3(2): 555608.

iii. Suman Das, Santanu Ghosh, **Asit Kumar De**, Tanmoy Bera. Oral delivery of Ursolic acid-loaded nanostructured lipid carrier coated with chitosan oligosaccharides: Development, characterization, in vitro and in vivo assessment for the therapy of leishmaniasis. International Journal of Biological Macromolecules. 2017; 102: 996-1008.

iv. Nabanita Kar, Shreyasi Chakraborty, **Asit Kumar De**, Tanmoy Bera, Development and evaluation of a Cedrol-loaded nanostructured lipid carrier system for in vitro and in vivo susceptibilities of a wild and drug resistant Leishmania donovani amastigotes. European Journal of Pharmaceutical Sciences. 2017; 104: 196-211.

v. Santanu Ghosh, Suman Das, **Asit Kumar De**, Nabanita Kar and Tanmoy Bera. Amphotericin B-loaded mannose modified poly(D,L-lactide-co-glycolide) polymeric nanoparticles for the treatment of visceral leishmaniasis: in vitro and in vivo approaches. Royal Society Of Chemistry Advances. 2017; 7: 29575-29590.

vi. Shreyasi Chakraborty, Nabanita Kar, Leena Kumari, **Asit De**, Tanmoy Bera. Inhibitory effect of a new orally active Cedrol-loaded nanostructured lipid carrier on compound 48/80-induced mast cell degranulation and anaphylactic shock in mice. International Journal of nanomedicine. 2017; 12: 4849-4868.

2. **List of patents: NIL**

3. **List of presentations in National/International seminar/webinar/Conferences/Workshops**

   i. Participated in the National workshop on "Small Molecules Analysis by API-Mass Spectrometry & NMR Spectroscopy", held on 25th - 27th Feb 2019,Organised by SAIF, CSIR-CDRI, Lucknow.

   ii. Participated in the National webinar "Bioactive Glass,Ceramics & Composites In Healthcare: Current Technological Trends", held on 27th-28th May 2021,Organised by Bio-Ceramic & Coating Dicision, CSIR-CGCRI, Kolkata.

   iii. Participated in the online International workshop on "Advanced Functional Materials" held on 15th-16th July, 2021 ,organised by JIS University,Kolkata,India & Hongik University,Sejong Campus,Republic of Korea (Indo-Korea Joint venture).

4. **List of Book Chapters:**

   Asit Kumar De, Tanmoy Bera. Analytical Method Development,Validation and stability studies by RP-HPLC method for simultaneous estimation of Andrographolide and Curcumin in Co-encapsulated nanostructured lipid carrier drug delivery system. Innovare Academic Sciences Pvt Ltd., Recent Advances in Pharmaceutical Sciences, Vol-5, Chapter-6.

CONTENTS

LIST OF ABBREVIATIONS

Abbreviation	Full form	Abbreviation	Full form
AG	Andrographolide	**AGNP**	Andrographolide nanparticle
AG-CMN NLC	Andrographolide-curcumin loaded nanostructured lipid carrier	**ANOVA**	Analysis of variance
ATR	Attenuated total reflectance	**AUC**	Area under curve
BP	British Pharmacopoeia	**C-48/80**	Compound 48/80
CCN	Curcumin-chitosan nanocomplex	**CMN**	Curcumin
CMN NP	Curcumin nanoparticle	**DAD**	Diode array detector
DL	Drug loading	**DMF**	Dimethyl formamide
DMSO	Dimethyl sulphoxide	**DSC**	Differential scanning calorimetry
EE	Entrapment efficiency	**FBS**	Fasting blood glucose
FDA	Food and drug administration	**FESEM**	Field emission scanning electron microscopy
FTIR	Fourier-transform infrared spectroscopy	**HLB**	Hydrophilic lipophilic balance
HPLC	High-performance liquid chromatography	**IP**	Indian Pharmacopeia

Abbreviation	Full form	Abbreviation	Full form
ICH	International council on harmonisation	**LC**	Liquid chromatography
LOD	Limit of detection	**LOQ**	Limit of quantification
min	Minutes	**ml**	Milli litre
mm	Millimeter	**mM**	Milli mole
ng	Nano gram	**NLC**	Nanostructured lipid carrier
nm	Nanometer	**PDI**	Polydispersity index
PDA	Photodiode array	**PLGA**	Poly lactic co glycolic acid
RP-HPLC	Reversed phase high performance liquid chromatography	**RSD**	Relative standard deviation
RT	Retention time	**SD**	Standard deviation
SLN	Solid-lipid nanoparticles	**SGF**	Simulated gastric fluid
SI	Selectivity index	**SIF**	Simulated intestinal fluid
STZ	Streptozotocin	**TEM**	Transmission electron microscope
USP	United States Pharmacopoeia	**UV**	Ultra violet
WHO	World Health organization	**XRD**	X ray diffraction
ZP	Zeta potential	**µg**	Micrograms
µl	Micro litre	**µm**	Micron

LIST OF TABLES

LIST OF FIGURES

Chapter I

Introduction

1.1 Diabetes mellitus

Diabetes mellitus also known as diabetes, is a metabolic disorder that affects the obstructions of proteins, carbohydrates and fats metabolism as well as an increase in blood glucose levels. In diabetic patients these pathophysiological complications are often responsible for a decline in the quality of life [Genuth et al, 2003]. It is a prominent global epidemic affecting 9 % of the world's population. It is estimated that by 2030, diabetes would be the world's seventh dominant cause of death. Nearly about 80% of diabetes-related deaths are currently reported in highly populated countries such as India, China, and Thailand [Samuel et al, 2011].

1.2 Classification of Diabetes

Diabetes is categorized in two types, type 1 and type 2 diabetes [American Diabetes Association, 2010].

1.3 Type-I diabetes

Type I diabetes is also called insulin-dependent diabetes mellitus or juvenile-onset diabetes. This results from the cellular-mediated autoimmune destruction of the pancreatic β-cells. This is an autoimmune disease [Veld et al, 2011].

1.4 Type-II diabetes

Type II diabetes is also called as non-insulin-dependent diabetes mellitus or adult-onset diabetes. This results from the development of insulin resistance and the affected individuals usually have insulin deficiency. This is the most common type of diabetes found in 90% of the diabetic community. It is apparently due to a family history of diabetes, obesity, smoking, less physical activity, and nutrition deficiency [Lin et al, 2010].

1.5 Treatment available for diabetes by antidiabetic drugs

Various synthetic drugs such as α-glucosidase, Biguanides, Dipeptidyl peptidase-4 (DPP-4) inhibitors, Meglitinides, Sulfonylurea, and Thiazolidinediones category along with insulin sensitizers are used in the treatment of diabetes mellitus. The reduction of the glycemic reaction occurs due to side effects of synthetic antidiabetic drugs. The classification of antidiabetic drugs is presented in Figure 1.1 [Trevor et al, 2015].

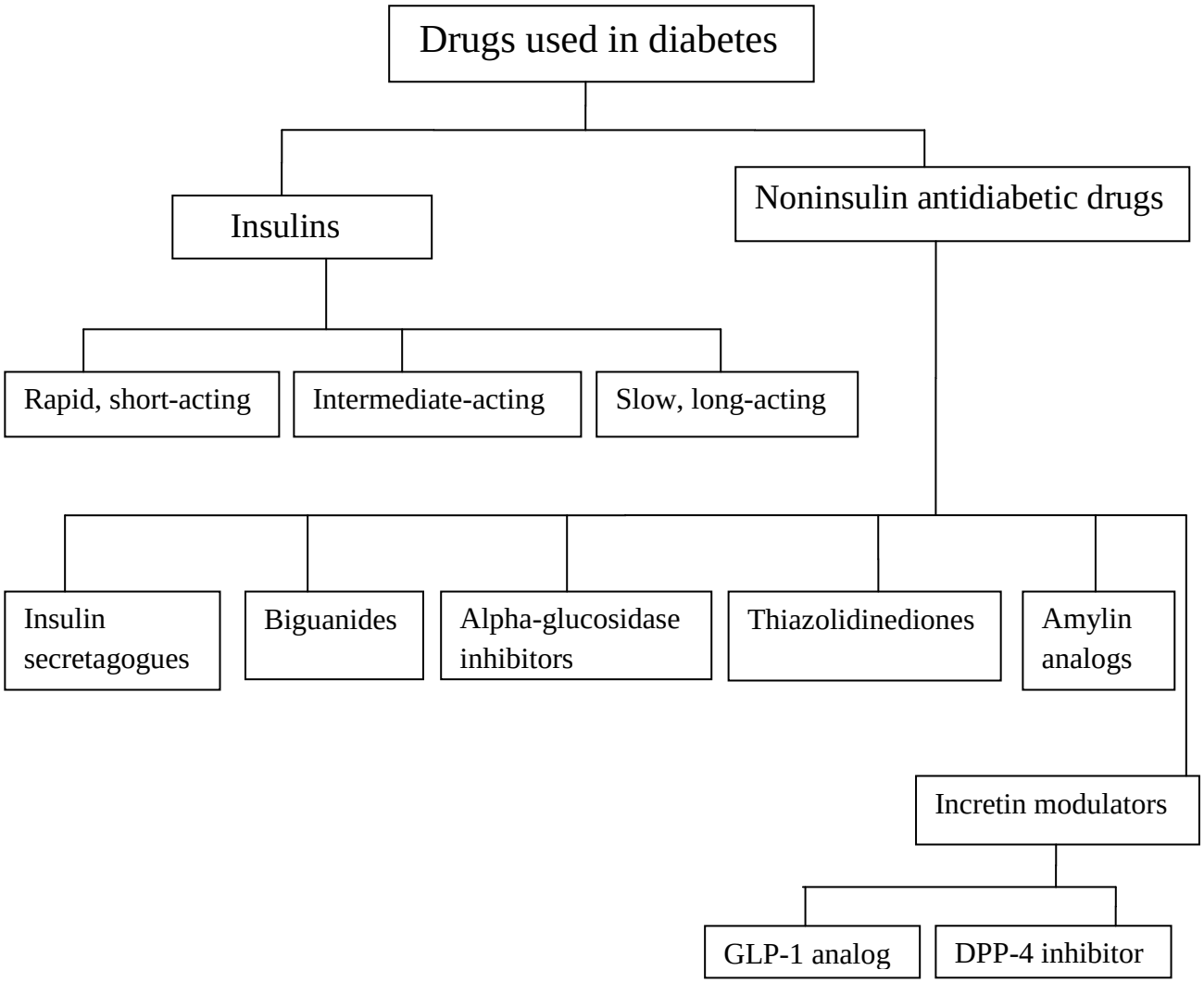

Figure 1.1: Classification of antidiabetic drugs

1.6 Alpha-glucosidase inhibitors

These medications aid in the digestion of starchy foods and sugar. This has the effect of lowering blood sugar levels. Acarbose and miglitol are examples of these drugs. [Van de Laar et al, 2005].

1.7 Biguanides

Biguanides reduce the amount of sugar which liver produces. They reduce the amount of sugar absorbed by intestines, increase insulin sensitivity, and aid glucose absorption in muscles. Metformin can also be combined with other drugs for type 2 diabetes and it can also be used as a sustained-release form [Hotta et al, 2019].

1.8 Dipeptidyl peptidase-4 (DPP-4) inhibitors

DPP-4 inhibitors aid in the body's continued production of insulin. They reduce blood sugar levels without producing hypoglycemia (low blood sugar). These medications can also assist the pancreas in producing more insulin. These drugs include Teneligliptin, Sitagliptin, Saxagliptin, Linagliptin, etc [Lim et al, 2015].

1.9 Meglitinides

These medications help the body to release insulin. However, in some cases, they may lower blood sugar too much. These drugs aren't suitable for everyone. These drugs include Repaglinide etc [Lim et al, 2015].

1.10 Sulfonylureas

These are among the oldest diabetes drugs still used today. They work by stimulating the pancreas with the help of beta cells. This causes the body to produce more insulin. These drugs include Glimepiride, Gliclazide, Glipizide, Glibenclamide, etc. [Monami et al, 2014].

1.11 Thiazolidinediones

Thiazolidinediones work by decreasing glucose in the liver. They also help fat cells to use insulin better. These drugs include: Pioglitazone, Rosiglitazone etc [Christos et al, 2016].

1.12 Limitations of allopathic Drugs

Though antidiabetic drugs are the best available treatment till now but they have several side effects when used long-term. Long-term use of these drugs has side effects like atherosclerotic cardiovascular disease, heart disease or chronic kidney disease may predominate over their diabetes [Valeron et al, 2013]. A large quantity of medication with repeated or sustained release dosage is required to attain an effective therapeutic concentration. After being diagnosed with diabetes and consuming antidiabetic drugs for the first time blood sugar may fall. In the case of diabetes, dosing is very important. Reduction of glycemic reaction occurs due to side effects of synthetic antidiabetic drugs [Ahmad et al, 2020].

1.13 Natural Products in the treatment of Diabetes

Nowadays, herbal drugs are gaining importance to treat type-2 diabetes. Furthermore, herbal compounds are frequently consumed in food and food additives. They're also secure from minimum side effects and effective for alternative drugs. Herbal compounds have numerous biological activities and help to enhance insulin secretion. Various types of phytoconstituents present in the plant material belonging to different chemical classes, such as terpenoids, alkaloids, flavonoids, phenolics, and some other categories also have anti-diabetic potential. Phytoconstituents like alkaloids inhibit alpha-glucosidase and decrease glucose transport through the intestinal epithelium [Sanjeev et al, 2020].

Herbs have also been shown to provide alternative therapy in the prevention of diabetes complications. Some of these herbs have also been confirmed to help in the redevelopment of β cells and overwhelming insulin resistance and there are a variety of poly-herbal formulations available on the market that may be used as an alternative therapy to treat DM complications.

The medicinal herbs were applied to treat a wide range of diseases [Yuan et al,2016]. The use of a medicinal herb, alone or in combination with other herbs can be regarded as a sort of combination treatment because of the complexity of the phytochemicals and bioactivities in the plant. As a result, a single antidiabetic plant containing thousands of phytochemicals might have various advantages by affecting different metabolic pathways. One study supported this principle by demonstrating that combination therapy of western medicine and herbal medicine exhibited a better (synergistic) effect than either medicine alone. Despite the development of various synthetic medications for the treatment of diabetes mellitus, a safe and effective therapy has yet to be found. Medicinal foods are prescribed widely even when their biologically active compounds are unknown because of their safety, effectiveness, and availability. Polysaccharides increase the level of serum insulin, reduce the blood glucose level and improve glucose tolerance. Flavonoids suppress the glucose level, reduce plasma cholesterol and triglycerides significantly and boost hepatic glucokinase activity probably by enhancing the insulin release from pancreatic islets. Previous research reported various natural compounds like rutin, quercetin, curcumin, silymarin, piperine, glycyrrhizin, thymoquinone etc when used separately or in combination have been demonstrated to have antidiabetic properties. Among the different classes of natural compounds, terpenoid is one of them. Terpenoids are classified as monoterpene, diterpene, and

sesquiterpene. Andrographolide and curcumin are two examples of terpenoids [Lehar et al, 2009; Kaur et al, 2016].

1.14 Andrographolide

Andrographolide, a diterpene lactone is the primary active ingredient in *Andrographis paniculate*. *Andrographis paniculata* is widely utilized in ayurvedic formulations. Andrographolide might be isolated and purified within the crystalline form. It has anti-diabetic, anticancer, antioxidant, anti-hyperlipidemic, and anti-allergic asthma activities. Andrographolide belongs to BCS class iv compound, having low water solubility, low intestinal permeability, and a low biological half-life of 2 hours [Rao et al, 2004; Liang et al, 2018].

1.15 Curcumin

Curcumin is the principal active ingredient present within the rhizome of turmeric (*Curcuma longa*). The main active ingredient in turmeric is curcumin, which is found in the rhizome (Curcuma longa). It was discovered to have anti-diabetic effects. Curcumin possesses hypoglycemic, nephroprotective, and cardioprotective effects in modest amounts. Several studies have demonstrated that curcumin has anticancer effects in humans. Its ability to induce apoptosis, prevent cancer cell proliferation, and reduce cell cycle progression makes it a viable treatment for cancers of the lung, breast, prostate, colorectal, liver, pancreatic, myeloma, and melanoma malignancies [Nair et al, 2012]. It has moderate hypoglycemic, nephroprotective, and cardioprotective properties. Despite its potential therapeutic effects, curcumin has poor bioavailability. Curcumin is a potent anti-inflammatory drug, and its anti-inflammatory effects are achieved via inhibiting enzyme activity, cytokine synthesis, and transcription factor activation. Curcumin's antimicrobial activity mechanism is strongly linked to the

interaction with the FtsZ protein-inducing cell division. Curcumin has potential inhibitory activity on renal cyst formation which is characterized by massive enlargement of fluid-filled cysts which eventually cause renal failure [Chattopadhyay et al, 2004; Martin et al, 2012].

1.16 Nano based Drug delivery system

Recently nanotechnology especially nanomedicine and nano-based drug delivery system is frequently used for loading different types of drugs due to several advantages such as improved bioavailability, sustained release, targeted delivery, reduced toxicity, improved permeability to biological membranes, and convenience in different routes of administration [Koo et al, 2005]. Different types of nanoparticles can be classified according to size and shape. These nanoparticles can be fabricated using different techniques. Among the different types of nanosystems polymeric nanoparticles, nanostructured lipid carriers, liposomes are commonly used in therapeutics [Patra et al, 2018].

1.17 Polymeric nanoparticle

Polymeric nanoparticles are synthetic polymers with a small size. Generally, biodegradable polymers are commonly used as this polymer easily hydrolyses in the body and produce biocompatible small molecules. [Wang et al, 2008]. Polymeric NPs have shown great potential for controlled release and targeted delivery of drugs for the treatment of several diseases. Polymeric molecules can be used to encapsulate both hydrophilic and lipophilic drug molecules. Polymeric nanoparticles can be used for the treatment of brain drug delivery, cancer therapy, and targeted antibiotics delivery with suitable polymer choice and the ability to adjust drug release [Bennet and Kim, 2014].

1.18 Nanostructured lipid carrier (NLC)

Nanostructured lipid carriers (NLCs) spring up as the second generation of lipid nanoparticles are the modifications of the first generation i.e. solid-lipid nanoparticles (SLN), in which biodegradable, compatible lipids (solid and liquid) and emulsifiers are used for the preparation of NLCs. In recent years, nanostructured lipid carriers became a popular drug delivery system over SLNs, polymeric nanoparticles, emulsions, microparticles, liposomes, etc. Incorporation of liquid lipids (oil) generates structural defcts in solid lipids, resulting to a less ordered crystalline arrangement which prevents drug leakage from the particle and provides a high drug payload [Pardeike et al, 2009]. These formulations possess the advantage in the delivery of hydrophilic as well as lipophilic drugs. In the case of many drugs, solubility in liquid lipid is higher than in solid lipid. As a result NLC offers a promising carrier system for the delivery of pharmaceuticals via oral, parenteral, ocular, pulmonary, topical, and transdermal routes [Kaur et al, 2015].

Chapter II

Literature Review

2.1 Nanotechnology and its applications

Nanotechnology is the study and application of extremely small things and can be used in the field of science, engineering, and technology conducted at the nanoscale [Saini et al, 2010]. Nanotechnology may be able to create many new materials and devices with a vast range of applications such as in nanomedicine, nanoelectronics, biomaterials energy production, and consumer products. These include more resistant building materials, therapeutic drug delivery, and higher-density hydrogen fuel cells that are eco-friendly. Being that nanoparticles and nanodevices are highly versatile through modification of their physiochemical properties, they have found uses in nanoscale electronics, cancer treatments, vaccines, hydrogen fuel cells, and nanographene batteries. The application of nanotechnology is presented in Figure 2.1 [Rao et al, 2014; Hussein et al, 2016]

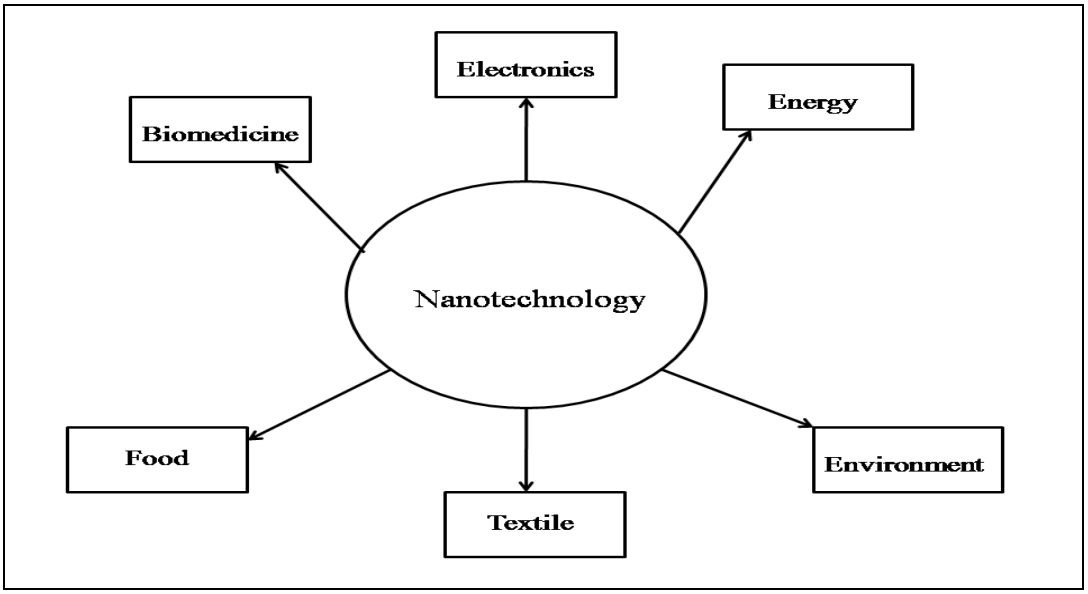

Figure 2.1: Applications of nanotechnology in different fields

2.2 Application of nanomedicine

The use of nanotechnology for medical purposes has been termed as nanomedicine. Nanomedicine is used for diagnosis, monitoring, control, prevention, and treatment of

diseases. Nanomedicine can be useful for both *in vivo* and *in vitro* biomedical research and applications such as diagnostic devices, contrast agents, analytical tools, physical therapy applications, and drug delivery vehicles. *In vivo* imaging is another area where tools and devices are being developed [Saini et al, 2010]. Using nanoparticle contrast agents, images such as ultrasound and MRI have a favorable distribution and improved contrast. In cardiovascular imaging, nanoparticles have the potential to aid the visualization of blood pooling, ischemia, angiogenesis, atherosclerosis, and focal areas where inflammation is present [Bansal et al, 2017].

Nanomedicine has exhibited great potential for the treatment of different diseases like cancer, cardiovascular and neurological disorders, asthma, inflammatory diseases HIV/AIDS, and diabetes as well as many types. The drugs which have low bioavailability and are poorly water-soluble can be delivered through nanomedicine. Nanomedicine is also applicable for drugs that are absorbed too quickly and removed from the body as waste before treatment can be effective. Nanomedicine can increase the period in which a drug remains active in the body. The drugs can be used for the specific target site, controlled delivery with minimum doses [Nikalje et al, 2015]. Common nanoparticles that have been used for drug delivery such as polymeric nanoparticles, liposomes, nanosuspension, nanostructured lipid carrier (NLC), micelles and hydrogel nanoparticles, etc [Patra et al, 2018].

2.3 Use of nanoparticles in Diabetes

Recently, many researchers are involved in the discovery of novel drug delivery systems for diabetes so that dosing frequency and drug-related toxicity can be reduced [Woldu et al, 2014]. Mohseni et al. reported water-insoluble drug resveratrol-loaded solid-lipid nanoparticles to improve insulin resistance in diabetes [Mohseni et al,2019]. According to Ahangarpour et al., solid lipid nanoparticles of myricitrin improved

diabetes and hyperglycemia complications [Ahangarpour et al, 2018]. Das et al. prepared engineered silybin nanoparticles for the experiment of diabetes [Das et al, 2014]. The drug is constrained due to solubility and bioavailability. They observed that blood glucose levels came down to normal values after 28 days of treatment with engineered silybin nanoparticles and restoration from hyperglycemic damage condition. In 2014, Alkaladi et al. reported, zinc oxide and silver nanoparticles act as potent antidiabetic agents and significantly reduced blood glucose levels [Alkaladi et al, 2014]. In the year 2017, Rani et al. showed enhanced antidiabetic activity with the treatment of combined nanoformulation of glycyrrhizin and nicotinamide which was better than free drugs [Rani et al, 2017].

2.4 Nanostructured lipid carrier (NLC)

In the early 1990s, solid lipid nanoparticles (SLNs) were discovered as first-generation lipid nanoparticles where solid lipids were used for preparation. SLNs were certain limitations like poor drug loading capacity, unpredictable gelation tendency, and drug leakage during storage [Ghasemiyeh et al, 2018].

In the late 1990s, nanostructured lipid carriers (NLC) grow up as the second generation of lipid nanoparticles to overcome the limitations of SLNs where a mixture of solid and liquid lipids is used for preparation. The excipients used for the preparative process of NLC are mostly non-toxic for *in vivo* and also biodegradable as well as biocompatible. Liquid lipids (oil) incorporation causes structural imperfections of solid lipids leading to a less ordered crystalline arrangement which prevents drug leakage providing a high amount of drug loading. Hydrophobic as well as hydrophilic drugs can be entrapped in the core of NLC to provide control and specific targeted delivery. The process of NLC preparation involves heating and cooling crystallization [Piazzini et al, 2019].

In recent years, NLCs have gained the attention of researchers as an alternative to SLNs, polymeric nanoparticles, microparticles, liposomes, etc. NLCs have sprung up as an encouraging carrier system for the delivery of pharmaceuticals via oral, parenteral, ocular, pulmonary, topical, and transdermal routes. Recently, NLCs are also being utilized for brain targeting, chemotherapy, and gene therapy [Salvi et al, 2019].

2.5 Chitosan Oligosaccharide

Chitosan oligosaccharide (COS) is an oligomer of β-(1 ➔ 4)-linked d-glucosamine. COS can be prepared from the deacetylation and hydrolysis of chitin, which is commonly found in the exoskeletons of arthropods and insects and the cell walls of fungi.COS's average molecular weight is less than 5000 Da. The main advantage of COS is water-soluble, non-cytotoxic, readily absorbed through the intestine, and mainly excreted in the urine. Many researchers prepared COS-based nanoparticles. Anter et al. prepared COS- apocynin nanoparticles for apocynin sustained release in gastric mucosa [Anter et al, 2019]. Cheng et al. were designed phycocyanin -functionalized and curcumin-loaded biotin-chitosan oligosaccharide-dithiodipropionic acid-curcumin nanoparticles to enhance the biocompatibility of CUR for tumor treatment [Cheng et al, 2019].

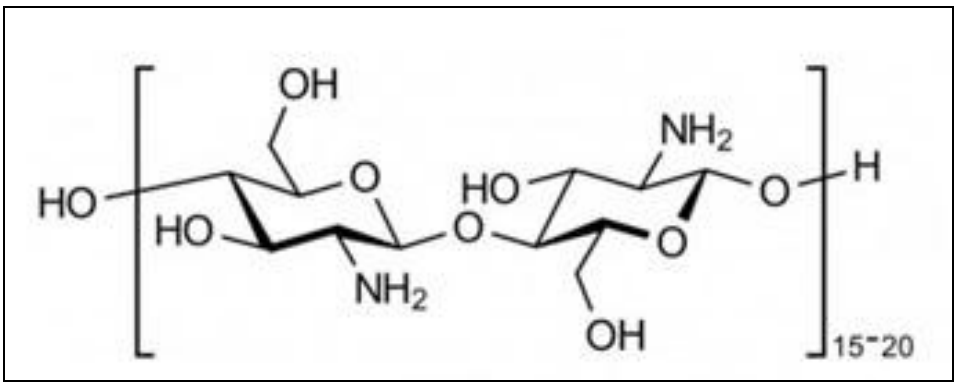

Figure 2.2: Chemical structure of Chitosan Oligosaccharide

2.6 Compritol 888 ATO

Compritol 888 ATO is a multifunctional lipidic excipient that is generally used for the preparation of prolonged-release dosage forms like solid lipid microparticles, solid lipid nanoparticles, nanostructured lipid carriers etc. It is prepared by esterification of glycerin through behenic acid without the addition of catalysts [Borgia et al, 2005]. It is a hydrophobic mixture of mono- (12 – 18% w/w), di- (45 – 54% w/w), and tri- (28 – 32% w/w) behenate of glycerol with a melting point in the range of 69 – 74°C and with hydrophilic-lipophilic balance (HLB) ≈ 2. It is available in the market in white flakes or powder form. Many researchers are preparing NLC by using compritol 888 ATO. Reddy et al, prepared clobetasol NLC made up with compritol 888 ATO to increase drug entrapment up to 85.4± 2.89% [Reddy et al, 2019]. Kar et al. formulated cedrol-loaded NLC using compritol 888 ATO to increase oral bioavailability and they reported 96.42 ± 0.876% encapsulation efficiency [Kar et al, 2017]. Spironolactone-loaded NLC was prepared using compritol 888 ATO by Kelidari et al for enhanced dissolution rates and stability that resulted in encapsulation efficiency of 90.6± 3.5% [Kelidari et al, 2016]. The chemical structure of Glyceryl monobehenate, Glyceryl dibehenate, and Glyceryl tribehenate are presented in Fig 2.3.

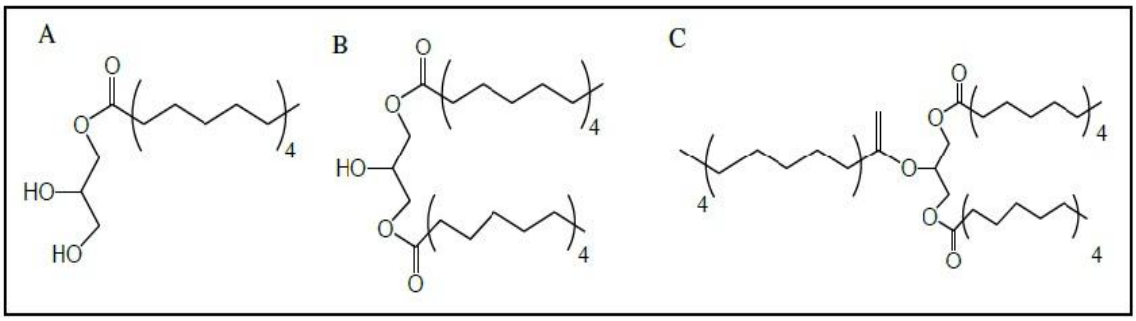

Figure 2.3: Chemical structure of (A) Glyceryl monobehenate (B) Glyceryl dibehenate (C) Glyceryl tribehenate

2.7 Triolein

Triolein is an asymmetrical triglyceride derived from glycerol and three units of the unsaturated fatty acid i.e. oleic acid. Most triglycerides are unsymmetrical, being derived from mixtures of fatty acids. Triolein represents 4 –30% of olive oil. In the pharma industry, it is used as an ointment, emulsifiable paste, suppository, lotion, emulsifier in air agent, stabilizing agent, lubricating agent, antifoaming agents [Naseri et al, 2015]. For the preparation of NLC, it is used as liquid lipid. Das et al. prepared ursolic acid-loaded NLC with the use of triolein for the therapy of leishmaniasis [Das et al, 2017]. Cedrol-loaded NLC was prepared with the use of triolein by Chakraborty et al. for mast cell degranulation that resulted in encapsulation efficiency of 88.71% [Chakraborty et al, 2017].

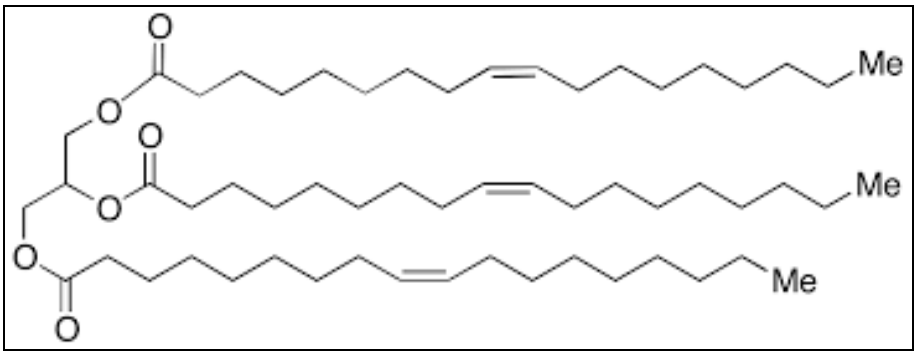

Figure 2.4: Chemical structure of Triolein

2.8 Soybean lecithin

Lecithin is a generic term to designate any group of yellow-brownish fatty substances occurring in animal and plant tissues that are amphiphilic. They attract both water and fatty substances (both hydrophilic and lipophilic) and are used for smoothing food textures, emulsifying, homogenizing liquid mixtures, and repelling sticking materials. Lecithins are mixtures of glycerophospholipids including phosphatidylcholine, phosphatidylethanolamine, phosphatidylinositol, phosphatidylserine, and phosphatidic

acid. It has emulsification and lubricant properties and is a surfactant. It acts as a good dispersing agent, stabilizing agent or helps in emulsification and encapsulation for the preparation of drug nanoparticles [Uprit et al,2012]. Minoxidil-loaded NLC was prepared with the use of soybean lecithin by Upright et al. for effective treatment of alopecia resulting the encapsulation efficiency of 86.09% [Uprit et al, 2013].

Figure 2.5: Soya lecithin powder

2.9 Streptozotocin (STZ)

Streptozotocin or streptozocin (STZ) is a naturally occurring alkylating antineoplastic agent that is particularly toxic to the insulin-producing beta cells of the pancreas in mammals. Due to its high toxicity to beta cells, in scientific research, streptozotocin has also been used for inducing insulitis and diabetes on experimental animals [Abdollahi et al, 2014]. Alkali et al worked for the antidiabetic activity of zinc oxide and silver nanoparticles on streptozotocin-induced diabetic rats [Alkaladi et al, 2014]. Karuppusamy C et al. reported evaluation of the antidiabetic activity of miglitol nanoparticles in streptozotocin-induced diabetic rats [Karuppusamy C et al, 2017].

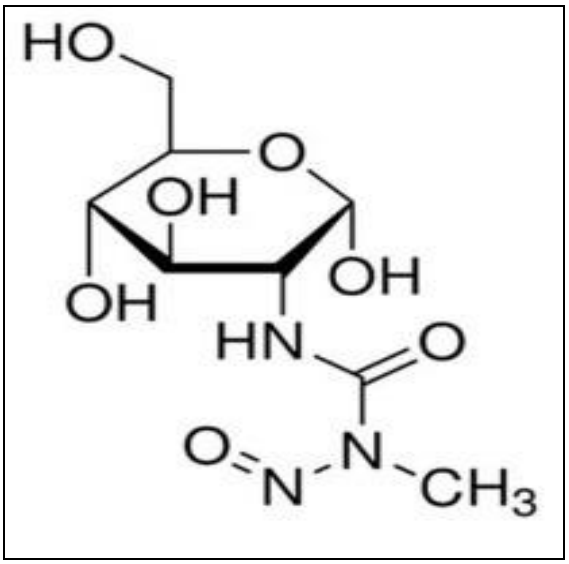

Figure 2.6: Chemical structure of Streptozotocin

2.10 Andrographolide

Source

Andrographolide (AG) is a labdane diterpene lactone isolated from stems and leaves of *Andrographis paniculata*. Andrographolide is used in different types of diseases in South East Asia countries, India and China.

Physical appearance

Andrographolide is a white powder when obtained in its pure form.

Chemistry of andrographolide

The IUPAC name of andrographolide is '3-2-[Decahydro-6-hydroxy-5-(hydroxymethyl)-5,8a-dimethyl-2-methylene-1-napthyl]ethylidene]dihydro-4-hydroxy-2(3H)-furanone', with molecular formula $C_{20}H_{30}O_5$ and molecular weight 350.455 $gmol^{-1}$ [Levita et al, 2010]. The chemical structure of andrographolide is shown in Fig. 2.7.

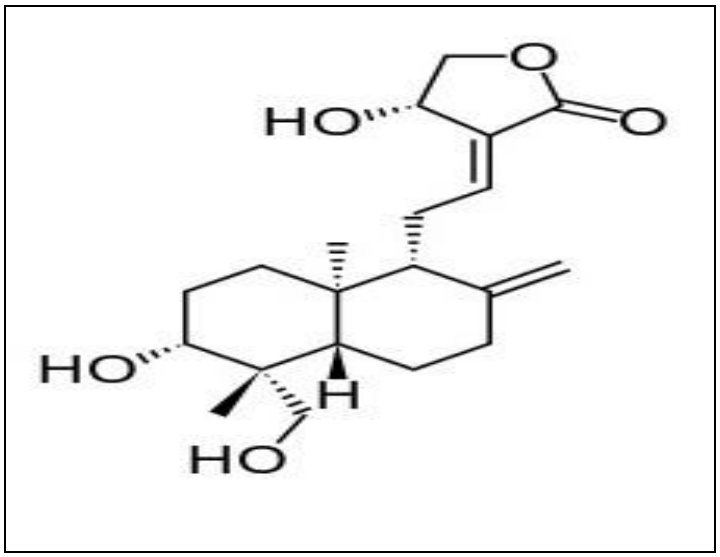

Figure 2.7: Chemical structure of Andrographolide

Solubility

Andrographolide is soluble in methanol, ethanol, transcutol (Diethylene Glycol Monoethyl Ether), dimethyl sulfoxide (DMSO), dimethylformamide (DMF), and acetone. Andrographolide is slightly soluble in chloroform and almost insoluble in water.

Biological activities of andrographolide

Many investigators have been reported different biological activities of andrographolide such as anti-inflammatory, antiallergic, antibacterial, antitumor, antidiabetic, antimalarial, and hepatoprotective. Andrographolide is well-known for its potential activity. It has been proven to attenuate inflammation by inhibiting NF-kappa B activation through the covalent modification of reduced Cys62 of p50. Andrographolide has been widely used for upper respiratory tract infections (URTIs). In a randomized, double-blind, and controlled study, Thamlikitkul et al. administered *A. paniculata* at a dose of 6 g/day for 7 days to 152 Thai adults suffering from pharyngotonsillitis and the efficiency has been reported to be similar to that of

acetaminophen in relieving the symptoms of fever and sore throat [Thamlikitkul et al, 1991]. A recent study [Uttekar et al, 2012] summarized that andrographolide derivatives may be promising candidates for preventing HIV infection suggesting that andrographolide inhibited the gp120-mediated cell fusion of HL2/3 cells with TZM-bl cells. AG also had been reported to prevent oxygen radical production by human neutrophils. Hidalgo et al. investigated the activity of AG on platelet-activating factor (PAF) induced NF- κβ activation. AG also inhibits the binding of NF-κβ on DNA which in turn reduces the expression of COX-2. AG at an oral dose of 300mg/kg successfully exhibited analgesic activity [Hossain et al, 2014]. It is also reported in their study that the anti-asthmatic activity of AG is mediated by the suppression of NF-κβ [Bao et al, 2009]. Li et al. further confirmed the inhibitory property of AG on the p65 translocation of NF- κβ [Li et al, 2009]. Chakraborty et al. reported the therapeutic potential of andrographolide-loaded nanoparticles on a murine asthma model [Chakraborty et al, 2019]. A study conducted by Xu et al. showed that andrographolide exhibited antidiabetic activity to decrease blood glucose levels in normal rats on streptozotocin-diabetic rats [Xu et al, 2012]. Zhang et al. reported the antidiabetic property of andrographolide in streptozotocin-induced diabetic rats [Zhang et al, 2000]. In a recent study, the antihyperglycemic activity of andrographolide in rats was reported by Verma et al [Verma et al, 2020].

Safety and toxicity

Many studies on rats, mice, or rabbits as well as *in vitro* studies and clinical trials have proven AG as a safe therapeutic agent. It is also reported that up to 2000 mg/kg dose of AG did not show any toxic effect [Sithisomwongse et al, 1989].

2.11 Curcumin

Source

Curcumin is the principal active ingredient present within the rhizome of turmeric (*Curcuma longa*). It's employed as a dietary supplement, cosmetics ingredient, and additive.

Physical appearance

Curcumin is a bright yellow to orange powder when obtained in its pure form.

Chemistry of Curcumin

The IUPAC name of curcumin is ' (1E,6E)-1,7-Bis(4-hydroxy-3-methoxyphenyl)hepta-1,6-diene-3,5-dione', with molecular formula $C_{21}H2_0O_6$ and molecular weight 368.385 $gmol^{-1}$. The chemical structure of curcumin is shown in Fig. 2.8.

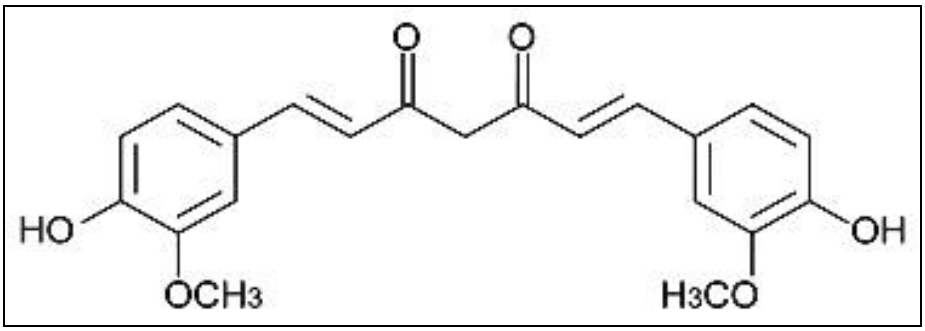

Figure 2.8: Chemical structure of Curcumin

Solubility

Curcumin is soluble in methanol, ethanol, transcutol(Diethylene Glycol Monoethyl Ether), chloroform, dimethyl sulfoxide (DMSO), and acetone. Curcumin is almost insoluble in water.

Biological activities of curcumin

Curcumin possesses several biological activities including anti-inflammatory, antioxidant, anticancer, antimutagenic, antimicrobial, antidiabetic, hypolipidemic, cardioprotective, and neuroprotective effects. Bhawana et al reported curcumin nanoparticles for antimicrobial properties [Bhawana et al, 2011]. It possesses anti-cancer and chemo-preventive activity. It acts by modulating various components of signaling cascades that are involved in cancer cell proliferation, invasion, and apoptosis process. It interacts with the adaptive and innate immune systems of our body and causes tumor regression. Bhawana et al reported curcumin nanoparticles for antimicrobial activities. It was found that nano curcumin was more effective against Gram-positive and also Gram-negative bacteria [Bhawana et al, 2011]. Curcumin has anti-inflammatory activity. Rebecca L. Edwards et al, reported curcumin analogs that undergo oxidative transformation potently inhibited the pro-inflammatory transcription factor nuclear factor κB (NF-κB), whereas stable, non-oxidizable analogs were less active, with a correlation coefficient (R^2) of IC50 versus the log of autoxidation rate of 0.75 [Rebecca L Edwards et al, 2017]. In a study conducted K Seo et al. showed that curcumin exhibited antidiabetic activity. In this study, curcumin supplement improved insulin resistance and hyperglycemia in diabetic mice, obese-diabetic animals with insulin resistance, but had no effects on non-diabetic db/+ mice and significantly lowered blood glucose levels and HOMA-IR when compared to those in the diabetic control dB/DB mice by 22 and 10%, respectively [K Seo et al, 2008]. In another study, the findings suggested that treatment of DM rats with curcumin nanoparticles decreased significantly the expression levels of insulin genes in liver and pancreas tissues

compared with those in DM rats [Gouda et al, 2019]. Ali et al. evaluated that curcumin–Zn complex has been exerted a dual action in diabetes, where the beneficial effect of curcumin in glycemic status was explored besides the action of Zn metal in insulin maintenance [Ali et al, 2016].

Safety and toxicity

Many studies on rats, mice, or rabbits as well as *in vitro* studies and clinical trials have proven curcumin as a safe therapeutic agent. It was also reported that up to 2000 mg/kg dose of CMN did not show any toxic effect [Srimal et al, 1973].

2.12 Procedure for the preparation of NLC

NLC can be prepared by different methods. This includes high-pressure homogenization (hot homogenization or cold homogenization), ultrasonication (bath sonication or probe sonication), a solvent evaporation method, a micro emulsion-based method [Naseri et al, 2015]

2.12.1 High-pressure homogenization

High-pressure homogenization is of two types, hot and cold homogenization processes [Naseri et al, 2015]. In the hot homogenization process, the lipid phase (lipids, lipophilic drugs, and lipophilic emulsifiers) is melted first before mixing with an aqueous phase. On another side, the aqueous phase (water, hydrophilic drugs, and hydrophilic emulsifiers) are heated separately. Poorly soluble drugs and lipophilic substances are suitable for making NLC through this procedure. Homogenization pressure, time of homogenization, and temperature are major parameters for reducing the particle size of NLC [Li et al, 2017].On the other hand in the cold homogenization

process, the melted lipid is rapidly cooled under liquid nitrogen or dry ice. This lipid mixture is emulsified with the cold aqueous phase. The aqueous phase is then emulsified with the molten lipid phase [Shi et al, 2011].

2.12.2 Ultrasonication

In this method, lipid and drugs are taken as oil phase which is then dispersed in an aqueous phase containing a high amount of surfactant by using probe/bath ultrasonicator. After forming a stable emulsion the organic phase is evaporated by applying heat under reduced pressure. The sample thus formed was cooled which allows solidification of particles of NLC. The drawback of this method is that it doesn't produce a small particle size which leads to instability of samples during storage [Li et al, 2017]. By using this method, Upright et al. reported NLC containing minoxidil, and entrapment efficiency was found to be 86.09% [Uprit et al, 2013].

2.12.3 Solvent evaporation

In this method, lipid and drugs are dissolved in a non-aqueous organic solvent which is then slowly added to the aqueous phase having emulsifier in it. Next, an emulsion is formed in an aqueous phase containing surfactant. The evaporation of solvent leads to the formation of nanoparticles in the aqueous phase. Then after centrifugation NLC is collected. This method is simple and useful for the preparation of NLC while the residual organic solvent is a disadvantage of the method [Li et al, 2017]. Abdolahpour et al. used the method for doxorubicin NLC preparation that resulted in 75 % entrapment efficiency and good stability [Abdolahpour et al, 2017].

2.12.4 Microemulsion

In the microemulsion method lipid phase (lipids, lipophilic drugs, and lipophilic emulsifiers) and the aqueous phase (water, hydrophilic drugs, and hydrophilic emulsifiers) are heated separately in a correct ratio. The lipid phase is mixed with the aqueous phase to form a transparent or translucent solution. The solution is dispersed in the cold aqueous medium (2~3°C) under mild stirring. Upon precipitation of fine particles, NLC is obtained [Joshi et al,2019]. Cirri et al. used this method for the preparation of hydrochlorothiazide NLC that gives rise to advantages in terms of smaller particle size ranging from 300-400 nm and increased entrapment efficiency reached to 93% [Cirri et al, 2018].

Chapter III

Objectives & Plan of Study

3.1. Objectives

The objectives of this research work were:

a) Preparation of nanoformulations loaded with combined drugs andrographolide and curcumin.
b) Characterization of the prepared nanoparticles.
c) Evaluation of the prepared nanoparticles as *in-vivo* pharmacokinetic antidiabetic study.

3.2. Plan of study

The study plan was as follows:

Nanostructured lipid carrier of combined andrographolide and curcumin

- Preparation of curcumin-chitosan nanocomplex (CCN)
- Preparation of andrographolide(AG) and curcumin(CMN) loaded nanostructured lipid carrier (AG-CMN NLC) by hot melt homogenization and ultrasonication.
- Determination of drug loading (%) and entrapment efficiency (%) of AG-CMN NLC
- HPLC method development for the estimation of andrographolide and curcumin
- Characterization of prepared nanoparticles employing particle size, polydispersity index, zeta potential, FESEM and TEM.
- Investigation of any interaction between drug and other excipients used in the formulation by FTIR, differential scanning calorimetry (DSC), and XRD study.

- *In-vitro* drug release study of AG-CMN NP in different release media like simulated gastric fluid (SGF, pH 1.2) and simulated intestinal fluid (SIF, pH 6.8).
- Assessment of nanoparticle characteristics of AG-CMN NLC during stability study after 90 days.

In-vivo studies

- Determination of plasma drug concentration in rat of free AG, CMN suspension, or AG-CMN NLC suspension through oral route of administration by HPLC method.
- Evaluation of antidiabetic study in mice model of free AG, CMN,AG-NLC,CMN-NLC and AG-CMN NLC.

Chapter IV

Materials and Methods

Materials and methods

4.1 MATERIALS

Table 4.1: List of reagents and solvents used

SL No.	Chemical name	Source
1	Acetic acid	Merck Life Science Pvt. Ltd, Bengaluru, India
2.	Acetone	Merck Life Science Pvt. Ltd, Bengaluru, India
3.	Acetonitrile	Merck Life Science Pvt. Ltd, Bengaluru, India
4.	Andrographolide	Sigma-Aldrich Co, St Louis, MO, USA
5.	Chloroform	Merck Life Science Pvt. Ltd, Bengaluru, India
6.	Chitosan Oligosaccharide	Sisco Research Laboratories Pvt. Ltd,Mumbai, India
7.	Compound 48/80	Sigma-Aldrich Co, St Louis, MO, USA
8.	Curcumin	Sigma-Aldrich Co, St Louis, MO, USA
9.	Dichloromethane	Merck Life Science Pvt. Ltd, Bengaluru, India
10.	Di potassium hydrogen orthophosphate	Merck Life Science Pvt. Ltd, Bengaluru, India
11.	Di sodium hydrogen orthophosphate	Merck Life Science Pvt. Ltd, Bengaluru, India
12.	Hydrochloric acid	Merck Life Science Pvt. Ltd, Bengaluru, India
13.	Hydrogen peroxide (30%)	Merck Life Science Pvt. Ltd, Bengaluru, India
14.	Methanol	Merck Life Science Pvt. Ltd, Bengaluru, India
15.	Orthophosphoric acid	Merck Life Science Pvt. Ltd, Bengaluru, India
16.	Polyvinyl alcohol (PVA, MW 85,000-124,000)	Merck Life Science Pvt. Ltd, Bengaluru, India

SL No.	Chemical name	Source
17.	Potassium dihydrogen Orthophosphate	Merck Life Science Pvt. Ltd, Bengaluru, India
18.	Potassium hydroxide	Merck Life Science Pvt. Ltd, Bengaluru, India
19.	Sodium chloride	Merck Life Science Pvt. Ltd, Bengaluru, India
20.	Sodium deoxycholate	Merck Life Science Pvt. Ltd, Bengaluru, India
21.	Sodium hydroxide	Merck Life Science Pvt. Ltd, Bengaluru, India
22.	Sorbitol	S.D. Fine Chem. Pvt. Ltd., Mumbai, India
23.	Soybean lecithin	Sigma-Aldrich Co, St Louis, MO, USA
24.	Stearylamine	Merck Life Science Pvt. Ltd, Bengaluru, India
25.	Streptozotocin	Sigma-Aldrich Co, St Louis, MO, USA
26.	Triolein	Sigma-Aldrich Co, St Louis, MO, USA
27.	Tween-80	Merck Life Science Pvt. Ltd, Bengaluru, India

Table 4.2: List of equipments used:

SL No.	Instrument name	Source
1	Bath sonicator	Trans-O-Sonic, Mumbai, India
2.	Cold Centrifuge	Rota 4R ‐ V/FM, Plastocrafts, India
3.	Differential scanning caloriemetry	Pyris Diamond TG/DTA, PerkinElmer,Singapore
4.	Digital weigh machine	Sartorius Corporate Administration, Otto-Brenner-Straße 20, Goettingen, Germany
5.	Field emission scanning electron Microscopy	JEOL JSM 6700 F, JEOL, Tokyo, Japan
6.	FTIR instrument	IR Affinity 1,Shimadzu, Japan
7.	High performance liquid Chromatography (HPLC)	Agilent 1260 series,Agilent,USA
8.	HPLC Column	Phenomenax,USA
9.	High speed homogenizer	IKA Laboratory Equipment, Model T10B Ultras-Turrax, Staufen, Germany
10.	Incubator shaker	BOD-INC-1S, Incon, India
11.	Laboratory freeze dryer (lyophilizer)	Instrumentation India, Kolkata, India
12.	Magnetic stirrer	Tarsons,Kolkata,India
13.	Particle size and zetasizer	Zetasizer nano ZS 90, Malvern Zetasizer Limited, Malvern, UK
14.	Refrigerator	Godrej,India
15.	Scanning electron microscope	JEOL JEM-2010 TEM, JEOL, Japan

SL No.	Instrument name	Source
16.	Transmission electron microscope	JEOL JEM-2010 TEM, JEOL, Japan
17.	Ultrasonication	MW sonicator, Vibra cell VCX750, Sonics, USA
18.	UV cabinet	Camag,Switzerland
19.	UV-VIS spectrophotometer	Shimadzu UV‐1800, Shimadzu,Japan
20.	Vortex mixture	CM-101 plus cyclomixer, Remi,India
21.	Water bath (Temperature control)	Remi,India

Experimental methodologies

4.3 Preparation of different buffers and reagents used in the experiments

Preparation of Simulated gastric fluid buffer, pH 1.2 (SGF) without enzyme

SGF buffer was prepared according to the method mentioned in United States Pharmacopoeia (volume 1). For 1000 ml SGF buffer, 2 g of sodium chloride and 7 ml concentrated hydrochloric acid, and 800 ml Milli-Q water was taken in a 1000 ml beaker. The beaker was then kept on a magnetic stirrer to dissolve the materials, pH was adjusted to 1.2 with sodium hydroxide or hydrochloric acid solution. Finally, the volume was made up to 1000 ml with Milli-Q water [USP, Vol. 1].

Preparation of Simulated intestinal fluid buffer, pH 6.8 (SIF) without enzyme

SIF buffer was prepared according to the method mentioned in United States Pharmacopoeia (volume 1). For 1000 ml SIF buffer, 6.8 g of potassium dihydrogen orthophosphate and 800 ml Milli-Q water were taken in a 1000 ml beaker. The beaker was then kept on a magnetic stirrer to dissolve the materials, pH was adjusted to 6.8 with sodium hydroxide or orthophosphoric acid solution. Finally, the volume was made up to 1000 ml with Milli-Q water [USP, Vol. 1].

4.4 Selection of polymer, lipids, and surfactants for the preparation of nanoparticles

The selection of polymer is important for preparing nanoparticles. The selected polymer was easily formed a complex with the drugs. Also, the choice of lipid is the main criteria for the preparation of lipid nanoparticles. The selected lipids easily form solid-liquid binary lipid (SLB) matrix and solubilize the drugs [Chakraborty et al,

2009]. Many studies had been done for the choice of the best suitable excipients to solubilize the drug in many solid and liquid lipids.

4.5 Preparation of Curcumin-Chitosan nanocomplex (CCN)

Briefly, 250 mg chitosan oligosaccharide (water-soluble) was dissolved in 20 ml acetic acid (1.4 % w/v). 250 mg curcumin was dissolved in a cold solution of 0.2 (M) potassium hydroxide to charge the curcumin drug particles. The charged curcumin solution was immediately mixed with chitosan solution with homogenizer. Then pH of the solution was adjusted to 4.4 with a dilute solution of KOH/CH_3COOH. Then the solution was first centrifuge at 4000 rpm for 10 minutes at 4°C. The obtained supernatant solution was again centrifuged at 16000 rpm for 10 minutes at 4°C. The combined product was lyophilized via freeze dryer and kept at 2- 8 °C for future use [Nguyen et al, 2015].

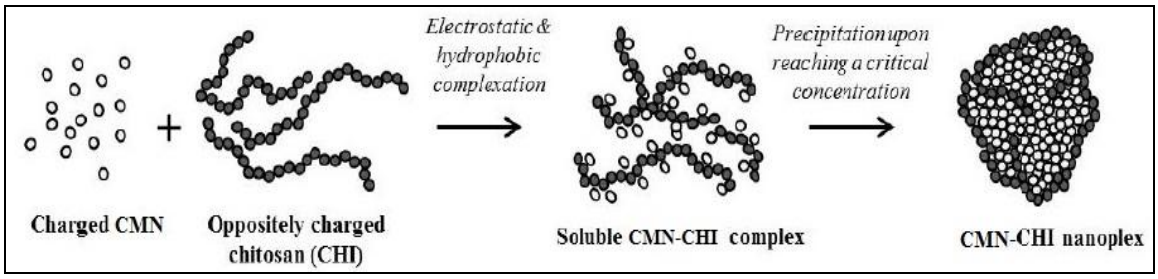

Figure 4.1: Schematic diagram for preparation of CCN by electrostatic & hydrophobic complexation mechanism

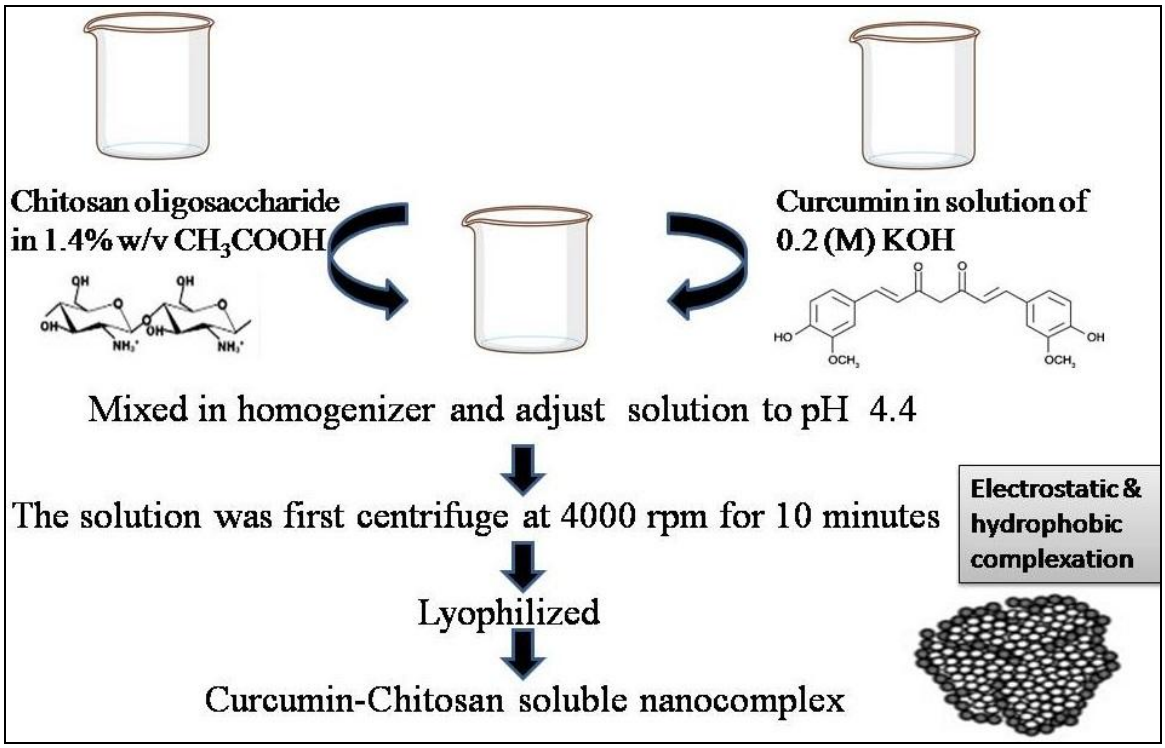

Figure 4.2: Schematic diagram for preparation of CCN by electrostatic & hydrophobic complexation method

4.6 Preparation of combined andrographolide-curcumin loaded nanostructured lipid carrier (AG-CMN NLC)

Combined andrographolide(AG) and curcumin(CMN) loaded nanostructured lipid carrier was prepared by hot-melt emulsification combined with high-speed stirring and ultrasonication [Fang et al, 2011]. Briefly, in a glass beaker necessary amounts of Compritol 888 ATO(500 mg), triolein(160 mg), and stearylamine(6 mg) were melted until it became transparent at 75 – 80°C to prepare the lipid phase. Required quantities of andrographolide(160 mg) and curcumin-chitosan nanocomplex(curcumin content 160 mg) were dissolved in transcutol (5 ml) and mixed with the lipid phase with a homogenizer. The mixture was stirred at 5000 rpm at 75 – 80°C to obtain a uniform transparent oil phase. In another beaker, an aqueous phase (30 ml water) was prepared by adding sodium deoxycholate (60 mg) and amphiphilic emulsifier soya lecithin (110

mg) and stirring at 5000 rpm for 1 hour then it was heated to 85°C for 15 min. The aqueous phase was dropwise added to the lipid phase at 75-80°C with continuous homogenization by a homogenizer at 20,000 rpm for 10 min according to the hot homogenization method. The obtained pre-emulsion was then put through ultrasonication for 10 min with maintaining the temperature at 85°C. Then sorbitol (7%) as cryoprotectants was added to this solution. The nanoparticles were separated by centrifugation at 4°C at 17000 rpm for 30 minutes. The obtained nanoparticles were frozen to (-) 80°C overnight and lyophilized by a Labogene-APS Lyophilizer (Labogene-APS 6-BDR- 3450Lynge, Denmark) until the dry powder was obtained and stored at 2-8°C for further studies. Single andrographolide nanoparticles (AG-NLC) and single curcumin (CMN-NLC) nanoparticles were also prepared by the above method. Blank nanoparticles were prepared by the same method except adding the drug at the first step [Das et al, 2017; Kar et al,2017].

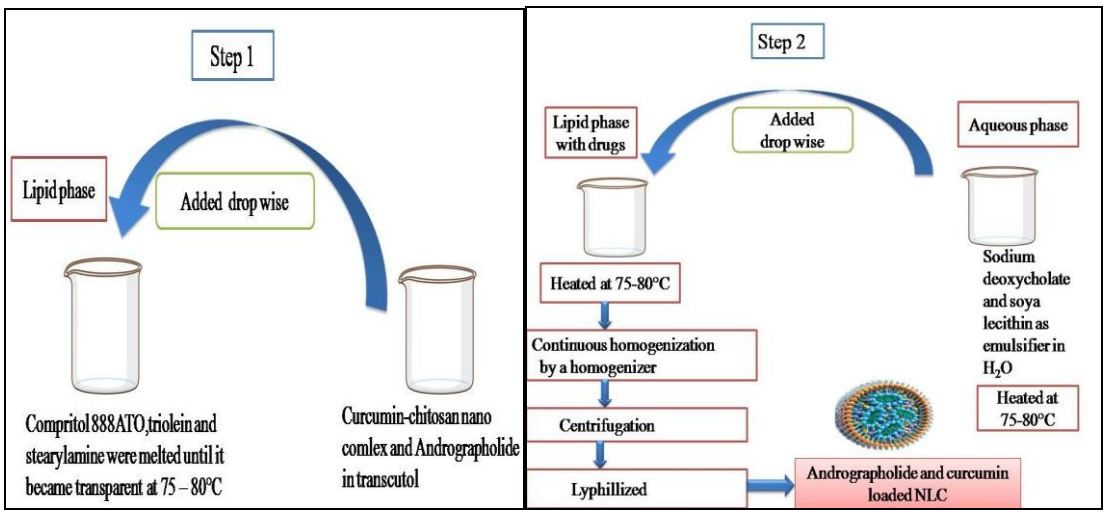

Figure 4.3: Schematic diagram for preparation of AG-CMN NP by hot homogenization method

Physicochemical characterization of AG - CMN NLC

4.7 Determination of drug loading (%) and entrapment efficiency (%)

Drug loading (DL%) and entrapment efficiency (EE%) were determined for AG-CMN NLC by the developed RP-HPLC method. Briefly, necessary quantities of nanoformulation were dissolved in methanol and sonicated for 15 minutes then centrifuged at 10,000 rpm for 10 minutes. After that, the supernatant was collected. From the supernatant, necessary dilution was carried out with the diluent to determine the entrapment efficiency and drug loading. The drugs in the NLC were quantified by the developed HPLC method.

Drug entrapment efficiency and drug loading were determined from equations (1) and (2) respectively [Das et al, 2017].

$$\text{Drug loading content}\,(\%) = \frac{\text{weight of the drug in nanoparticles}}{\text{weight of the nanoparticles}} \times 100\% \qquad (1)$$

$$\text{Encapsulation efficiency}\,(\%) = \frac{\text{weight of the drug in nanoparticles}}{\text{initial amount of drug}} \times 100\% \qquad (2)$$

4.8 HPLC method development for the estimation of andrographolide and curcumin

To develop a straightforward RP-HPLC method, validation, and quantification of combined andrographolide (AG) and curcumin (CMN) in novel NLC formulation. The HPLC method was validated as per ICH recommendations for system suitability criteria within the acceptable limit [ICH. Q2(R1); 2005; Chaudhari et al, 2020].

4.8.1 Choice of detection wavelength for HPLC method

Andrographolide and curcumin primary standard stock solutions (100 µg/ml) were prepared in methanol and further diluted to a secondary standard stock solution (10 µg/ml). The solutions were scanned by Ultraviolet-Visible (UV-VIS)

spectrophotometer in the range of 200- 400 nm. Andrographolide showed absorption maxima at 223 nm while that for curcumin was found to be at 262 nm. Two standard UV spectrum crosses at a common wavelength at 240 nm, which is the isosbestic wavelength of andrographolide and curcumin and hence 240 nm was taken as a detection wavelength for HPLC analysis. The overlay UV spectrum of andrographolide and curcumin is represented in Fig. 4.4.

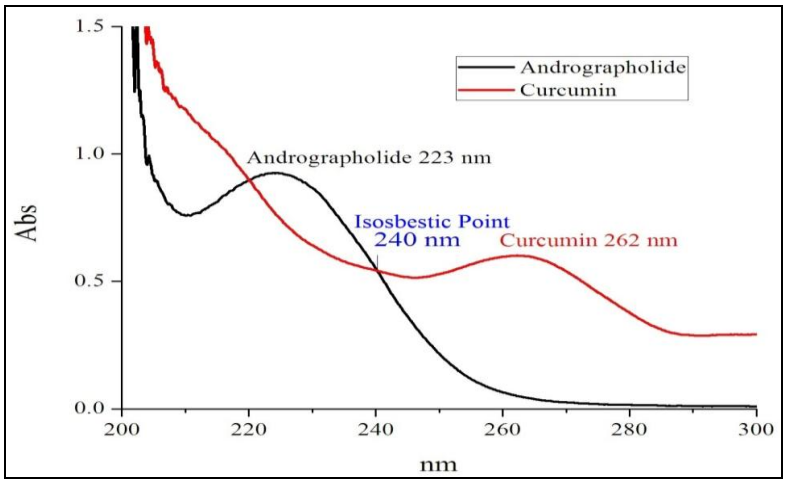

Figure 4.4: UV overlay spectrum of Andrographolide and Curcumin

4.8.2 Instrumentation and chromatographic conditions

The UV 1800 UV- Visible spectrophotometer make of Shimadzu equipped with UV probe software was used for recording the UV spectrum. The HPLC system consisted of a quaternary pump (Model: Agilent 1260 series) with an autosampler, photodiode array detector (PDA), and thermostat column compartment(TCC). EZ chrome Elite software was used for data collection and analysis. Phenomenex octadecylsilane column with 1.5 ml/min flow rate in an isocratic mode of elution was used for the separation of two drugs. The mobile phase contains 0.02 M monobasic potassium phosphate solution of pH 3.0 and acetonitrile as a ratio of 50: 50 (v/v). The mobile phase was degassed and filtered before use. All the tests were performed at a 35 °C constant column oven temperature with 240 nm UV detection and 20 µl injection load. The established chromatographic conditions are given in table 4.3.

Table 4.3: Optimized chromatographic condition for developed RP-HPLC method

Parameter	**Conditions**
Column	Phenomenex, octadecylsilane (250 mm × 4.6 mm, 5 µm) column
Mobile phase	Buffer (0.02 M KH_2PO_4, pH 3.0) : Acetonitrile = 50 : 50 v/v
Solvent	First dilution in methanol and subsequent dilution in the mobile phase
Flow rate	1.5 ml/ min
Column oven tempt	35 °C
Detection wavelength	240 nm
Injection volume	20 µl

4.8.3 Preparation of primary standard and sample solutions

A mixed standard solution of andrographolide and curcumin (500 µg/ml) was prepared in methanol as the primary stock solution. The final standard solution was obtained with an actual dilution of the standard stock solution.

Necessary quantities of nanoformulation were dissolved in methanol followed by dilution with diluent to determine the entrapment efficiency, drug loading, and cumulative *in vitro* drug release study by the suggested method.

4.8.4 Method validation

Method validation was executed by ICH recommendations for system suitability, accuracy, specificity, linearity, precision, sensitivity, and robustness [ICH. Q2(R1); 2005].

4.8.4.1 Specificity

Specificity stipulates the proposed method's capability to separate the principal peaks from any other impurity/degradation products. To carry out the specificity analysis, blank nanoparticle (without drugs) solutions and stress degradation solutions under different conditions were analyzed into the HPLC method. The acquired peaks were compared with standard drug solutions peaks. No interference peak was observed apart from the peak of andrographolide and curcumin.

4.8.4.2 Linearity

To develop the calibration curve, andrographolide and curcumin standards were mixed to prepare 500 µg/ml of stock solution and 12.5, 25, 50, 75, 100, and 125 µg/ml concentrations were prepared for linearity from the stock solution. Each solution was injected in replicate (n = 3) and the calibration curves for andrographolide and curcumin were established by plotting peak area versus concentration.

4.8.4.3 Accuracy

Accuracy was ascertained by using the standard addition method or recovery study by spiking standard andrographolide and curcumin to the nanoformulation followed by analysis using the proposed method. To each flask, the measured amount of andrographolide and curcumin standards (at 80 %, 100 %, and 120 % levels of andrographolide and curcumin contributed from the sample) were added. Eventually, five concentration solutions were prepared with the diluent and injected into replicate (n = 3).

4.8.4.4 Precision

For estimation of method precision of the developed method, three different standard concentration levels were prepared which contained 12.5 µg/ml (lower concentration),

50 µg/ml (middle concentration), and 125 µg/ml (higher concentration) each of andrographolide and curcumin. The intra-day precision was determined by analyzing sample solutions (n = 6) at a single batch in duplicate sets in a single day but the inter-day precision was determined on another day. The relative standard deviations (% RSD) were determined for every batch.

4.8.4.5 LOD and LOQ

Analytical method sensitivity was ascertained by the limit of detection (LOD) to detect the lowest amount of substance and the limit of quantification (LOQ) to quantify the lowest amount of substance that can be measured within the acceptable system suitability criteria.

4.8.4.6 Robustness

To assess the robustness study of the proposed method for andrographolide and curcumin, some intentional changes in the chromatographic conditions were employed. System suitability parameters were estimated after such changes for robustness study.

4.8.4.7 System suitability

System suitability was estimated from the mixed standard solutions of andrographolide and curcumin under optimized chromatographic conditions. Retention time, theoretical plates, tailing factor, resolution, and injection precision was considered for system suitability.

4.8.4.8 Forced degradation studies

The degradation property of andrographolide and curcumin was carried out by various forced conditions. Each 5 ml individual standard stock solution of andrographolide and curcumin was applied to various stress conditions separately like photolytic, heat,

oxidative hydrolysis, UV light, acidic and alkaline hydrolysis for specified times. Finally, every 5 ml of stress-induced solution was diluted to have a final concentration of andrographolide around 51 µg/ml and curcumin around 50.4 µg/ml. Each solution was analyzed against a freshly prepared mixed standard of andrographolide (52 µg/ml) and curcumin (51 µg/ml). Optimized conditions for the forced degradation study of andrographolide and curcumin are given in Table 4.4.

Table 4.4: Optimized condition for forced degradation study of andrographolide and curcumin

Stress type	**Stress condition**
Acidic	5 ml of 0.1 (N) HCl for 4 h at 80 °C
Alkali	5 ml of 0.1 (N) NaOH for 4 h at 80 °C
Peroxide	5 ml of 5 % v/v H_2O_2 for 4 h at 80 °C
Photolytic	Kept in sunlight for 4 h
Thermal	80 °C for 4 h
UV light	254 nm UV light for 4 h

4.9 Particle size, polydispersity index, and zeta potential

The lyophilized AG-CMN NLC (10 mg) was suspended in Milli Q water (10 mL) and was sonicated for 15 min. Average particle size, polydispersity index (PDI), and zeta potential of the samples were analyzed at 25°C by a dynamic light scattering method (DLS) using Data Transfer Assistance (DTA) software by Zetasizer Nano ZS90 [Zetasizer Nano ZS, Malvern Instrument Limited, UK] [Wolfgang S, 2007; Martin A, 1993].

Morphology study of nanoparticles

4.10 Field emission scanning electron microscopy (FESEM)

The surface morphology of the prepared NLCs were investigated by FESEM. The lyophilized AG-CMN NLC, CCN nanoparticles and blank nanoparticles (each 10 mg) were suspended in Milli Q water (10 mL) and was vortexed for 5 min and it was centrifuged at 10,000 rpm for 20 min. The final pellet was resuspended in Milli Q water and placed on the stub. The stub was then coated with platinum using a sputter coater (JEOL JFC 1100) and was observed under field emission scanning electron microscope (JEOL JSM 6700 F, JEOL, Tokyo, Japan) [Kar et al, 2017].

4.11 Transmission electron microscopy (TEM)

The internal morphology of AG-CMN NLC was studied by transmission electron microscopy (Jeol JEM 2100F, JEOL-France, Paris), with an accelerating voltage of 200kV. The lyophilized AG-CMN NLC (10 mg) was suspended in Milli Q water (10 mL) and was shaken for 1 min it was centrifuged at 10,000 rpm for 5 min. One drop of NLC was sprayed on copper grids by the formation of a thin liquid film. The copper grid was air-dried overnight before being observed with a transmission electron microscope [Chakraborty et al, 2017].

4.12 FTIR analysis

FTIR analysis was done to investigate any possible interaction between the drug and other excipients used in the formulation. Briefly, pure andrographolide, pure curcumin, physical mixture of all components used in the formulation, blank NLC and andrographolide-curcumin NLC (AG-CMN NLC) were scanned in the range of 400-4000 cm^{-1} at a resolution of 4 cm^{-1} by ATR techniques (IR Affinity 1, Shimadzu, Japan) and the data were acquired [Maji et al, 2014].

4.13 Differential scanning calorimetry (DSC) study

Differential scanning calorimetry analysis (DSC) study was performed for pure andrographolide, pure curcumin, physical mixture of all components used in the formulation, blank NLC, and andrographolide-curcumin NLC (AG-CMN NLC) on a DSC 60 detector (Pyris Diamond TG/DTA, PerkinElmer, Singapore). Briefly, 5 mg of each sample was taken in a platinum crucible and sealed hermetically. DSC scan was recorded in the range of 30ºC to 600°C at a heating rate of 5°C/min under a nitrogen purge, using alpha aluminum powder as a reference [Ghosh et al, 2017].

4.14 X-ray diffraction (XRD) analysis

To characterize the physical form (crystalline/amorphous) of standard andrographolide, standard curcumin, physical mixture, blank nanoparticles, combined andrographolide and curcumin-loaded nanoparticles were accomplished by XRD study. The diffraction angle was 10-80°C with a scanning rate of 10° min^{-1} [Das et al, 2017].

4.15 Stability study of AG-CMN NLC

The NLCs were stored in a closed polypropylene bottle in a refrigerator at 2-8°C for 90 days. The stability of NLC was estimated in terms of particle size, polydispersity index, zeta potential, and drug loading (DL).

4.16 *In vitro* drug release study of AG-CMN NLC

The release of AG and CMN from the core of AG-CMN NLC was studied using the dialysis bag diffusion technique. Briefly, in vitro drug release study was carried out in two separate mediums of simulated gastric fluid (SGF without enzyme) and also simulated intestinal fluid (SIF without enzyme) containing polysorbate 80 (1% v/v). 10 $mg.ml^{-1}$ combined drug-loaded NLC solution was prepared with two release mediums separately and placed into a 12 kDa, molecular weight cut off of a pre-swelled dialysis

bag. The dialysis bag was kept in a 250 ml conical flask containing 200 ml of release medium and placed in an orbital shaker at 100 rpm content shaking at 37.5°C temperature.1 ml sample solution was withdrawn by replacing 1 ml release medium at a predetermined time interval (1 h, 2 h, 3.5 h, 6 h, 9 h, 11 h, 24 h,33 h,48 h, and 72 h) to maintain sink condition [Hasan et al, 2019]. The drug content from all the samples was analyzed by the developed HPLC method [Das et al, 2017].

4.17 *In-vitro* drug release kinetic models

To evaluate the drug- release kinetics patterns, drug release data were fitted to different kinetic models like zero order, first order, Higuchi, Hixon-Crowell and Korsmeyer-Peppas models. The equation with highest correlation coefficient (R^2) value was used as indicator of the best fitting of the models in the different dissolution media. The equations are listed below [Rudra et al, 2010].

Zero-Order	$\mathbf{Q_t = Q_0 + K_0 t}$	**(% CDR vs. time)**
First-Order	$\mathbf{Log\ Q_t = Log\ Q_0 - Kt / 2.303}$	**(log % ADR vs. time)**
Higuchi model	$\mathbf{Q_t = K_H\ (t)^{1/2}}$	**(% CDR vs. root of time)**
Hixson-Crowell model	$\mathbf{Q_0^{1/3} - Q_t^{1/3} = K_{HC}\ t}$	**(Cube root of % ADR vs. time)**
Korsmeyer-peppas model	$\mathbf{M_t/M_\infty = Kt^n}$	**(log % CDR vs. log t)**

4.18 *In-vivo* Pharmacokinetic study

In vivo pharmacokinetic study was carried out for the comparison of drugs available in blood plasma upon treatment of pure drugs/drug-loaded nanoparticles. Female Wistar rats (150-200 g) were used for pharmacokinetic study. The rats were fasted for 12 hours before the experiment but water was allowed and the rats were divided into three groups as follows:

Group-1: Rats received combined andrographolide and curcumin-loaded NLC.

Group-2: Rats received mixed andrographolide and curcumin-free drugs.

Group-3 (control group): Rats received vehicle.

The necessary quantities of pure drugs were mixed and the nanoformulation was separately dissolved in carboxymethyl cellulose sodium salt solution (0.2% v/v) containing polysorbate 80 (0.1 % v/v) and 150 $mg.Kg^{-1}$ of each andrographolide and curcumin-free-drugs/NP oral dose was given to rats. Blood samples were withdrawn from the rat tail vein at predetermined time intervals (at 30 min,1,2,4,8,12,24, and 48 h) post drug administration. At each point blood (~1 ml) was collected in a centrifuge tube containing 0.1 ml of a saturated solution of EDTA as an anticoagulant. The tube was vortexed for one minute and centrifuge immediately at 1000 rpm for five minutes at 4°C for separation the of plasma. All plasma samples were collected and stored at -20°C until analyzed [Dutta et al, 2018].

AG and CMN content in plasma were determined by the developed HPLC method. Briefly, control or test plasma was thawed at room temperature and 100 µl of plasma was mixed with 300 µL of ice-cold acetonitrile to precipitate the plasma protein. The sample was mixed by vortexing and after centrifugation at 10,000 rpm for 10 min and the supernatant was collected. AG and CMN stock was prepared in methanol and working stocks (WS) were prepared by serial dilution in the mobile phase. Calibration control (CC) and quality control (QC) samples were prepared by spiking WS in blank plasma. Next, 100 µl of CC/QC plasma homogenate sample was precipitated with 300µl of ice-cold acetonitrile. The samples were mixed using a vortexer and it was followed by centrifugation at 10,000 rpm for 10 min. The supernatants were collected

and injected into HPLC system and the drugs were quantified [Paul et al, 2018; Chakraborty et al, 2019].

4.19 *In-vivo* antidiabetic activity study

4.19.1 Animals and induction of diabetes

Swiss albino mice (25 -30 g) either or sex were used for this study. Streptozotocin (STZ) with a dose of 45 $mg.kg^{-1}$ body weight intraperitoneal injection was given to the fasting animals (10-12 hours) . After six-hour of STZ administration, a 10 % glucose solution was fed for 12- 24hour to all the diabetic animals to prevent hypoglycemic shock. After three days of STZ injection fasting blood glucose was measured. Mice with fasting blood glucose (FBGL) > 200 $mg.dl^{-1}$ were considered as diabetic [Alkaladi et al, 2014; Rani et al, 2017].

4.19.2 Experimental protocol

Experimental animals were divided into seven groups with five animals in each group. Regular oral doses were given for successive six weeks. Blood glucose was measured weekly of overnight fasted animals (mice). The animal groups were as follows:

Group I: Normal control (No drug)

Group II: Diabetic + ve control (STZ-induced mice).

Group III: Standard drug control Diabetic mice (STZ-induced) treated with 1 $mg.kg^{-1}$ glibenclamide.

Group IV: Pure drug control Diabetic mice (STZ-induced) treated with pure andrographolide (150 $mg.kg^{-1}$) plus curcumin (150 $mg.kg^{-1}$) .

Group V: Andrographolide nanoparticles (AG-NLC) Diabetic mice (STZ-induced) treated with andrographolide nanoparticles (15 $mg.kg^{-1}$)

Group VI: Curcumin nanoparticles (CMN-NLC) Diabetic mice (STZ-induced) treated with curcumin nanoparticles (15 $mg.kg^{-1}$)

Group VII: Combined andrographolide and curcumin loaded nanoparticles (AG-CMN NLC) Diabetic mice (STZ-induced) treated with combined andrographolide and curcumin loaded nanoparticles (15 $mg.kg^{-1}$ of each drug).

4.20 Statistical analysis

The experimental data were reported as mean ± SD. One-way analysis of variance (ANOVA) followed by Tukey's test has been performed to compare all the data given in different groups.

$P < 0.05$ was contemplated as the statistical level of significance.

Chapter V

RESULTS

Results

5.1 Preformulation study of NLC

In our study, we have developed an effective and stable NLC formulation by using Generally Recognized As Safe (GRAS) ingredients, like triolein, compritol 888ATO, soya lecithin, and sodium deoxycholate as excipients (Table 5.1).

Table 5.1: The composition of nanostructured lipid carrier system

Formulation code	Solid lipid	Liquid lipid	Hydrophillic emulsifier	Amphiphillic emulsifier
AG-CMN NLC	Compritol® 888ATO Stearylamine	Triolein	Sodium deoxycholate	Soya lecithin

5.2 Drug loading and entrapment efficiency of AG-CMN NLC

All the NLC formulations were developed by altering the lipid-drug ratio. The drug loading and entrapment efficiency value of different nanoparticles has been given in Table 5.10. In our study, drug loading was increased with an increase in the concentration of andrographolide and curcumin in the formulation. The experiment was run in triplicate for each formulation. The drug loading (DL) varied from 17.52 % to 19.21% for AG and 16.93% to 18.12% for CMN and entrapment efficiency (EE) varied from 89.56 % to 91.63% for AG and 83.52% to 90.56% for CMN in NLC-F1 and NLC-F2 respectively. Due to the higher drug loading and entrapment efficiency of NLC-F1 was chosen for further characterization.

5.3 HPLC method development for the estimation of andrographolide and curcumin

5.3.1 Development of the Method

A series of trials in terms of choice of buffer in the mobile phase and its pH, composition of the mobile phase, detection wavelength, choice of the stationary phase i.e. column, flow rate, and column oven temperature was carried out for succeeding the suggested RP-HPLC method. To select the detection wavelength, UV spectrum in the range of 200 to 400 nm of standard andrographolide (50 μg/ml), curcumin (51 μg/ml) in methanol were recorded. Finally, the ideal chromatographic parameters were achieved. Andrographolide and curcumin peaks were found at 2.4 and 4.9 min. One small peak was found at the retention time of 2.85 minutes due to the keto form of curcumin produced little amount by the solvent. System suitability parameters were found within the acceptable limit. Typical chromatograms of standard andrographolide, curcumin, and mixed drugs are in Fig. 5.1, 5.2, and 5.3 respectively.

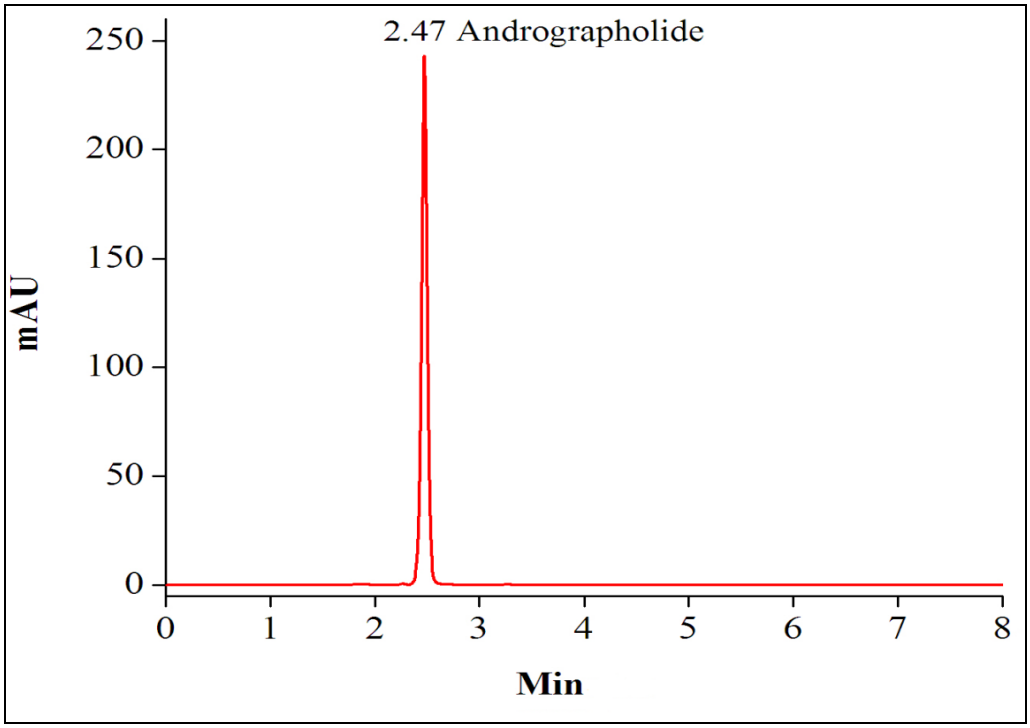

Figure 5.1: Chromatogram of Andrographolide standard

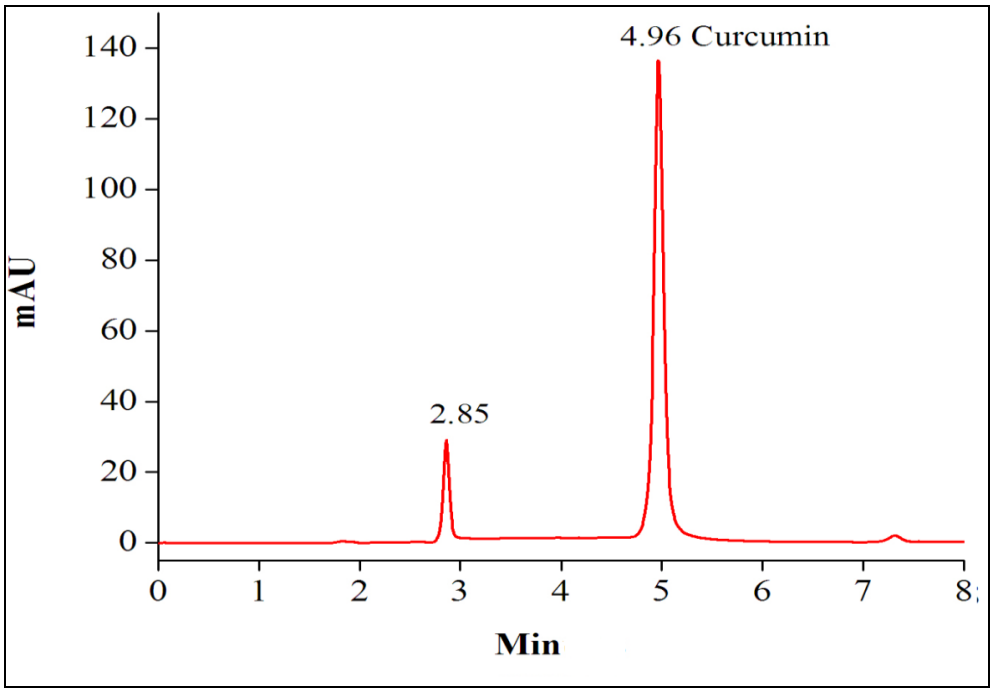

Figure 5.2: Chromatogram of Curcumin standard

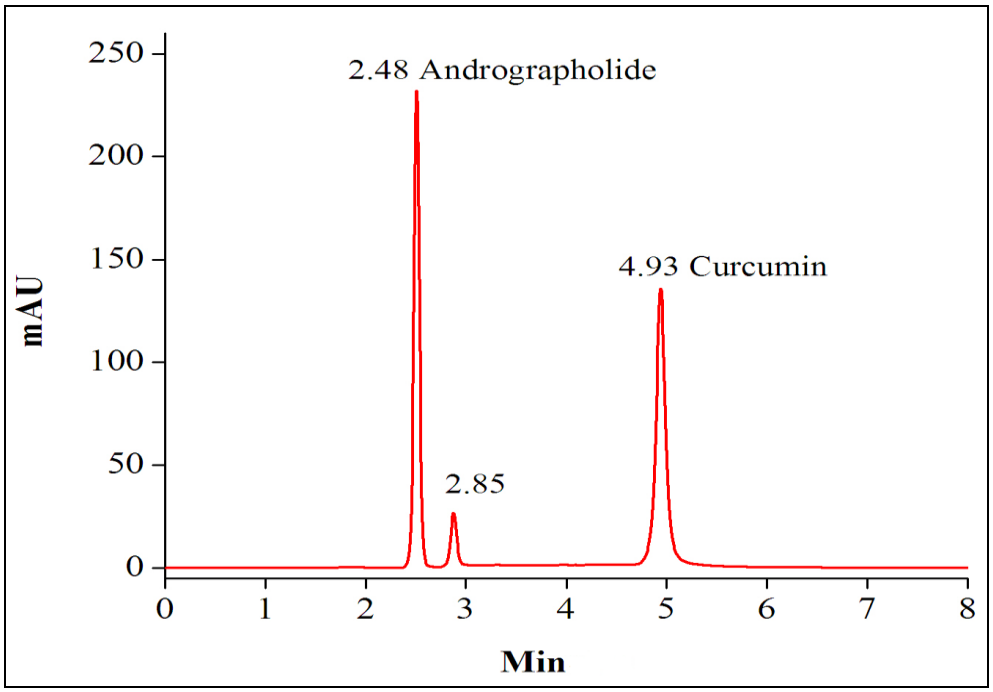

Figure 5.3: Optimised chromatogram of mixed Andrographolide and Curcumin standard

5.3.2 Method Validation

5.3.2.1 Specificity

Andrographolide and curcumin were eluted at 2.4 min and 4.9 min, respectively. The absence of interfering peaks from the NLC matrix is a piece of evidence for method specificity. Furthermore, andrographolide and curcumin peaks were well separated from the degradation products after different stress degradation studies.

5.3.2.2 Linearity

Regression equations for andrographolide and curcumin were found to be y = 42258 x + 1170 and y = 44390 x – 61969 , respectively. The linear concentration range was found to be 10 - 140 µg/ml with a value of 0.999 for the regression coefficient of both compounds. Calibration curves of andrographolide and curcumin are given in Fig. 5.4.

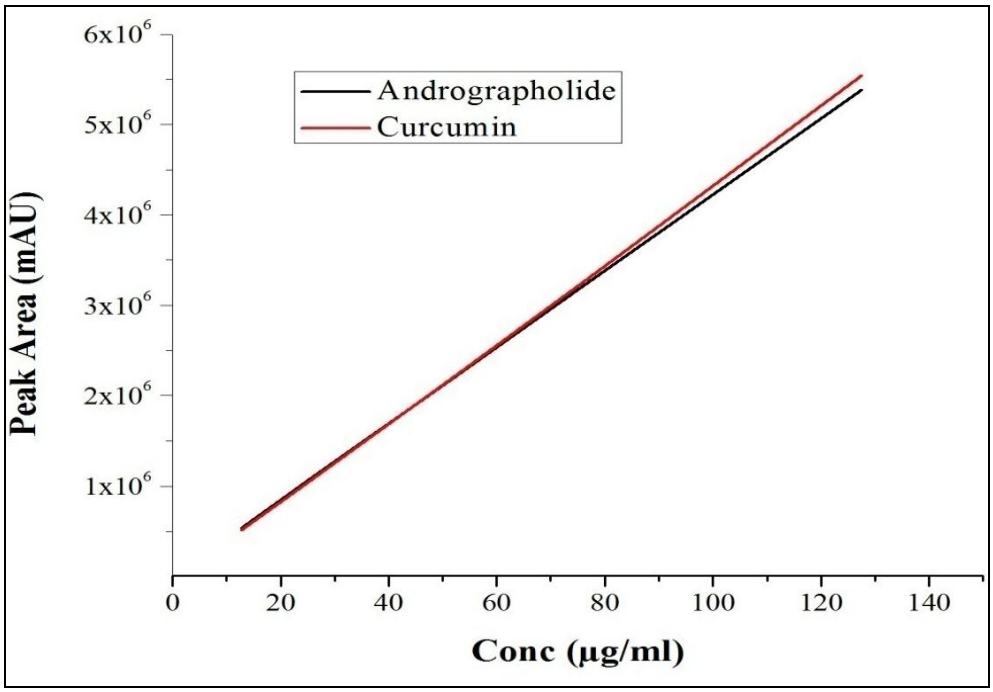

Figure 5.4: Calibration curve of standard Andrographolide and Curcumin

5.3.2.2 Accuracy

The mixed standard concentration of andrographolide and curcumin was considered to be 50 µg/ml. The overall % recovery was found to be in the range of 97.83 - 99.67 for both andrographolide and curcumin which indicated that the method was very accurate. Accuracy data for the andrographolide and curcumin are tabulated in Table 5.2.

Table 5.2 : Accuracy data by the proposed HPLC method

Drugs	Spiked level (%)	Spiked amount (mg)	Recovered amount (mg)	Recovery (%)	RSD* (%)
Andrographolide	80	8.3 ± 0.15	8.25 ± 0.12	99.39	0.82
	100	12.2 ± 0.25	12.16 ± 0.35	99.67	0.56
	120	15.4 ± 0.31	15.2 ± 0.21	98.70	0.31
Curcumin	80	8.40 ± 0.16	8.32 ± 0.17	99.04	0.45
	100	12.50 ± 0.33	12.4 5± 0.38	99.60	0.28
	120	15.50 ± 0.23	15.30 ± 0.25	98.70	0.61

*RSD –Relative Standard Deviation; All the values are presented as mean±SD, n=3

5.3.2.3 Precision

The relative standard deviation (%) of the same day (Intra) and another day (Inter) precision was found 0.085 - 0.520 for andrographolide and 0.128 - 0.625 for curcumin which was within the acceptable limit (RSD < 2 %). Precision results are summarised in Table 5.3 & 5.4.

Table 5.3: Intraday precision data by the proposed HPLC method

Drugs	Nominal concentration (µg/ml)	Recovered concentration (µg/ml)	Recovery (%)	Precision (Repeatability) %RSD
Andrographolide	12.5	12.12 ± 0.83	96.96 ± 1.02	0.120
	50	49.19 ± 0.75	98.38 ± 0.87	0.085
	125	124.36 ± 0.91	99.48 ± 0.16	0.096
Curcumin	12.5	12.21 ± 0.68	97.68 ± 0.92	0.312
	50	49.15 ± 0.71	98.30 ± 0.65	0.520
	125	124.22 ± 0.57	99.37 ± 0.35	0.136

RSD –Relative Standard Deviation; All the values are presented as mean ± SD, n=6

Table 5.4 : Interday precision data by the proposed HPLC method

Drugs	Nominal concentration (µg/ml)	Recovered concentration (µg/ml)	Recovery (%)	Precision (Repeatability) % RSD
Andrographolide	12.5	11.85 ± 0.52	94.80 ± 0.89	0.231
	50	48.92 ± 0.67	97.84 ± 1.03	0.128
	125	123.72 ± 0.83	98.97 ± 0.50	0.625
Curcumin	12.5	11.72 ± 0.49	93.76 ± 0.78	0.505
	50	48.73 ± 0.78	97.46 ± 0.69	0.212
	125	123.56 ± 0.62	98.84 ± 0.32	0.150

RSD –Relative Standard Deviation; All the values are presented as mean ± SD, n=6

5.3.2.4 LOD and LOQ

The LOD for andrographolide and curcumin were found 0.128 µg/ml and 1.008 µg/ml respectively. The LOQ were found 0.323 µg/ml for andrographolide and 3.054 µg/ml for curcumin, respectively.

5.3.2.5 Robustness

Robustness was determined by intentional modifications in method parameters like change in the rate of flow (± 0.1 ml/min), wavelength detection (± 2 nm), column oven temperature (± 2 ºC), buffer: acetonitrile ratio and pH of buffer (± 0.1 unit) used in the mobile phase were done. The acquired result showed that the percent of relative standard deviation (% RSD) values (< 2) remained within the acceptable limit which indicates the developed HPLC method is highly robust. The obtained robustness results are presented in Table 5.5.

Table 5.5: Robustness parameter of the proposed HPLC method

Parameters	% RSD of the area of andrographolide	% RSD of area of curcumin
A. Change in buffer pH of mobile phase		
2.9	0.061	0.052
3.0	0.081	0.521
3.1	0.056	0.610
B. Change in mobile phase composition (Buffer : Acetonitrile) (% v/v)		
48:52	0.136	0.196
50:50	0.142	0.256
52:48	0.164	0.604
C. Change in UV detector wavelength (nm)		
238	0.100	0.136
240	0.164	0.325
242	0.098	0.360
D. Change in flow rate (ml/min) of mobile phase		
1.4	0.053	0.024
1.5	0.125	0.226
1.6	0.035	0.258
E. Change in column oven tempt (°C) of mobile phase		
33	0.109	0.458
35	0.131	0.316
37	0.047	0.859

RSD –Relative Standard Deviation; All the values are presented as mean±SD, n=3

5.3.2.6 System suitability

The resolution was found from mixed standards solution of andrographolide and curcumin to be 17.78 ± 0.03 which specified the good separation of two peaks. The tailing factor was found to be 1.02 ± 0.02 and 1.01± 0.01 for andrographolide and curcumin which represents the peaks were symmetric. According to chromatographic peak results, the developed analytical method satisfies the criteria for system suitability [Chaudhari et al, 2020]. The system suitability parameters are given in Table 5.6.

Table 5.6: System suitability parameters of the validated analytical HPLC method

Parameters	Andrographolide (Mean ± SD)	Curcumin (Mean ± SD)
Retention time	2.4 ± 0.05	4.9 ± 0.06
Theoretical plates/meter	9344 ± 120	12628 ± 114
Tailing factor	1.02 ± 0.02	1.01 ± 0.01
Resolution	-	17.78 ± 0.03
Injection precision	0.089 ± 0.03	0.07 ± 0.04

SD -Standard Deviation; All the values are presented as mean ± SD, n=6

5.3.2.7 Forced degradation studies

The percentage recovery from degradation study of andrographolide and curcumin after forced conditions are given in Table 5.7.

Table 5.7: % Recovery and degradation of andrographolide and curcumin after stress conditions

Stress conditions	Recovery (%) (± SD)		Degradation (%) (± SD)	
	Andrographolide	**Curcumin**	**Andrographolide**	**Curcumin**
Acidic	94.99 ± 0.59	83.42 ± 1.21	5.01 ± 2.1	16.58 ± 0.95
Alkali	18.40 ± 0.12	24.37 ± 0.67	81.60 ± 0.36	75.63 ± 1.07
Peroxide	85.83 ± 0.89	81.30 ± 1.09	14.17 ± 1.53	18.7 ± 0.88
Photolytic	100.06 ± 0.22	99.12 ± 0.36	0 ± 0.17	0.88 ± 0.29
UV light	100.67 ± 0.35	97.55 ± 0.88	0 ± 0.35	2.45 ± 0.51
Thermal	99.05 ± 0.11	99.28 ± 0.30	0.95 ± 0.16	0.72 ± 0.23

SD -Standard Deviation; All the values are presented as mean ± SD, n=3

Andrographolide was degraded by 0.1 (N) HCl (assay 94.99 %), 5 % v/v H_2O_2 (assay 85.83 %) and 0.1 (N) NaOH solution(assay 18.40 %).

Acid degradation of andrographolide produced nearly one degradation product, base degradation produced nearly two degradation products, peroxide degradation produced nearly two degradations, and thermal degradation produced about one degradation product.

Curcumin was found to be degraded by 0.1 (N) HCl (assay 83.42%), 5 % v/v H_2O_2 (assay 81.3 %) and 0.1 (N) NaOH solution (assay 24.37 %) and UV light (97.55 %) under all stressed conditions.

Acid degradation of curcumin produced about two degradation products, base degradation produced about three degradation products, peroxide degradation produced about two degradation products, photolytic degradation produced one degradation product and UV degradation produced one degradation product.

The UV absorption maxima of each degradation product of standard andrographolide and curcumin were produced at the specified retention time and determined by the HPLC with PDA detector. The retention time and UV absorption maxima of each degradation product produced by degradation studies are represented in Table 5.8.

Table 5.8: Retention time and UV absorption maxima of degradation products of andrographolide and curcumin after stress conditions

Stress conditions	**Degradation products RT (min)**		**Degradation products λ_{max} (nm)**	
	Andrographolide	**Curcumin**	**Andrographolide**	**Curcumin**
Acidic	2.10	2.59	228	336
	-	3.43	-	376
Alkali	1.79	1.46	220	330
	4.53	1.75	234	232
	-	1.97	-	336
Peroxide	3.51	2.26	230	322
	7.34	2.53	220	268
Photolytic	-	4.07	-	302
UV light	-	2.17	-	236
Thermal	3.51	-	252	-

RT - Retention time; λ_{max} - UV absorption maxima; nm – Nanometer

The HPLC chromatograms after forced degradation are represented in Fig. 5.5 -5.16, respectively.

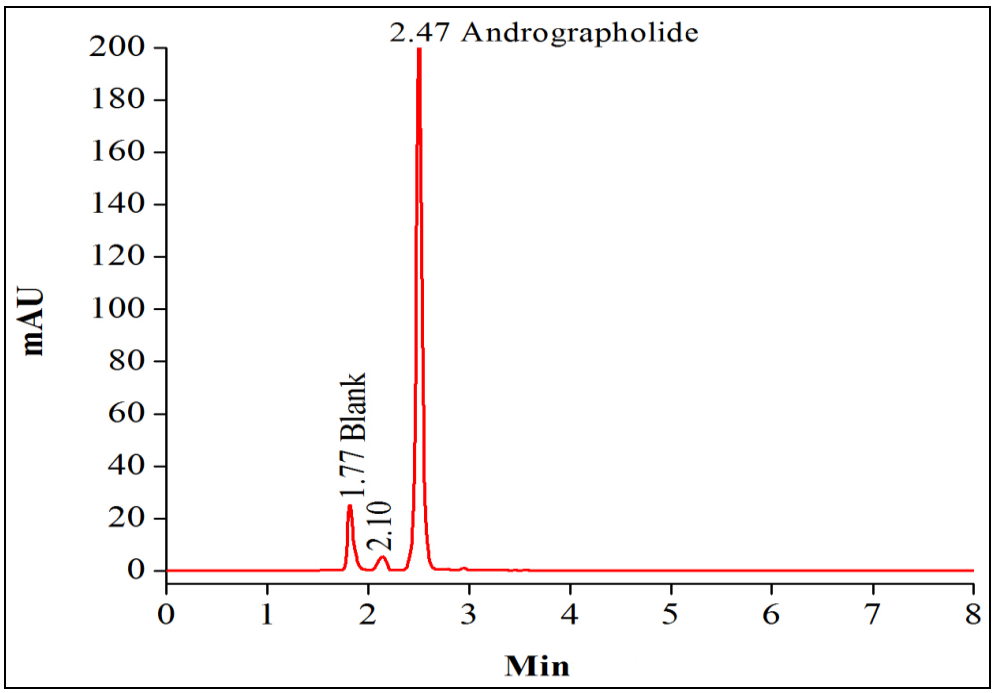

Figure 5.5: Forced degradation of standard Andrographolide in 0.1(N) HCl

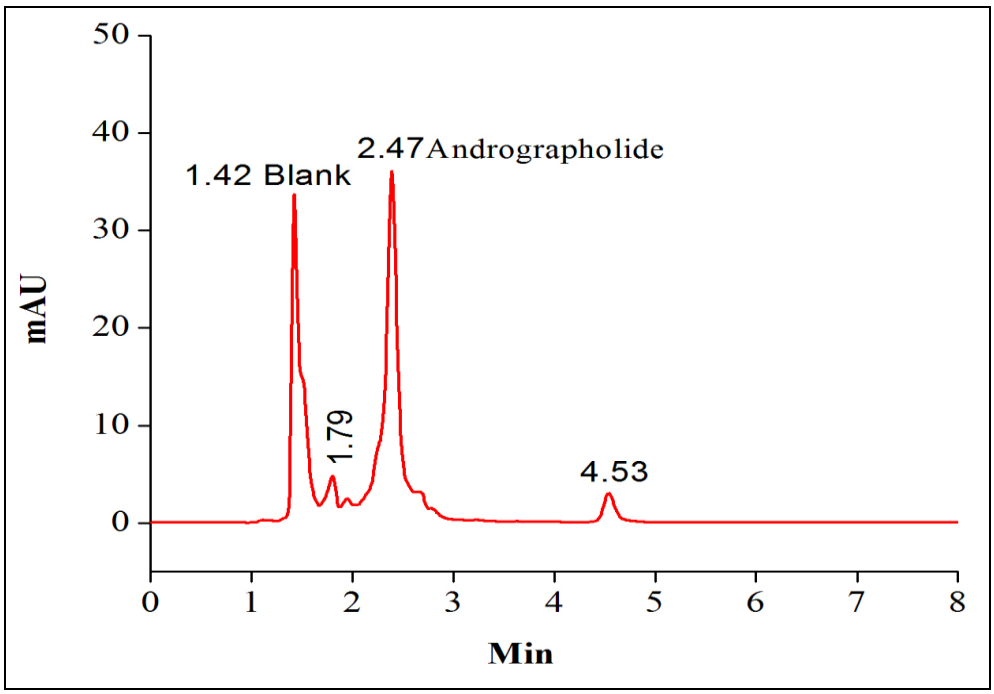

Figure 5.6: Forced degradation chromatogram of standard Andrographolide in 0.1(N) sodium hydroxide

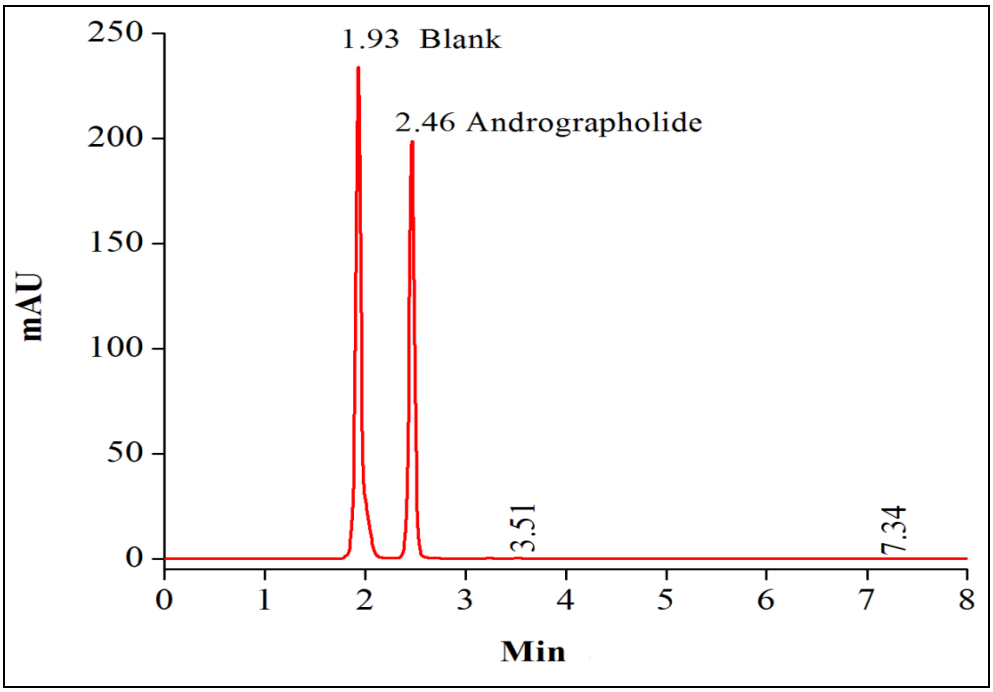

Figure 5.7: Forced degradation chromatogram of standard Andrographolide in 5 % v/vhydrogen peroxide

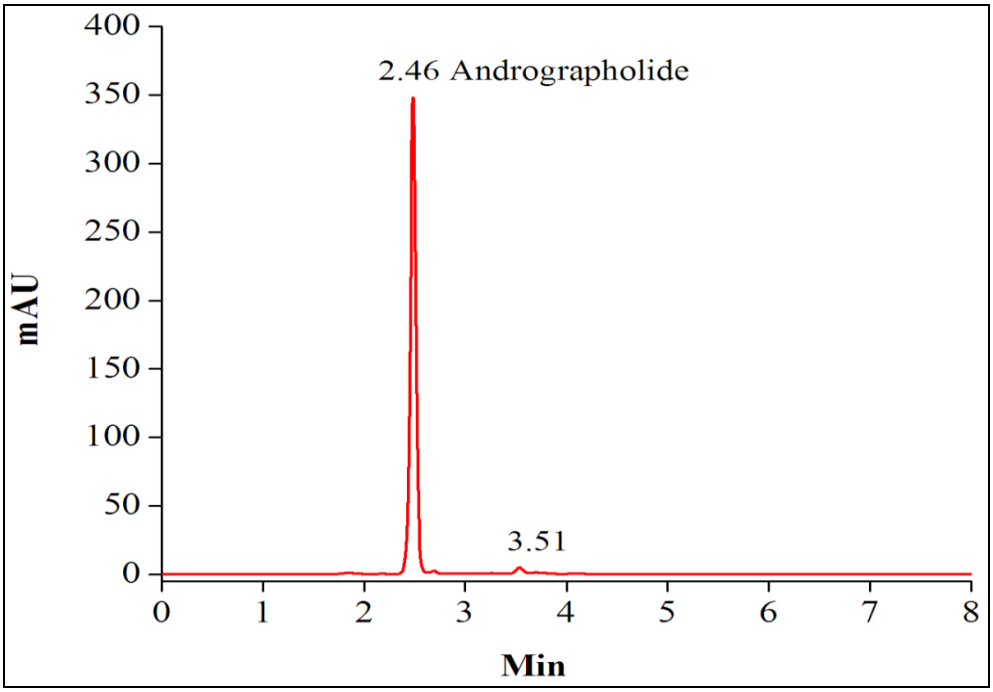

Figure 5.8: Forced degradation chromatogram of standard Andrographolide in heat

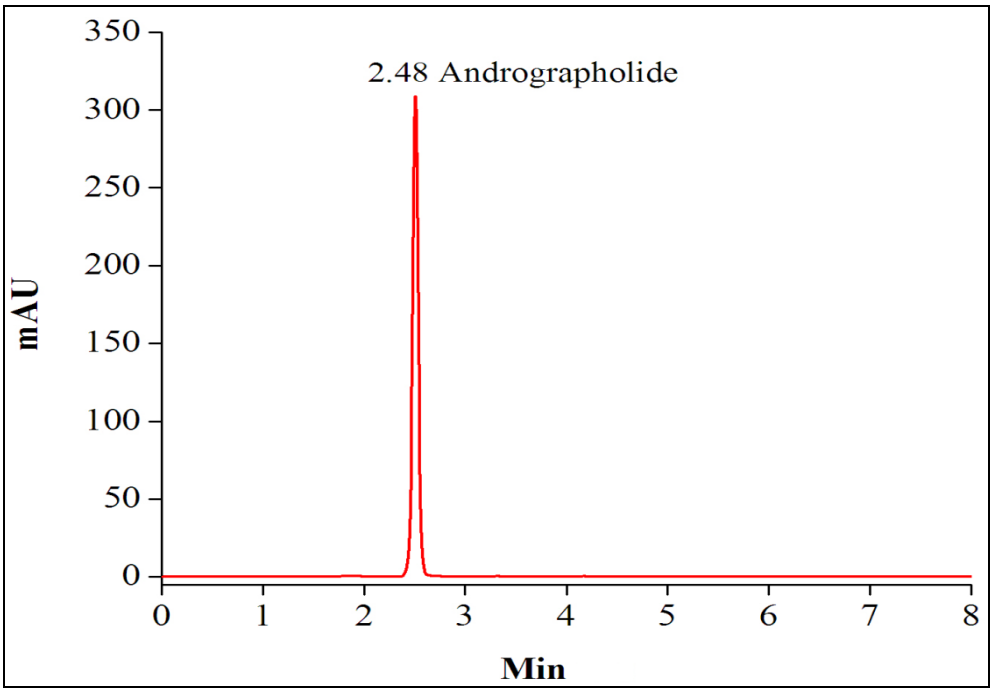

Figure 5.9: Forced degradation chromatogram of standard Andrographolide in photolytic

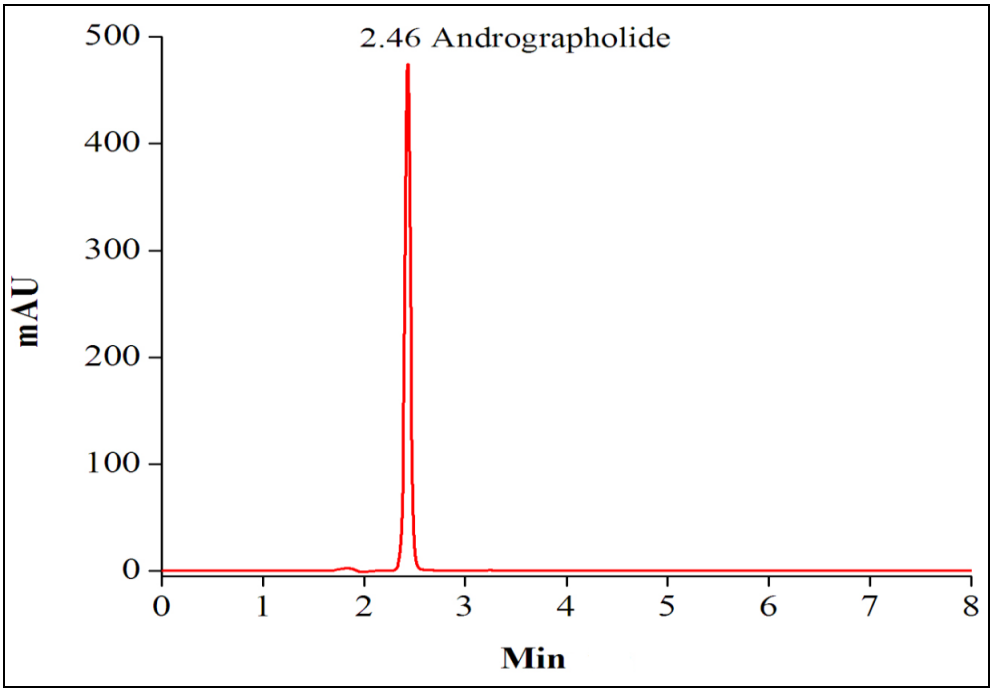

Figure 5.10: Forced degradation chromatogram of standard Andrographolide in UV light

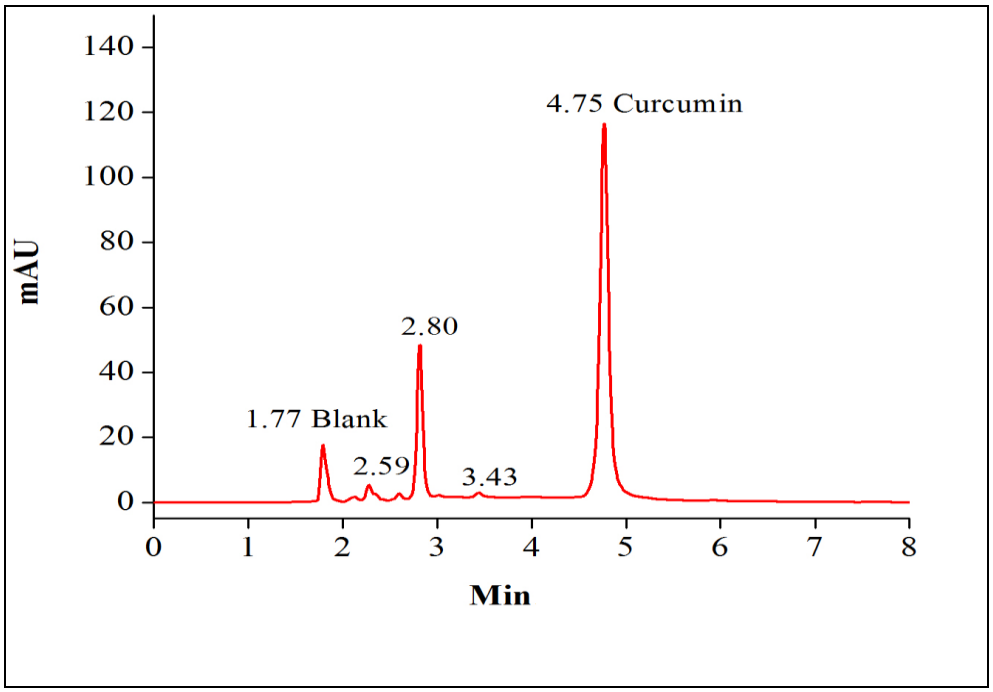

Figure 5.11: Forced degradation chromatogram of standard Curcumin in 0.1(N) HCl

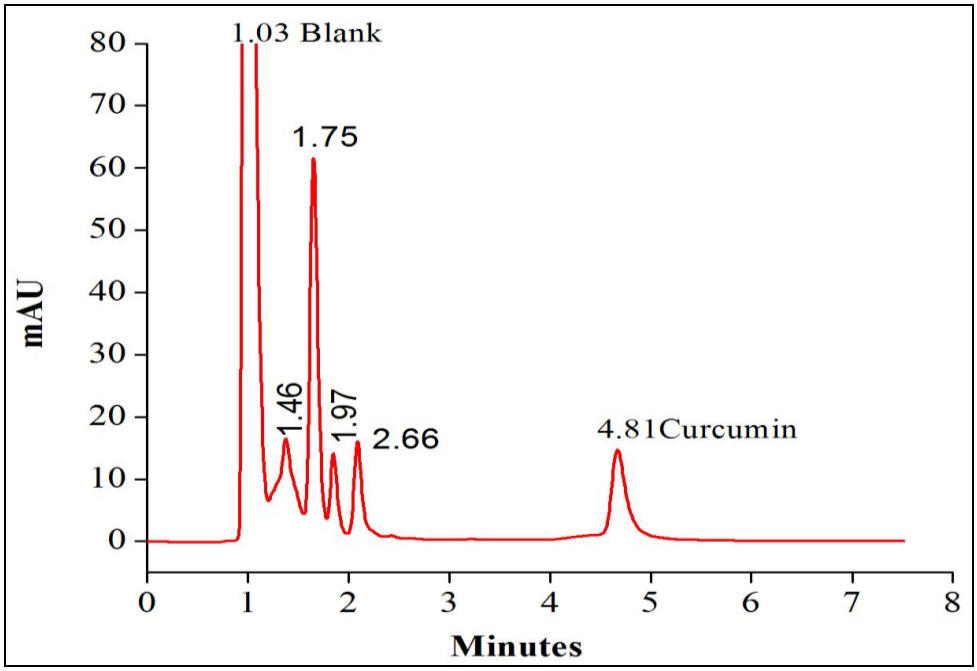

Figure 5.12: Forced degradation chromatogram of standard Curcumin in 0.1(N) sodium hydroxide

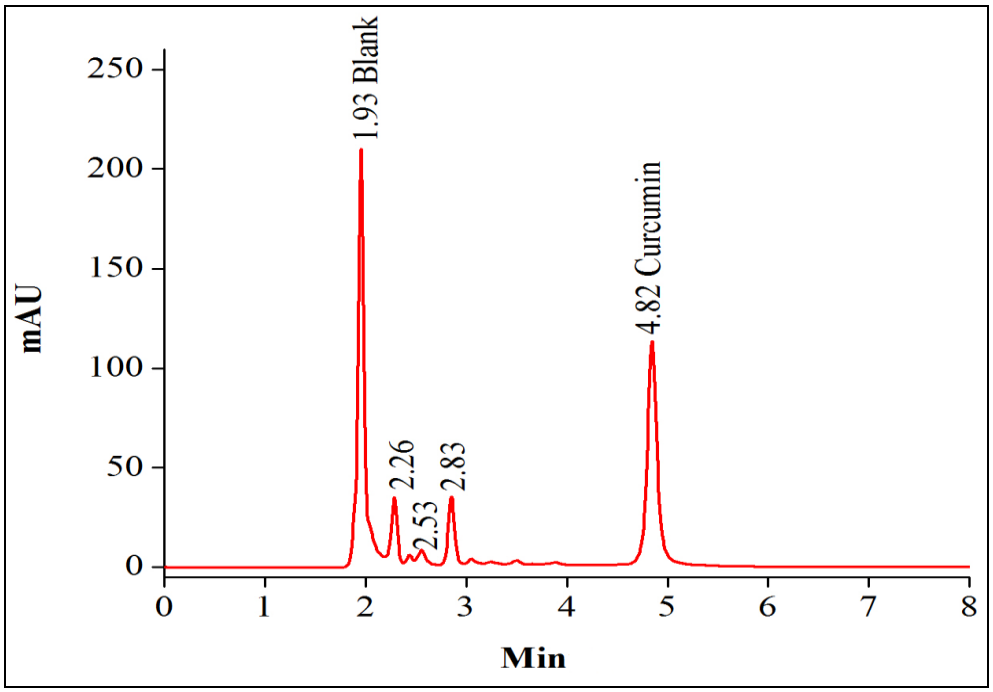

Figure 5.13: Forced degradation chromatogram of standard Curcumin in 5 % v/v hydrogen peroxide

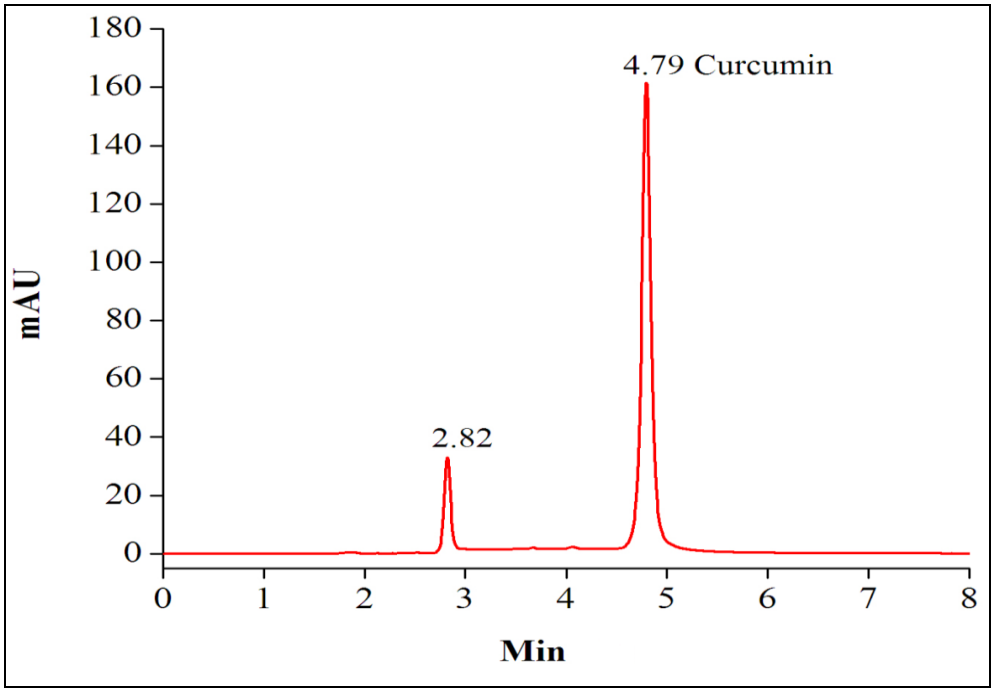

Figure 5.14: Forced degradation chromatogram of standard Curcumin in heat

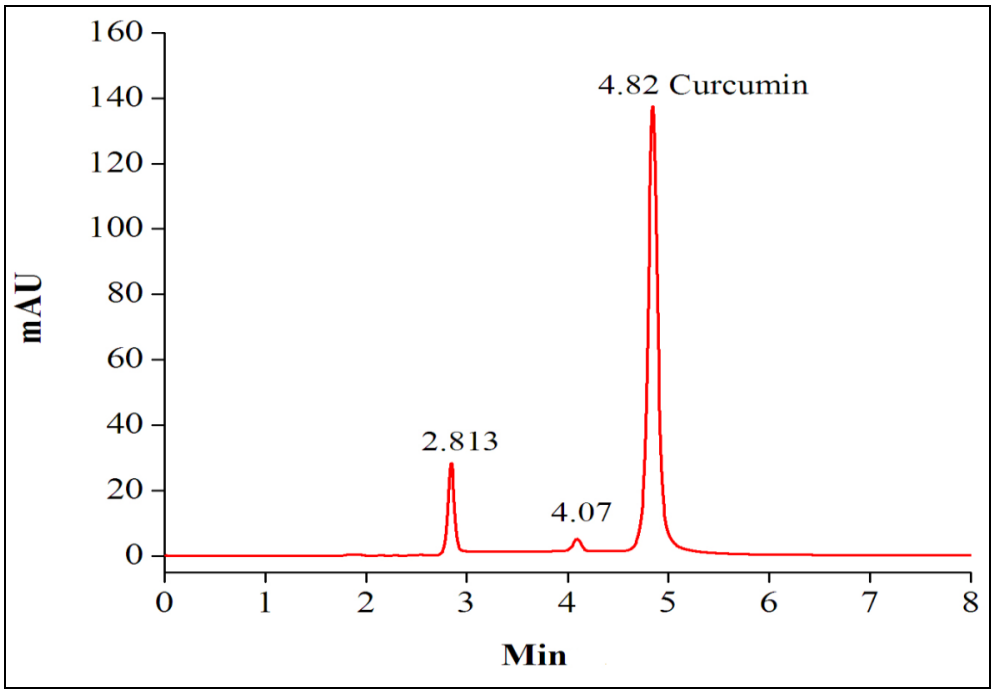

Figure 5.15: Forced degradation chromatogram of standard Curcumin in photolytic

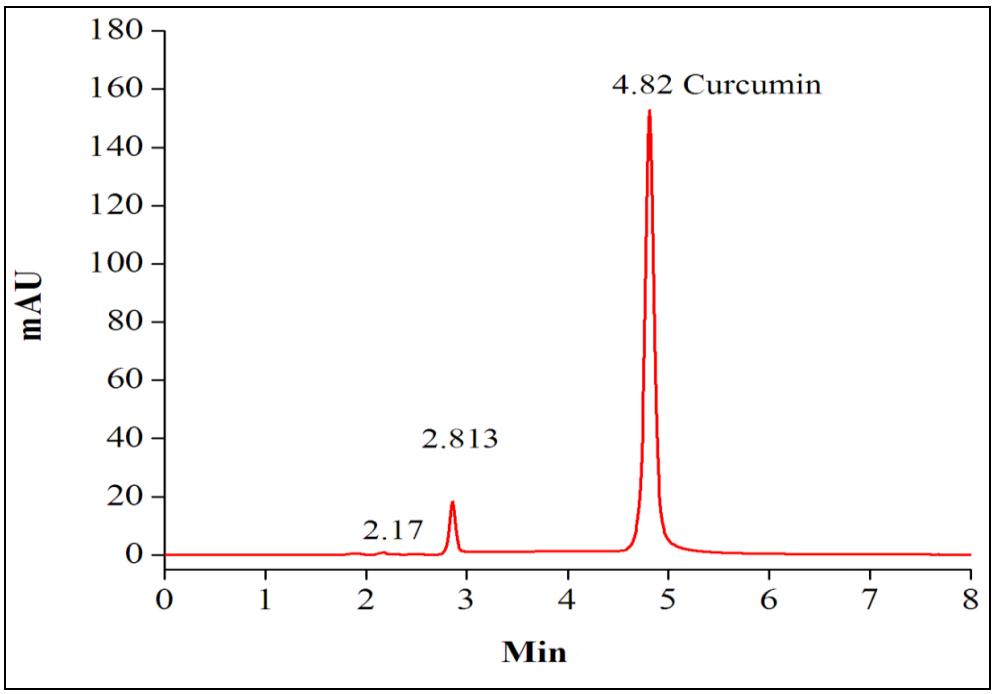

Figure 5.16: Forced degradation chromatogram of standard Curcumin in UV light

Physicochemical characterization of nanoparticles

5.4 Particle size, polydispersity index, zeta potential, drug loading(%) and entrapment efficiency (%) of curcumin-chitosan nanocomplex (CCN)

The mean particle size of the prepared curcumin-chitosan nanocomplex (CCN) formulations of A and B were found 204.5± 1.2 nm and 215.3 ± 1.6 nm respectively. The mean polydispersity index (PDI) was found at 0.149 and 0.242. The zeta potential was observed (-) 21.6 ± 1.1 and (-) 14.98 ± 1.3 respectively. Formulation A was found higher drug loading and entrapment efficiency so it was used for further experiment.

Table 5.9 :Characterization of CCN by Avg. particle size,Zeta Potential,PDI, drug loading and entrapment efficiency.

Formulations	Avg. Particle Size (nm)*	Zeta Potential (mV)*	PDI	%DL*	% EE*
A	204.5± 1.2	(-) 21.6 ± 1.1	0.149	37.58 ± 0.2	91.32 ± 0.3
B	215.3 ± 1.6	(-) 14.98 ± 1.3	0.242	34.32 ± 0.3	85 ± 0.5

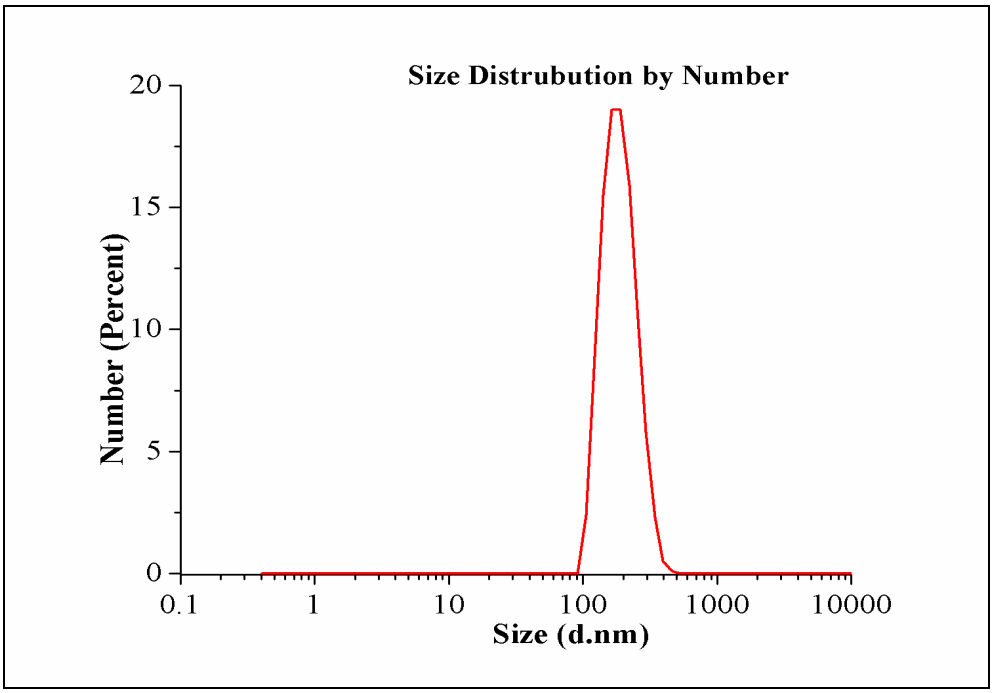

Figure 5.17: Particle Size of CCN sample A

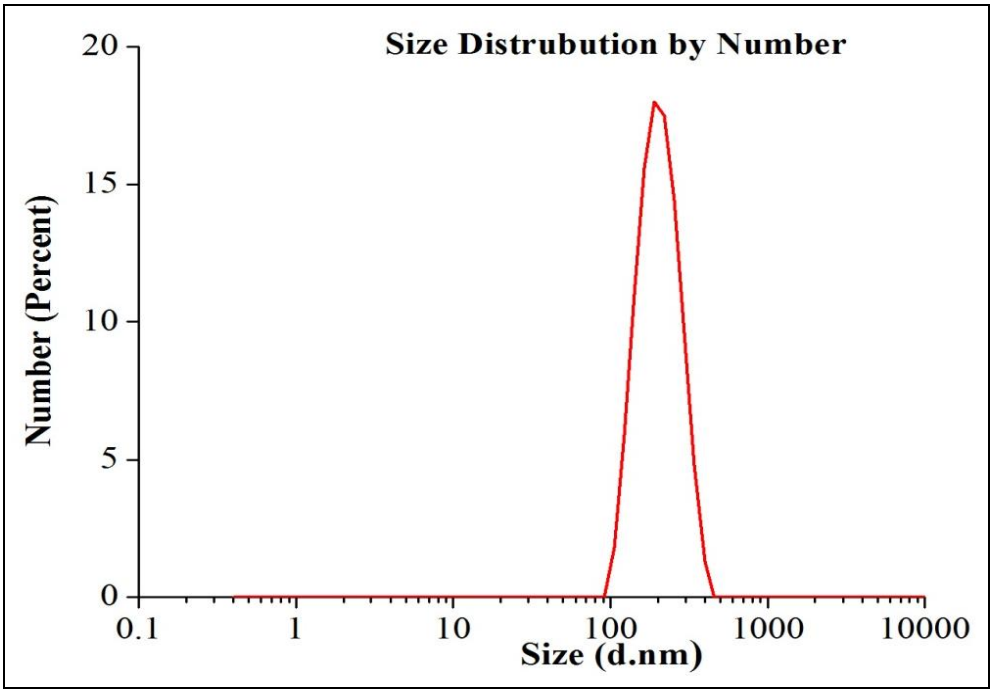

Figure 5.18: Particle Size of CCN sample B

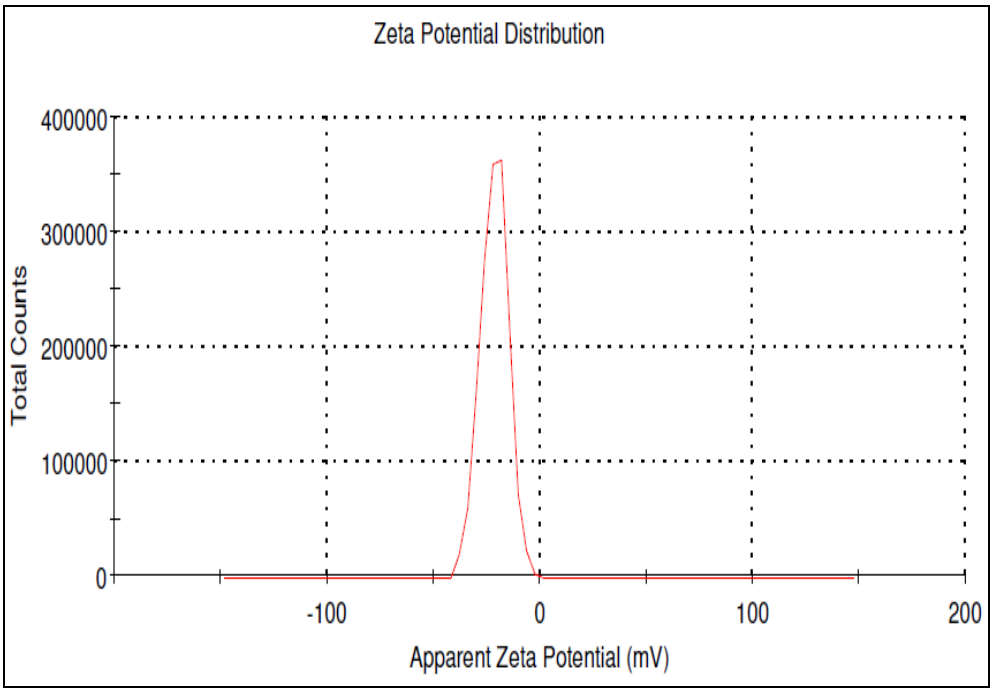

Figure 5.19: Zeta potential of CCN sample A

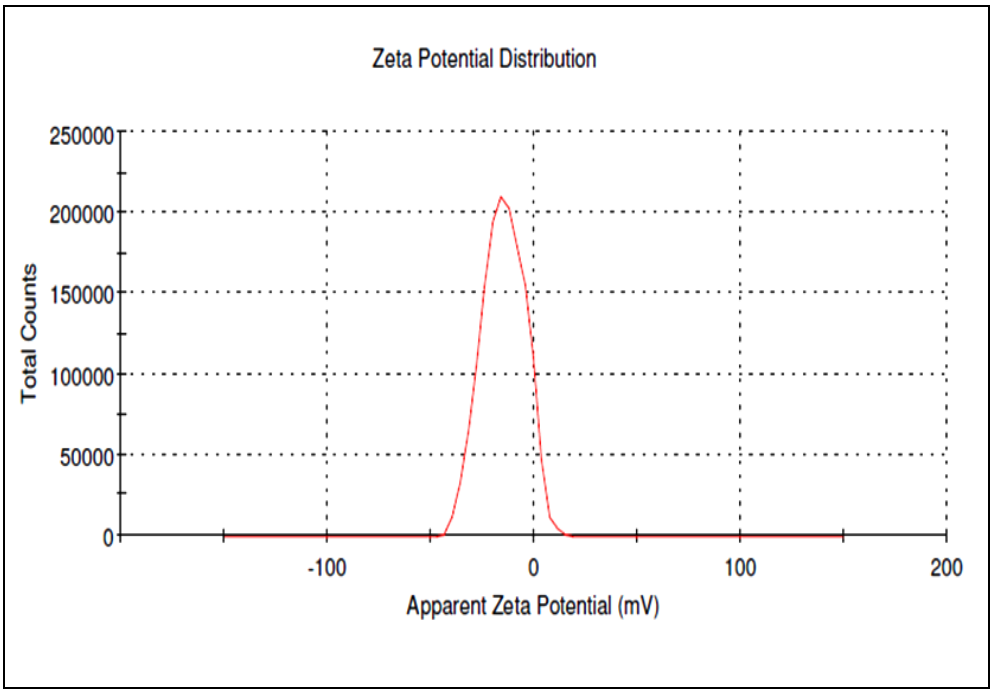

Figure 5.20: Zeta potential of CCN sample B

5.5 Particle size, polydispersity index, zeta potential, drug loading(%), and entrapment efficiency (%) of AG-CMN-NLC

The effect of the drug-lipid ratio on the physical parameters of nanoparticles was determined in terms of particle size, polydispersity index, and zeta potential.

The mean particle size of the prepared combined drug-loaded formulations of F1 and F2 were found 145.6 ± 4.1 nm and 98.32± 3.2 nm respectively. The mean polydispersity index (PDI) were found 0.233 and 0.288 respectively.The zeta potential were observed (+) 18.3 ± 2.2 and (+) 6.64 ± 1.5 respectively.Formulation F1 was found larger particle size due to higher drug loading.

Table 5.10: The average particle size, zeta potential,polydispersity index, drug loading(%) and entrapment efficiency (%) of AG-CMN nanoparticles.

Formulations	**Avg. Particle Size (nm)***	**Zeta Potential (mV)***	**PDI**	**%DL***		**% EE***	
				AG	**CMN**	**AG**	**CMN**
F1	145.6 ±4.1	(+) 18.3 ± 2.2	0.233	19.21 ± 0.5	18.12 ± 0.2	91.63 ± 0.5	90.56 ± 0.4
F2	98.32 ±3.2	(+) 6.64 ± 1.5	0.288	17.52± 0.3	16.93 ± 0.3	89.56 ± 0.6	83.52 ± 0.7

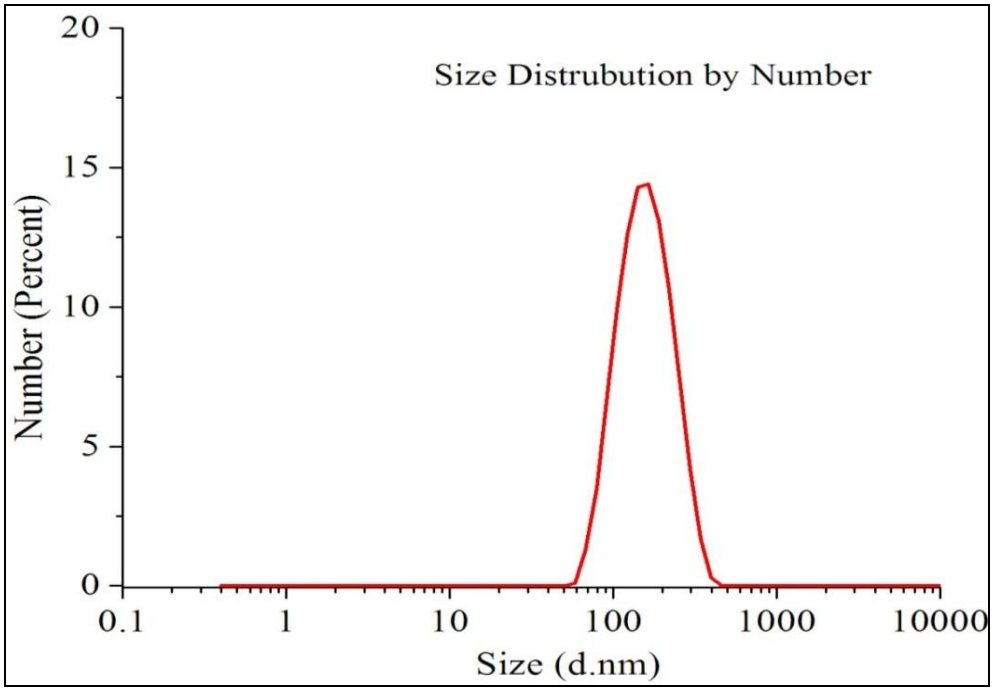

Figure 5.21: Particle Size of AG-CMN nanoparticle sample F1

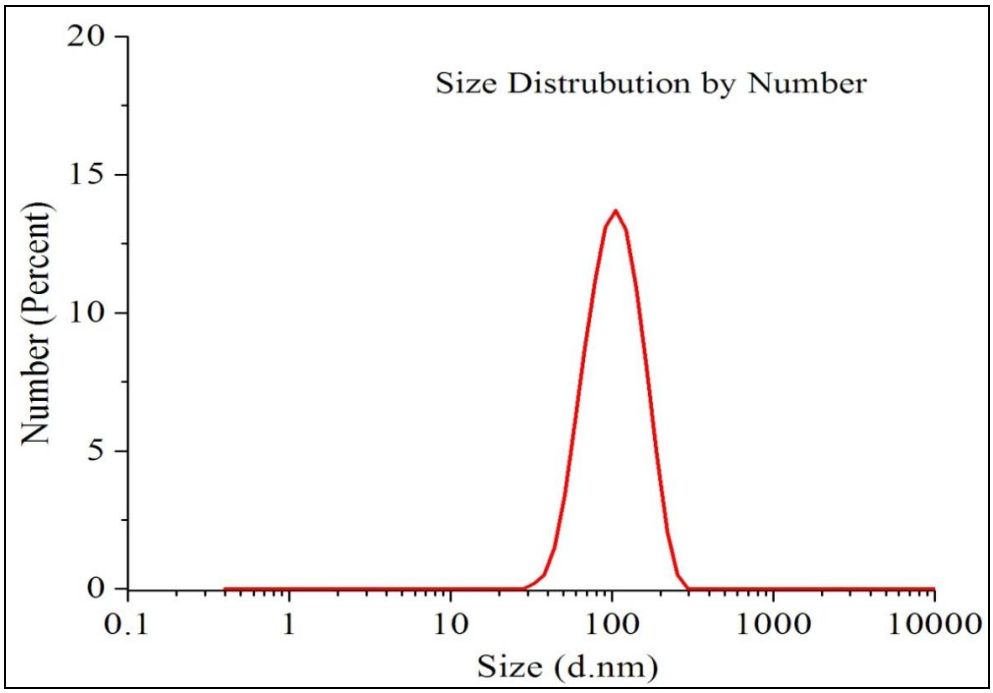

Figure 5.22: Particle Size of AG-CMN nanoparticle sample F2

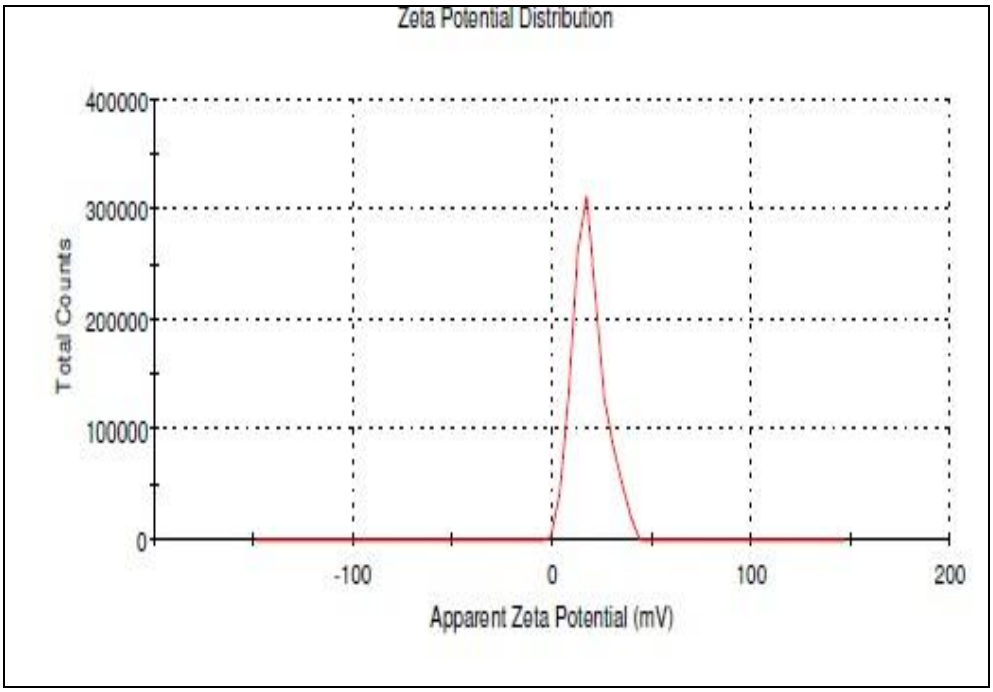

Figure 5.23: Zeta potential of AG-CMN nanoparticle sample F1

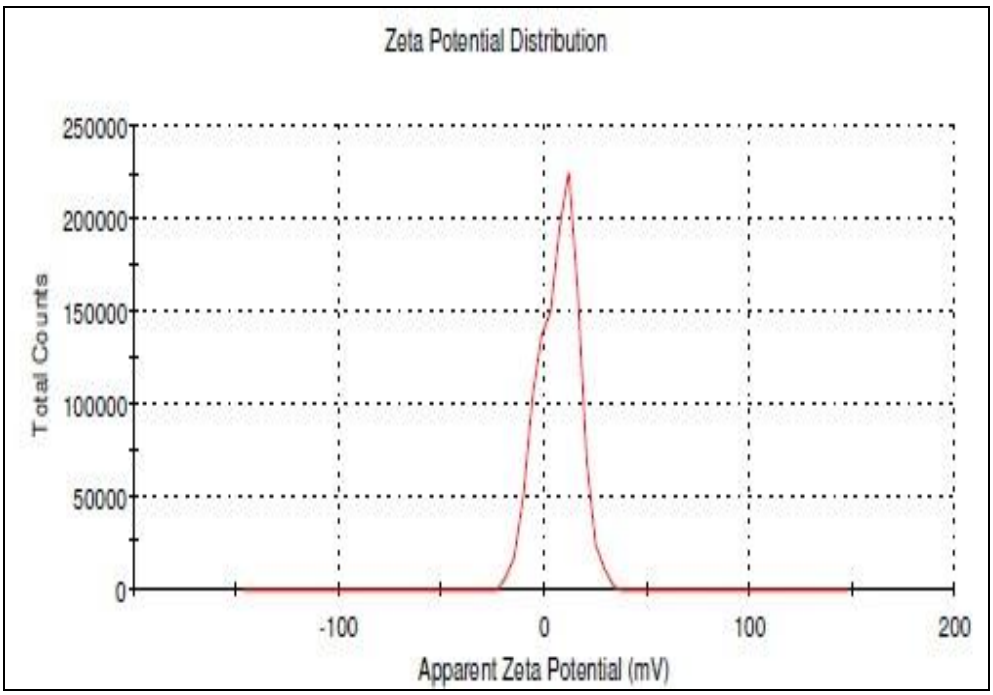

Figure 5.24: Zeta potential of AG-CMN nanoparticle sample F2

5.6 Drug loading and Drug Entrapment Efficiency of AG- NLC, and CMN-NLC

The drug loading of AG-NLC and CMN-NLC were found 18.32 ± 0.4 and 17.71 ± 0.5. The entrapment efficiency of AG- NLC, and CMN-NLC were found 82.45 ± 0.3 and 81.87 ± 0.2.

5.7 FESEM

Surface morphology property of CHI-CMN nanocomplex, combined drug-loaded nanoparticles, and blank nanoparticles was obtained from FESEM instrumental study. The combined drug-loaded NLCs were spherical and nano-size range.No drug particles were observed from blank nanoparticles of FESEM image picture. The FESEM picture of AG-CMN NLC, blank nanoparticles, and CHI-CUR nanocomplex are shown in Fig. 5.25, 5.26 & 5.27.

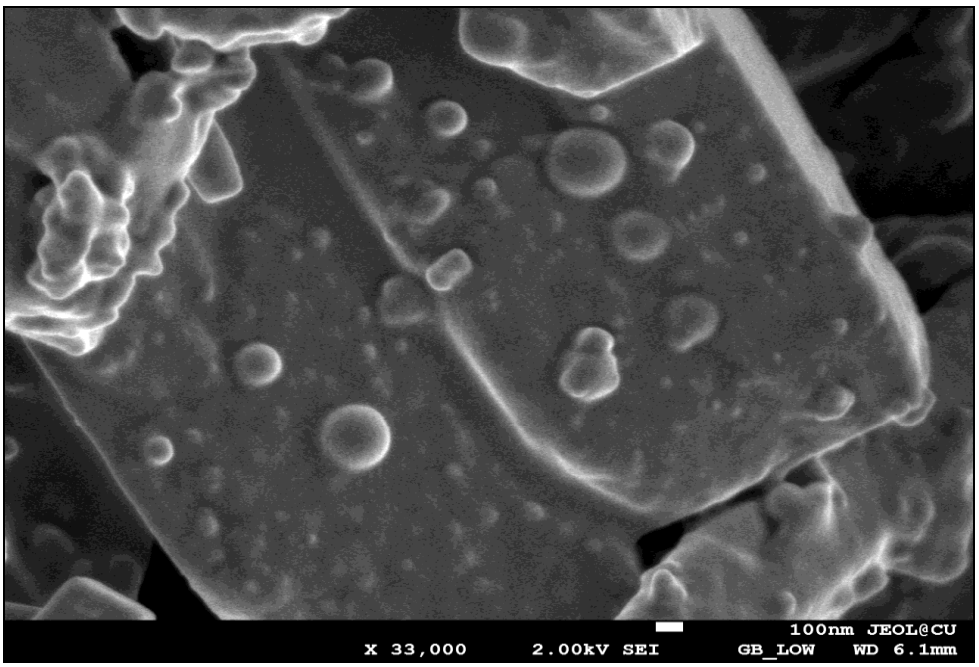

Figure 5.25: The FESEM picture of CCN nanoparticles

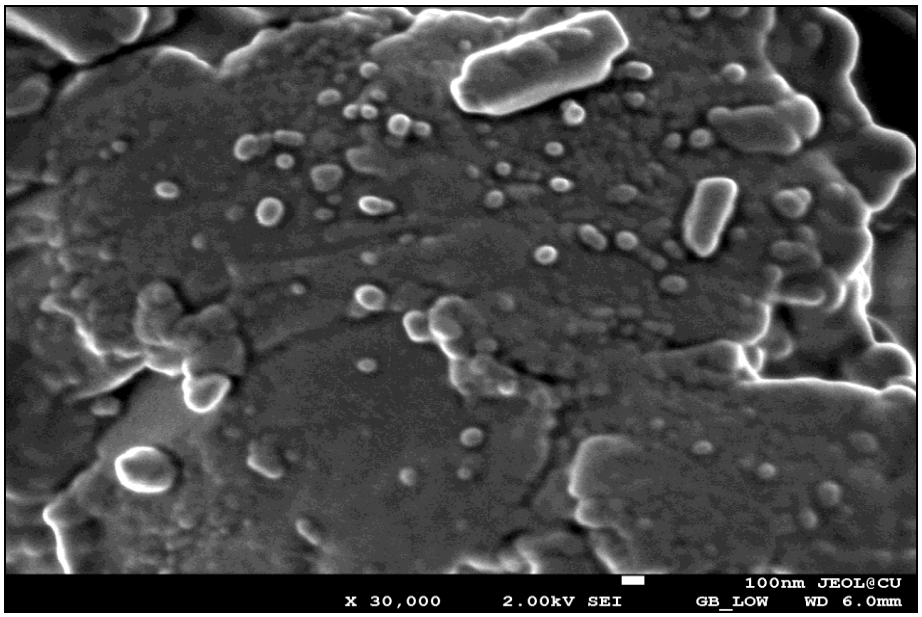

Figure 5.26: The FESEM picture of AG-CMN nanoparticle

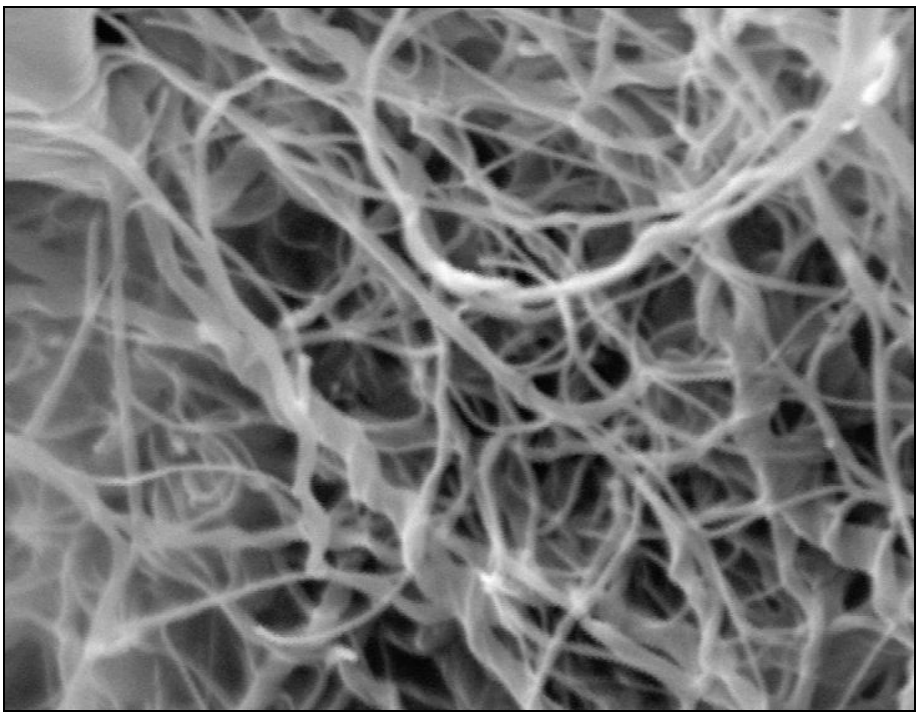

Figure 5.27: The FESEM picture of blank nanoparticle

5.8 Transmission electron microscopy (TEM)

The diameters of nanoparticles were observed by TEM as shown in Fig. 5.28. The nanoparticles were confirmed with a spherical shape, distinct and dense structure of TEM images.

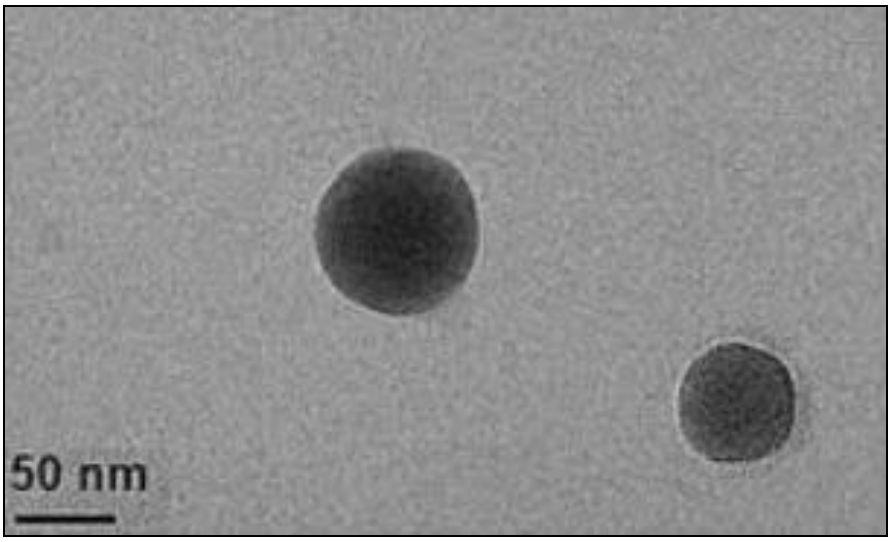

Figure 5.28: The TEM picture of AG-CMN nanoparticle

5.9 FTIR study

FTIR spectra of the physical mixture, blank nanoparticles, pure andrographolide, pure curcumin, and combined drug-loaded formulation are represented in Fig.5.29. The spectrum of pure andrographolide shows C=O stretching frequency for lactone ring at 1720.5 cm^{-1}, C=C conjugated stretching frequency at 1674.21 cm^{-1},-OH stretching frequency for the alcoholic group was observed at 3371 cm^{-1}, -OH bending vibration is present at 1414.85 cm^{-1}, primary and secondary alcoholic groups have appeared at 1029.99 cm^{-1} and 1076.12 cm^{-1} respectively. The spectrum of curcumin shows C=O stretching vibration at 1627.92 cm^{-1}, C=C stretching at 1600.92 cm^{-1}, C-O-C ether linkage at 1111.00 cm^{-1}, C-OH stretching at 1026.13 cm^{-1}, and C-OH stretching for the alcoholic group at 3282.84 cm^{-1}. All the frequencies shown in pure drugs were present in combined drug-loaded nanoparticles. So, it is proved that andrographolide and curcumin both are present in combined drug-loaded nanoparticles.

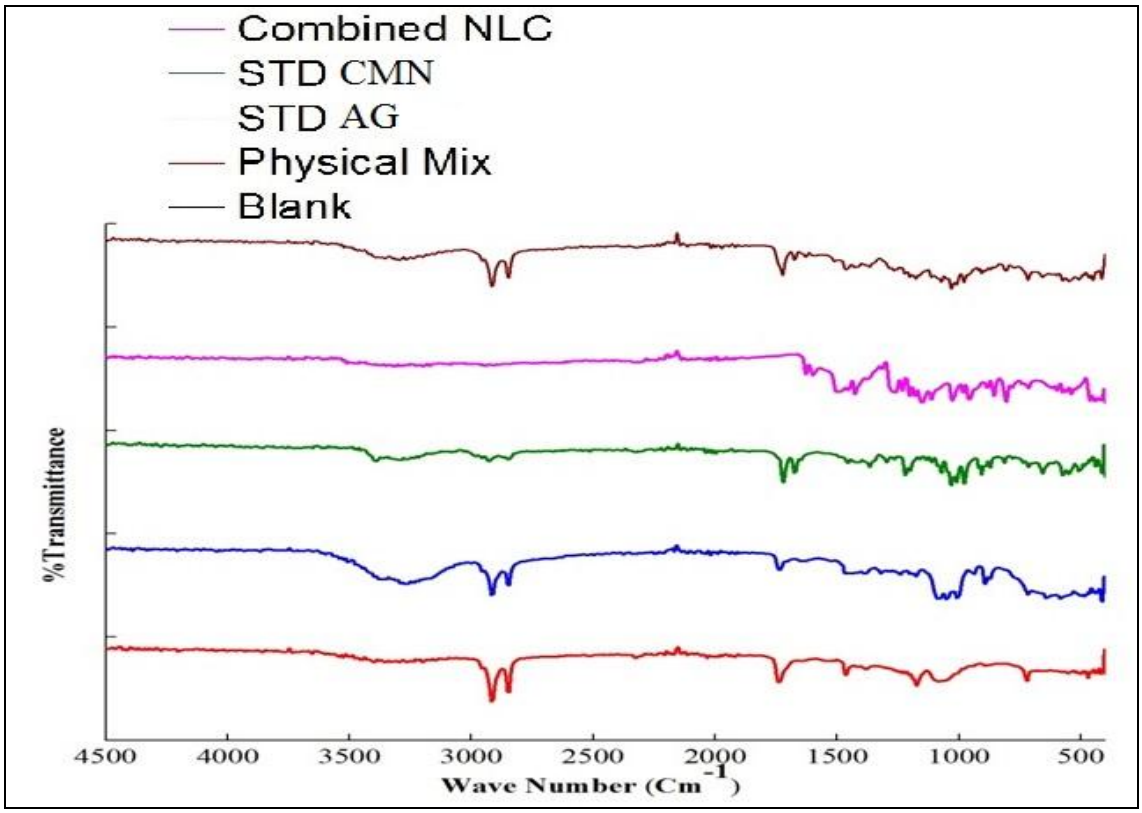

Figure 5.29: FTIR analysis of drug-excipient interactions

5.10 Differential scanning calorimetry (DSC) study

Differential scanning calorimetry(DSC) is a thermoanalytical technique. DSC curves of the physical mixture, blank nanoparticles, pure andrographolide, pure curcumin, and combined drug-loaded formulation are represented in Fig. 5.30. The sharp endothermic peak was found at the melting point of pure andrographolide at 230°C and curcumin at 183°C respectively due to the crystalline form of compounds. Blank nanoparticle and physical mixture show the same thermal behavior. But the thermal behavior of combined drug-loaded nanoparticles showed different from the physical mixture, blank nanoparticles, and pure drugs, and no such sharp endothermic peaks were observed due to the change of amorphous nature of drugs in the prepared formulation. The melting homogenization process has prevented the recrystallization of andrographolide and curcumin. The absence of a redundant endothermic peak in NLC suggests that there is

homogenous encapsulation of andrographolide and curcumin inside the AG-CMN NLC.

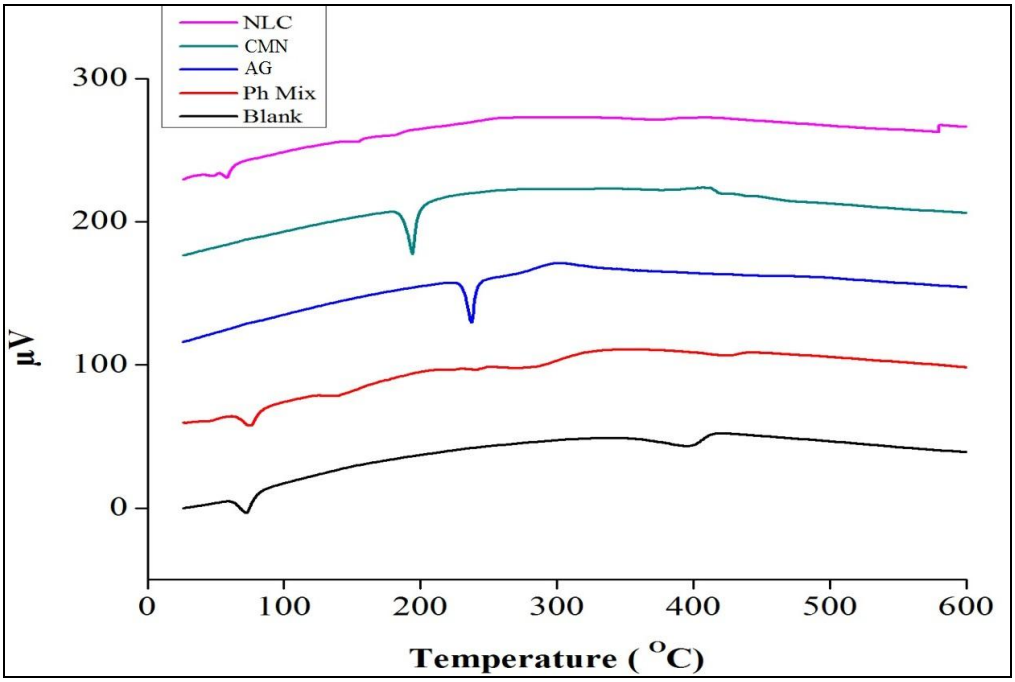

Figure 5.30: DSC analysis for depiction of drug-excipient interactions

5.11 XRD Study

XRD patterns of the physical mixture, blank nanoparticles, pure andrographolide, pure curcumin, and combined drug-loaded formulation are shown in Fig. 5.31. The diffraction pattern of the pure drug showed sharp and intense peaks due to crystallinity in nature. Whether the reduction of such sharp and intense peaks was observed for blank nanoparticles and combined drug-loaded nanoparticles. The results clearly showed that the crystallinity of drugs changed to an amorphous state due to the entrapment of drugs in the NLC matrix.

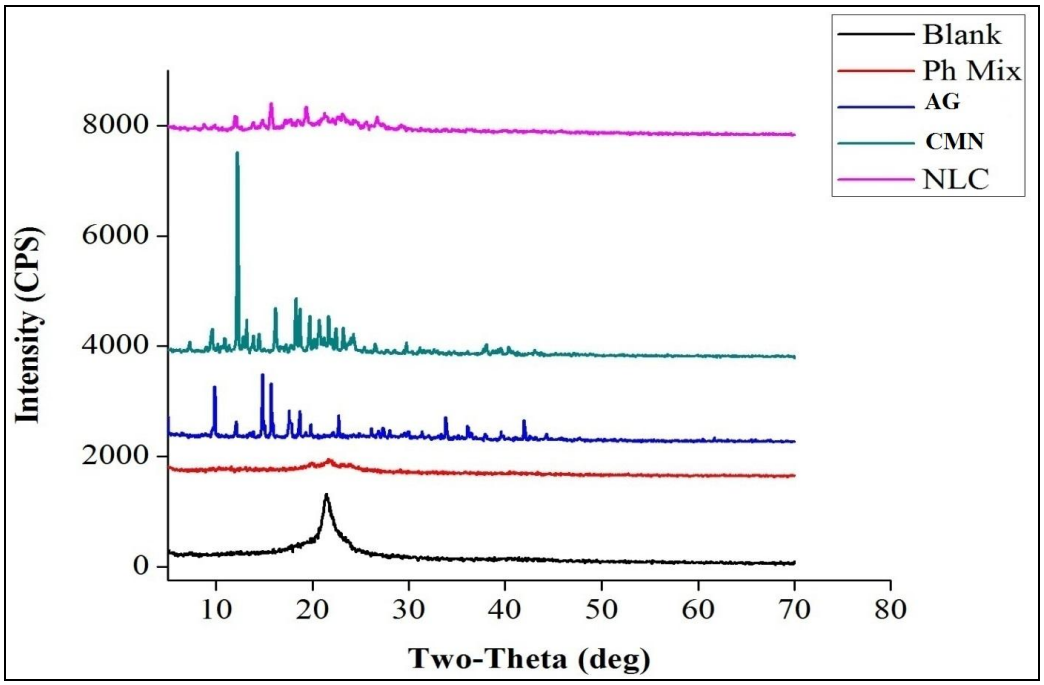

Figure 5.31: XRD analysis of drug-excipient interactions

5.12 Stability study of AG-CMN nanoparticles

The stability of the andrographolide and curcumin-loaded formulations was measured in terms of particle size, polydispersity index, zeta potential, and drug loading (Table 5.11). A slight increase in particle size, PDI, and a slight decrease in zeta potential, loading capacity has been observed after storage at 2-8°C for 90 days.

Table 5.11: Particle size parameters, polydispersity index, zeta potentials,drug loading & entrapment efficiency of AG-CMN NLC after storage at 2-8°C for 90 days

Sample	**Size (nm)**		**PDI**		**ZP (mV)**		**Drug loading (% w)**			
	Before storage	**After storage**	**Before storage**	**After storage**	**Before storage**	**After storage**	**Before storage**		**After storage**	
							AG	**CMN**	**AG**	**CMN**
F1	145.6 ± 4.1	147.2 ± 2.3	0.233 ± 0.03	0.235 ± 0.05	18.3 ± 2.2	19.1 ± 2.5	19.21 ±0.5	18.12 ±0.2	18.65 ±0.3	17.53 ± 0.4
F2	98.32 ± 3.2	99.56 ± 2.5	0.288 ± 0.02	0.291 ± 0.04	6.64 ± 1.5	7.85 ± 1.7	17.52 ± 0.3	16.93 ±0.3	16.87 ± 0.4	16.25 ± 0.5

5.13 *In vitro* drug release study

In vitro, drug release studies for combined drug-loaded nanoparticles were carried out in two medium SGF and SIF for 72 hours. The release of andrographolide and curcumin from the NLC core showed a phase release behavior where an initial burst has been observed and it was extended up to 24 hours. After 72 hours of experiment, andrographolide showed 83.39 % release in SGF medium and 79.28 % release in SIF medium. Whereas curcumin showed 77.19 % release in SGF medium and 89.31 % release in SIF medium. In vitro drug release study picture is given in Fig. 5.32 and 5.33 respectively. Andrographolide showed a higher percentage of drug release in the SGF medium whereas curcumin showed a higher percentage of drug release in the SIF medium. Both drugs showed extended-release behavior according to *in-vitro* study.

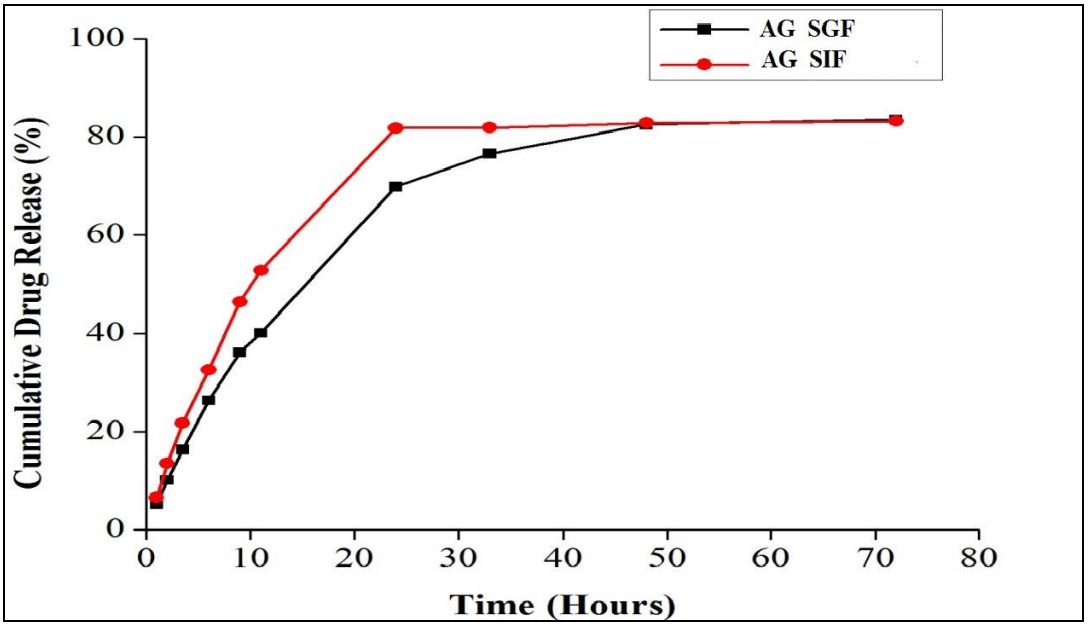

Figure 5.32: *In-vitro* release profile of Andrographolide in AG-CMN nanoparticle

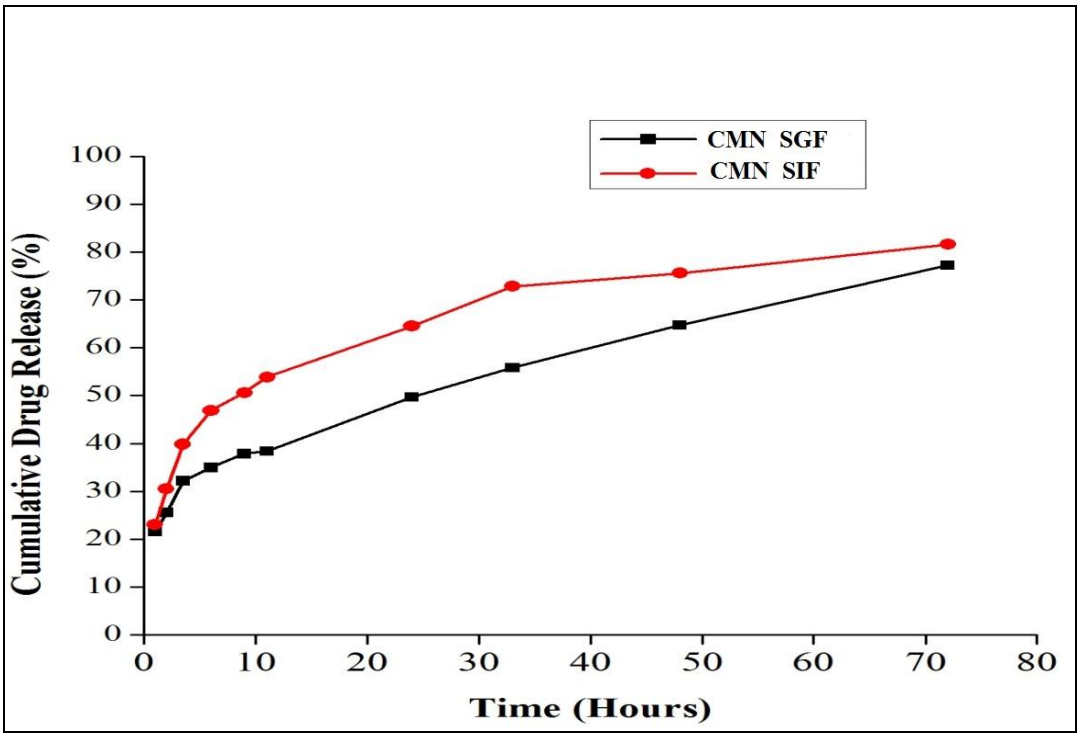

Figure 5.33: *In-vitro* release profile of Curcumin in AG-CMN nanoparticle

Drug release kinetics

To understand the mechanism behind drug release from matrix core, the drug release data were fitted to different kinetic models. From Table 5.12 and 5.13, a higher correlation coefficient (R^2) value was observed in the Korsmeyer-Peppas model (R^2= 0.957 for SGF and R^2= 0.917 for SIF) for andrographolide whereas more linearity was observed in the Higuchi model (R^2= 0.993 for SGF and R^2= 0.990 for SIF) for curcumin which means good linearity was observed in both the media. The first 60 % drug release data were fitted to Korsmeyer-Peppas and the release exponent (n) values were found to be 0.67 and 0.59 in SGF and SIF for andrographolide and 0.28 value both in SGF and SIF respectively for curcumin. Based on Korsmeyer-Peppas models, the magnitude of release exponent 'n' indicates the release mechanism (Fickian diffusion, case II transport, or anomalous transport). The limits were considered n ≤ 0.43 (For classical Fickian controlled drug release) and n= 0.85 indicates a case II

release transport, non-Fickian, zero-order release. The value of 'n' between 0.43 and 0.85 can be regarded as an indicator of both phenomena (drug diffusion in the hydrated matrix and erosion controlled dissolution) usually called anomalous transport (Nayak and Pal, 2011). In our formulation for andrographolide, the 'n' value fits well within 0.43 and 0.85, suggesting an anomalous or non-Fickian diffusion, which is related to a combination of both diffusions of the drug and dissolution from the NLC matrix. The release exponent value ≤ 0.43 represents Fickian diffusion where the drug release is related to diffusion pattern for curcumin [Maji et al, 2014].

Table 5.12 : Data of various *in vitro* drug release kinetic equations obtained by fitting experimental drug release data to different release kinetic models along with corresponding R^2 values and release exponent (n) (Korsmeyer–Peppas model) for andrographolide from AG-CMN nanoparticles.

Drugs	**Different Kinetics model**	**Equations and R^2 value of corresponding release kinetics model**	
		Release in SGF (pH 1.2)	**Release in SIF (pH 6.8)**
Andrographolide	Zero order	Y= 1.705X+14.29 R^2=0.895	Y= 1.04X+27.56 R^2=0.683
	First order	Y= -0.012X+1.913 R^2=0.884	Y= -0.010X+1.851 R^2=0.774
	Higuchi	Y= 11.86X-1.734 R^2=0.929	Y= 10.99X+6.347 R^2=0.861
	Hixon–Crowell	Y= -0.031X+4.319 R^2=0.855	Y= -0.028X+4.149 R^2=0.747
	Korsmeyer–Peppas	Y= 0.670X+0.833 R^2=0.957 n=0.67 Mechanism=Non-Fickian	Y= 0.594X+0.982 R^2=0.917 n=0.59 Mechanism=Non-Fickian

All values represent mean ± SD, n=3

Table 5.13 : Data of various *in vitro* drug release kinetic equations obtained by fitting experimental drug release data to different release kinetic models along with corresponding R^2 values and release exponent (n) (Korsmeyer–Peppas model) for curcumin from AG-CMN nanoparticles.

Drugs	**Different Kinetics model**	**Equations and R^2 value of corresponding release kinetics model**	
		Release in SGF (pH 1.2)	**Release in SIF (pH 6.8)**
Curcumin	Zero order	Y= 0.733X+28.43 R^2=0.952	Y= 0.838X+33.63 R^2=0.939
	First order	Y= -0.007X+1.872 R^2=0.991	Y= -0.010X+1.861 R^2=0.978
	Higuchi	Y= 7.057X+16.20 R^2=0.993	Y= 8.110X+19.48 R^2=0.990
	Hixon–Crowell	Y= -0.019X+4.183 R^2=0.985	Y= -0.026X+4.111 R^2=0.984
	Korsmeyer–Peppas	Y= 0.284X+1.323 R^2=0.984 n=0.28 Mechanism= Fickian	Y= 0.285X+1.391 R^2=0.989 n=0.28 Mechanism= Fickian

All values represent mean ± SD, n=3

5.14 *In-vivo* pharmacokinetic study

In vivo pharmacokinetic study of andrographolide and curcumin after oral administration of combined drug-loaded nanoparticles were compared to pure drug. The pharmacokinetic data are represented in Table 5.14 and Fig. 5.34 and 5.35. The C_{max} value for prepared nanoparticles increases 4.8 and 9.08 folds for andrographolide and curcumin compared to pure drugs. AUC $_{0\text{-}t}$ value for prepared nanoparticles increases 5.62 and 5.18 folds for andrographolide and curcumin compared to pure

drugs. Half-life ($t_{½}$) of andrographolide and curcumin in nanoparticles were found 1.69 and 2.18 fold higher than that of pure drugs. The AUC $_{0-\infty}$ value for nanoparticles were found 5.622 and 5.177 times higher compared to pure andrographolide and curcumin respectively. All the values were increased for nanoparticles may be due to an increase in bioavailability and sustained behavior of both drugs after developing the nanoparticles.

Table 5.14 : Pharmacokinetic parameters of andrographolide and curcumin from AG-CMN NP and mixed andrographolide, curcumin free drug.

Parameters	**Andrographolide Nano**	**Andrographolide Std**	**Curcumin Nano**	**Curcumin Std**
C_{max} (ng.mL^{-1})	1260.13 ± 1.56	260.44 ± 0.89	2657.27 ± 2.31	292.41 ± 1.22
T_{max} (Hr)	4	4	8	4
AUC_{0-t}(ng.mL^{-1}.hr)	25826.12 ± 3.19	4593.53 ± 4.52	22927.3 ± 0.72	4422.56 ± 1.23
$AUC_{0-\infty}$(ng.mL^{-1}.hr)	25836.8 ± 1.31	4595.17 ± 1.13	22928.4 ± 2.11	4428.57 ± 2.67
$t_{1/2}$ (Hr)	10.38 ± 0.87	6.14 ± 0.95	12.17 ± 0.79	5.57 ± 0.82
K_{EL}	0.06679	0.11285	0.0569	0.012436

All values represent mean ± SD, n=3

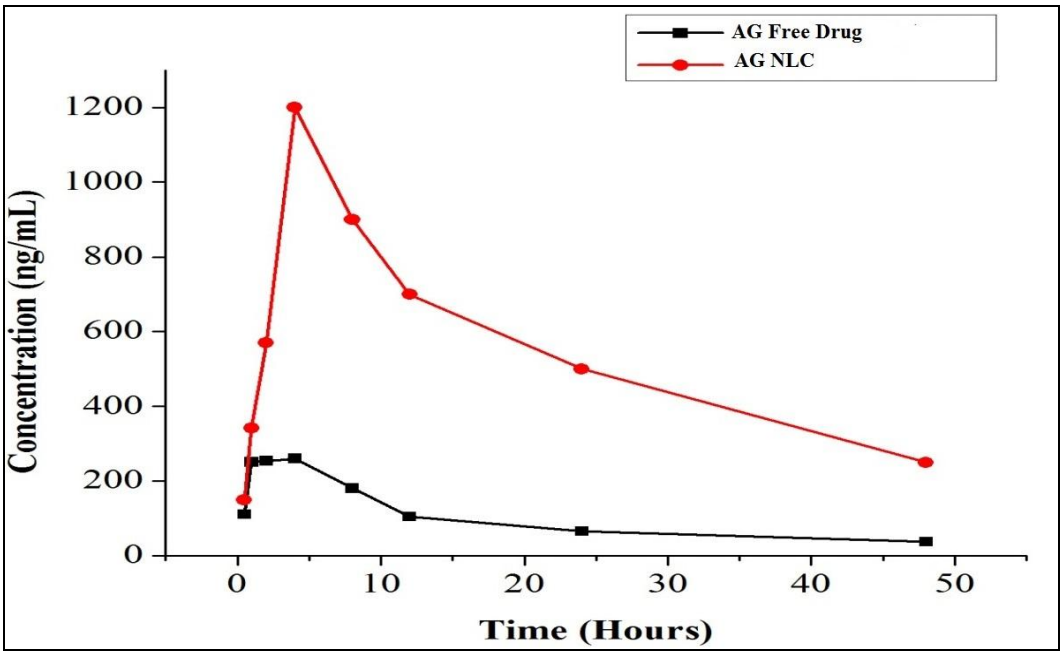

Figure 5.34: *In-vivo* pharmacokinetic profiles of AG in plasma upon administration of free- drug/AG-CMN NP by oral route in rat

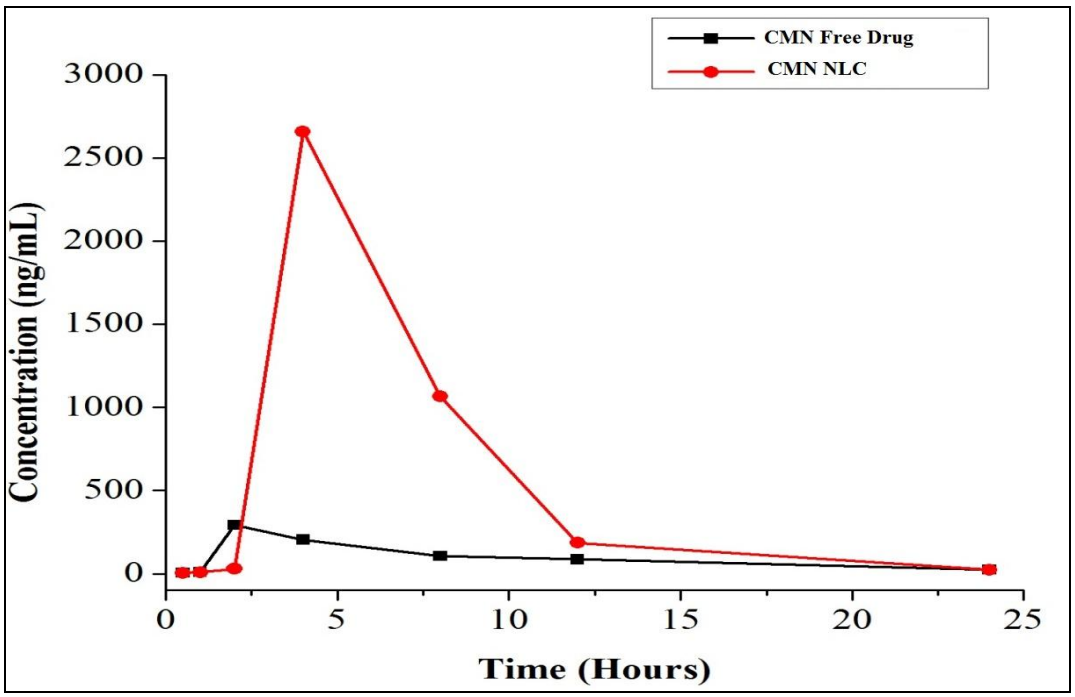

Figure 5.35: *In-vivo* pharmacokinetic profiles of CMN in plasma upon administration of free- drug/AG-CMN NP by oral route in rat

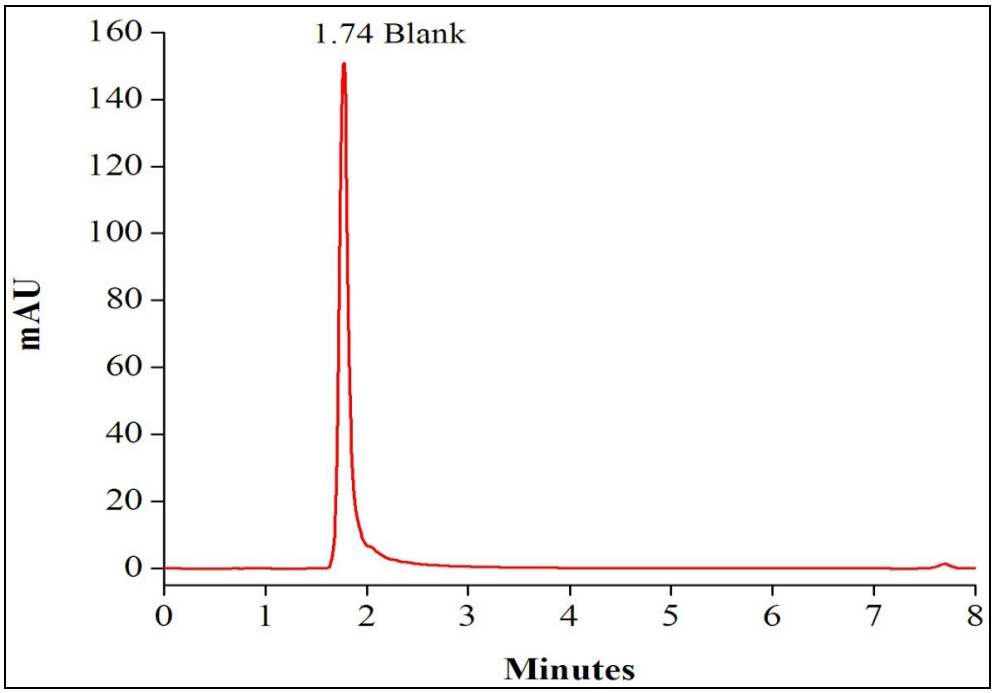

Figure 5.36: Chromatogram of blank rat plasma

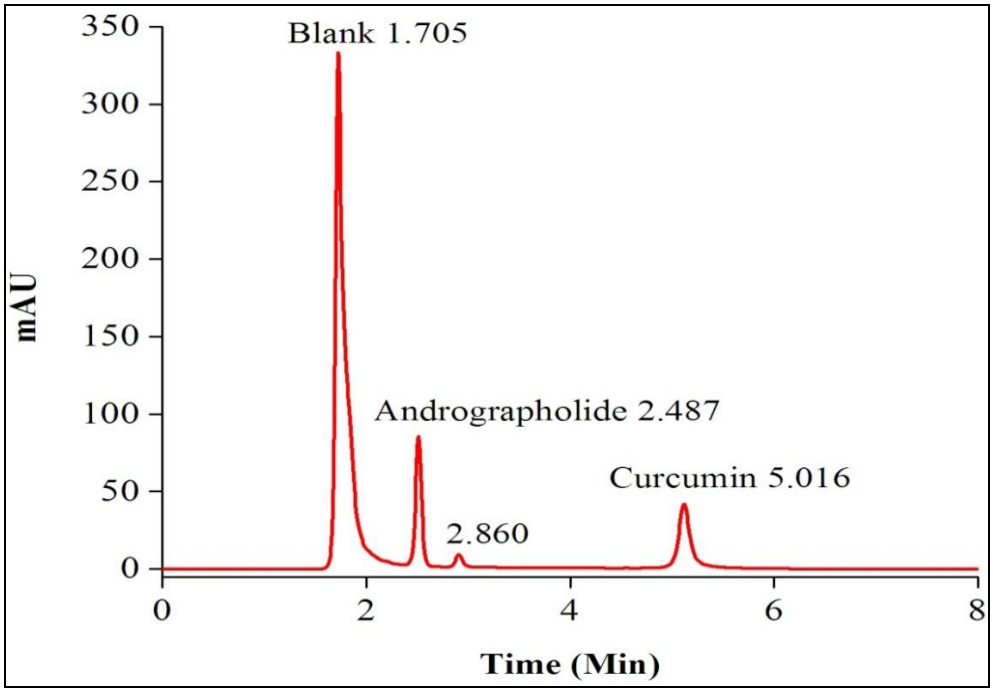

Figure 5.37: Chromatogram of mixed standard of AG and CMN spiked with blank rat plasma

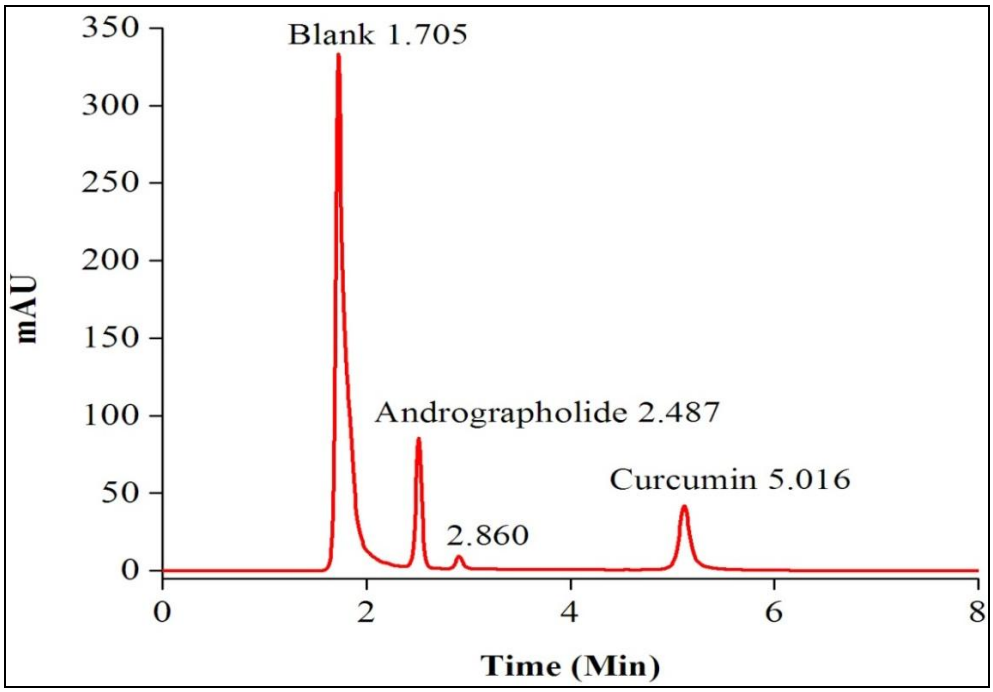

Figure 5.38: Chromatogram of AG and CMN from plasma sample upon administration of free- drug/AG-CMN NP by oral route in rat

5.15 *In- vivo* antidiabetic activity study

After six weeks treatment of diabetic mice (animals), Group III and Group VII animals fasting blood glucose levels reduced to normal levels. Group III animals fasting blood glucose was reduced to 55.04% whereas Group VII animals fasting blood glucose was reduced to 52.94%. Combined pure drug(Group IV), andrographolide and curcumin independent NLC (Group V and VI) when applied, fasting blood glucose level moderate decreases but could not reach normal levels. But when combined drug-loaded NLC (Group VII) was applied, fasting blood glucose remarkably reduced to normal levels compared to standard drug control(Group III). So, our developed formulation exhibited a better outcome upon type 2 diabetic mice.

Table 5.15: Antidiabetic activity of andrographolide and curcumin from AG-NP, CMN-NP, AG-STD, CUR-STD and AG-CMN NP.

Group	Day 0	After STZ	Week I	Week II	Week III	Week IV	Week V	Week VI
I	88±1.02	-	99±1.21	98±1.53	100±2.02	103±1.94	102±3.23	101±2.35
II	90±1.12	220±2.13	224±1.39	227±1.42	230±1.82	240±1.79	246±2.87	252±1.33
III	85±2.11	218±1.21	202±1.56	183±1.35	162±3.06	141±1.52	120±1.89	98±1.42
IV	92±3.56	216±1.39	211±1.45	202±1.62	191±2.32	182±1.76	171±1.43	152±3.08
V	80±1.59	217±2.16	212±1.86	198±1.29	182±1.82	169±2.03	154±2.42	141±1.55
VI	87±2.62	215±3.13	213±1.92	195±1.93	176±1.87	165±1.24	152±1.58	147±2.11
VII	83±1.19	221±1.19	210±1.76	191±1.83	171±1.49	152±3.13	132±1.37	108±1.88

All values represent mean ± SD, n=3

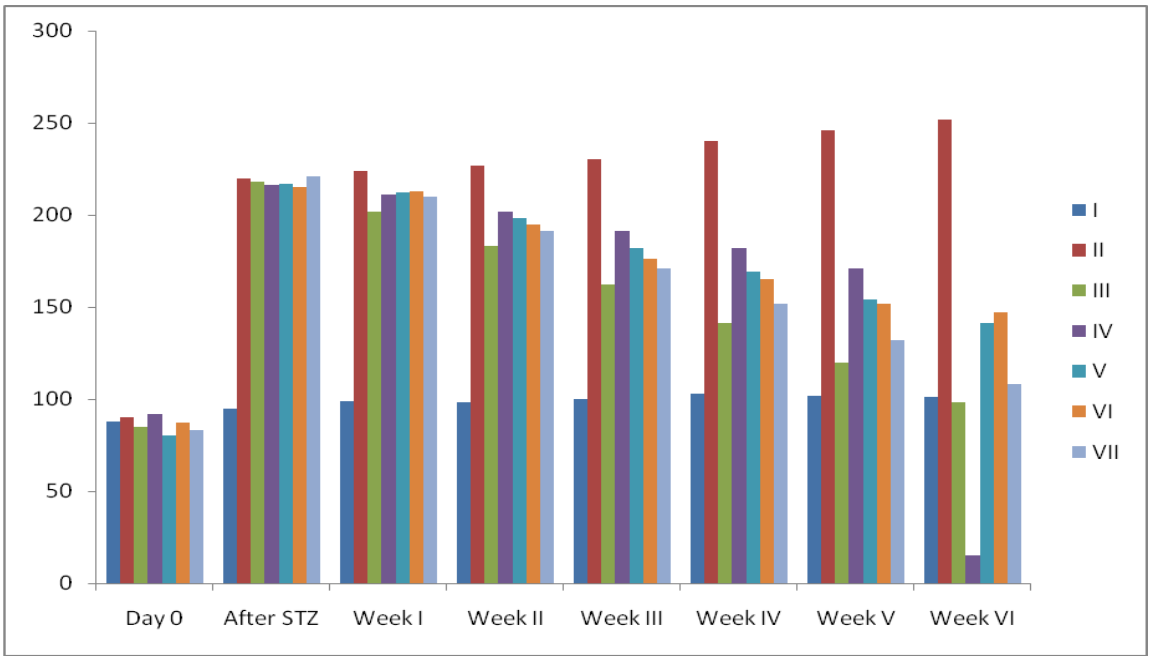

Figure 5.38: Effects of various treatments on blood glucose level of diabetic mices

Chapter VI

Discussion

Discussion

In recent years, combination medicinal therapy has been popular for lowering blood glucose in diabetic patients to provide additional benefits from single drug treatment [Alkaladi et al,2014].

Over the last few years researcher found, AG and CMN have antidiabetic effects for lowering blood glucose levels. Though these drugs are effective in treating diabetes, their limited bioavailability prevents them from being administered directly [Priyadarsini et al,2014; Verma et al,2020]. So we develop a combined AG and CMN nanostructured lipid carrier drug delivery system (NLC) to successfully deliver for diabetes mellitus. We developed a simple reverse phase HPLC method for the simultaneous estimation of AG and CMN for drug loading, entrapment efficiency, in-vitro release study, and in-vivo pharmacokinetic study. In the HPLC system, both drugs were estimated by using a single isosbestic UV wavelength by PDA detector. The absorption maxima of AG and CMN were measured using a spectrophotometric method. Andrographolide absorption maxima was identified at 223 nm, while curcumin was found at 262 nm [Chakraborty et al,2019; Syed et al,2015]. Two standard UV spectrum crosses at a common wavelength at 240 nm, which is the isosbestic wavelength of andrographolide and curcumin and hence 240 nm was chosen as the HPLC detection wavelength. Andrographolide and curcumin were eluted at 2.4 and 4.9 minutes respectively. For both drugs, quantification and linearity were obtained in the 10-140 µg/ml range. The method is specified as the presence of excipients utilized in the formulation failed to interfere with the estimation of andrographolide and curcumin.

In the present study, we have first investigated the physicochemical parameters of AG-CMN nanoparticles as they are essential for their better efficiency. The absence of any

chemical interaction between the drug and the excipients was demonstrated by FTIR data, which revealed no distinctive peak shift of the drug and other excipients and both drugs were completely encapsulated in the NLC. However, some physical interactions (such as weak hydrogen bond, van der Waals force of attraction, dipole moment, etc.) might play a role in the formation of nanoparticle structures [Rudra et al, 2010]. The particle size of AG-CMN NP was confirmed to be in the nanometer size range by particle size analysis. The polydispersity index (PDI) is the measure of the width of the particle size distribution, ranging from 0 to 1 [Masarudin et al, 2015]. The PDI value was found to be less than 0.5 which was indicate uniform homogeneity and a narrow distribution range [Gharib et al, 2014]. The zeta potential value of AG-CMN NP was found (+) 18.3 mV which indicates that the particles have a good amount of surface charge and form stable suspension in water [Maji et al, 2014]. The morphological study of AG-CMN NP by FESEM and TEM instruments confirmed that the nanoparticles were spherical shape with no visible fissures. *In vitro* release study of AG and CMN from nanoparticles showed an initial burst release throughout 8 h followed by a prolonged drug release pattern in SGF and SIF medium which indicates slower diffusion of AG and CMN from NLC core [Das et al,2017].

AG exhibited a higher percentage of drug release in SGF medium whereas CMN showed a higher percentage of drug release in SIF medium This is most likely owing to the tightly bound CMN with the formation of with curcumin-chitosan nano complex.

The *in-vivo* pharmacokinetic study furnishes AUC data by measuring drug concentration in plasma of treated laboratory animals. For comparison of drug levels in the blood, AG-CMN nanoparticles and free medicines were administered by oral route [Santos et al, 2019]. The pharmacokinetic data represented an increase in AUC_{0-t}

value 5.62 and 5.18 folds, half-life ($t_{½}$) 1.69 fold and 2.18 and C_{max} value 4.8 and 9.08 folds for AG and CMN compared to pure drugs. Even the drugs were present after 48 hours of oral administration of combined drug-loaded nanoparticles. However, encapsulation of the drug in the nanoparticle may have protected it from the intestinal degradation that helps in higher plasma concentration and longer residence time of the drug administered through nanoparticle.

In the present study, we have studied and evaluated the antidiabetic activity of combined drug-loaded NLC, independent drug loaded NLC and free drug compared to standard drug glibenclamide for six weeks. Our developed formulation (AG-CMN NLC), remarkably reduced fasting blood glucose to normal levels as compared to standard drug glibenclamide.

These observations emphasized the fact that AG and CMN in the form of AG-CMN NP have better bioavailability and effectiveness as an antidiabetic agent than the free drug which is poorly water-soluble and may degrade in intestinal pH ranges. Our AG-CMN NP experimental findings revealed improved efficacy and the benefit of significantly lower dose frequency for the treatment of diabetes mellitus.

Chapter VII

Conclusion

Conclusion

From this experiment, it can be concluded that poorly water-soluble and bioavailable drugs AG and CMN loaded NLC are suitable delivery for the treatment of diabetes mellitus.

The purpose of this study was to assess the feasibility of using NLC to promote the oral absorption of andrographolide and curcumin. The prolonged drug release was achieved by the formation of curcumin-chitosan nanocomplex and the lipid matrix with compritol® 888 ato and triolein stabilized by soya lecithin and sodium deoxycholate and stearylamine Our study reveals AG-CMN are suitable delivery for the treatment of diabetes mellitus by reducing blood glucose levels.NLC could be a potential vehicle for oral delivery of andrographolide and curcumin to ameliorate its anti-diabetic properties.

Chapter VIII

Summary

Summary

Diabetes mellitus is a metabolic disorder that has increased alarmingly all over the world. Type 2 diabetes is characterized by insulin resistance, which may be combined with relatively reduced insulin secretion. Type 2 diabetes is the most common type of diabetes mellitus and this type of patient is increasing day by day worldwide. It is estimated that by 2030, diabetes would be the world's seventh dominant cause of death. The oral antidiabetic agents currently used in clinical practice have a characteristic profile of unwanted side effects, leading to increasing demand for herbal products with antidiabetic activity having minimum side effects with prolonged efficacy. Two medicines are in that category, one is andrographolide isolated from *Andrographis paniculate* and another is curcumin, isolated from *Curcuma longa*.

These compounds have the potential in controlling the complications of diabetes, but poor water solubility and bioavailability restrict them from direct administration. In our study, combined AG and CMN were encapsulated in lipid core to prepare AG-CMN NLC. The nanoparticle was found to be in nano-size range, spherical in shape, and the drug is distributed homogeneously within the particle. FTIR data confirms that no chemical interaction existed between the drug and excipients used. DSC thermograms of AG-CMN NLC showed the absence of the sharp peak, confirming that drugs are completely encapsulated within the nanoparticle. We have developed an unique RP-HPLC method for the estimation of AG and CMN drugs intercalated in nanoformulation.

The developed HPLC method was also validated as per ICH guidelines Q 2 (R1). Drug release from AG-CMN NP in SGF (pH 1.2) and SIF (pH 6.8) was in a sustained manner which was extended up to 3 days. The drug release followed the Korsmeyer-

Peppas model for andrographolide with release exponent value (n) between 0.43 and 0.85 can be regarded as an indicator of both phenomena (drug diffusion in the hydrated matrix and erosion controlled dissolution) usually called anomalous transport non-Fickian diffusion. The drug release followed the Higuchi model for curcumin with release exponent value $n \leq 0.43$ suggests Fickian diffusion.

In-vivo pharmacokinetic study of AG-CMN NP was found to maintain a steady-state level in blood plasma after oral administration. The pharmacokinetic parameters like C_{max}, T_{max}, elimination half-life ($t_{1/2}$) of developed nanoparticles were improved than free drugs. This data suggest that better bioavailability has been achieved by AG-CMN NP.

The antidiabetic effect of AG-CMN NP was studied on streptozotocin induced diabetic model in mice. Thus, it can be said that oral administration of AG-CMN NP efficiently controlled diabetes mellitus by reducing fasting blood glucose levels to normal values. Finally, the effect of co-administration of these two drugs on the antidiabetic profiles showed additive or synergistic effects.

References

References

Abdolahpour S, Mahdieh N, Jamali Z, Akbarzadeh A, Toliyat T, Paknejad M. Development of Doxorubicin-Loaded Nanostructured Lipid Carriers: Preparation, Characterization, and In Vitro Evaluation on MCF-7 Cell Line. BioNanoScience. 2017; 7 (1): 32-39.

Abdulmumeen H, Risikat AN, Sururah AR. Food:Its Preservatives,additives and applications.International journal of chemical and biochemical sciences. 2012;1: 36-47.

Activity via Inhibition of NF-kappaB Activation from Computational Chemistry Aspects. Int J Pharmacol. 2010; 6(5): 569-576.

Aggarwal BB, Sung B. Pharmacological basis for the role of curcumin in chronic diseases: an age-old spice with modern targets. Trends Pharmacol Sci. 2009 ;30(2):85-94.

Ahangarpour A, Oroojan AA, Khorsandi L, Kouchak M, Badavi M. Solid Lipid Nanoparticles of Myricitrin Have Antioxidant and Antidiabetic Effects on Streptozotocin-Nicotinamide-Induced Diabetic Model and Myotube Cell of Male Mouse. Oxid Med Cell Longev.2018;7496936:1-18.

Ahmad AS, Sharma R. Comparitive Analysis of Herbal and Allopathic Treatment systems. European Journal of Molecular & Clinical Medicine.2020;07:2869-2876.

Akowuah GA, Zhari I, Norhayati I, Mariam A. HPLC and HPTLC densitometric determination of andrographolides and antioxidant potential of Andrographis paniculata. J Food Compos Anal. 2006;19: 118–126.

Al-Ali K, Abdel Fatah HS, El-Badry YA. Dual Effect of Curcumin-Zinc Complex in Controlling Diabetes Mellitus in Experimentally Induced Diabetic Rats. Biol Pharm Bull. 2016;39(11):1774-1780.

Al-Enazi MM. Protective effects of combined therapy of Rutin with Silymarin on experimentally-induced diabetic neuropathy in rats. Pharmacol. & Pharm.2014; 5(9) :876-889.

Alkaladi A, Abdelazim AM, Afifi M. Antidiabetic activity of zinc oxide and silver nanoparticles on streptozotocin-induced diabetic rats. Int J Mol Sci. 2014;15(2):2015-2023.

American Diabetes Association. Diagnosis and Classification of Diabetes Mellitus; Diabetes Care; 2010 : S62–S69.

Anand P, Kunnumakkara AB, Newman RA, Aggarwal BB. Bioavailability of curcumin: problems and promises. Mol Pharm. 2007;4(6):807-18.

Anand P, Nair HB, Sung B, Kunnumakkara AB, Yadav VR, Tekmal RR, Aggarwal BB. Design of curcumin-loaded PLGA nanoparticles formulation with enhanced cellular uptake, and increased bioactivity in vitro and superior bioavailability in vivo. Biochem Pharmacol. 2010;79(3):330-338.

Anter HM, Abu Hashim II, Awadin W, Meshali MM. Novel chitosan oligosaccharide-based nanoparticles for gastric mucosal administration of the phytochemical "apocynin". Int J Nanomedicine.2019;14:4911-4929.

Application of NLCs, PNPs, and PLNs. Nanomaterials (Basel). 2017; 7(6):122.

Atkinson MA, Maclaren NK. The pathogenesis of insulin-dependent diabetes mellitus. N Engl J Med. 1994;331(21):1428-36.

Balachandran P,Govindarajan R.Cancer--an ayurvedic perspective.Pharmacol Res.2005 ;51(1):19-30.9.

Banerjee S, Roy S, Bhaumik KN, Pillai J. Mechanisms of the effectiveness of lipid nanoparticle formulations loaded with anti-tubercular drug combinations toward overcoming drug bioavailability in tuberculosis. J Drug Target 2020; 28: 55-69.

Bennet D and Kim S. Polymer nanoparticles for smart drug delivery. Application of Nanotechnology in Drug Delivery.2014;8:257-310.

Bhawana, Basniwal RK, Buttar HS, Jain VK, Jain N. Curcumin nanoparticles: preparation, characterization, and antimicrobial study. J Agric Food Chem. 2011;59(5):2056-61.

Bisht S, Feldmann G, Soni S, Ravi R, Karikar C, Maitra A, Maitra A. Polymeric nanoparticle-encapsulated curcumin ("nanocurcumin"): a novel strategy for human cancer therapy. J Nanobiotechnology. 2007;5:3.

Chakraborty S, Kar N, Kumari L, De A, Bera T. Inhibitory effect of a new orally active cedrol-loaded nanostructured lipid carrier on compound 48/80-induced mast cell degranulation and anaphylactic shock in mice. Int J Nanomedicine .2017; 12: 4849-4868.

Chakraborty S, Ehsan I, Mukherjee B, Mondal L, Roy S, Saha KD, Paul B, Debnath MC,Bera T. Therapeutic potential of andrographolide-loaded nanoparticles on a murine asthma model. Nanomedicine. 2019 ;20:102006.

Chakraborty S, Shukla D, Mishra B, Singh S. Lipid – an emerging platform for oral delivery of drugs with poor bioavailability. Eur J Pharm Biopharm. 2009; 73(1):1–15.

Chattopadhyay I, Biswas K, Bandyopadhyay U, Banerjee RK. Turmeric and curcumin: biological actions and medicinal applications. Curr Sci.2004; 87(1): 44–53.

Chaudhari VS, Borkar RM, Murty US, Banerjee S. Analytical method development and validation of reverse-phase high-performance liquid chromatography (RP-HPLC) method for simultaneous quantifications of quercetin and piperine in dual-drug loaded nanostructured lipid carriers. J Pharm Biomed Anal 2020; 186: 113325.

Chaudhari VK,Pathak D,Hussain Z,Kumar P,Yadav V.Importance of herbal drug for new drug development.Journal of Applied Pharmaceutical Sciences and Research.2019;1(4):19-22.

Chen YT, Zheng RL, Jia ZJ, Ju Y. Flavonoids as superoxide scavengers and antioxidants. Free Radic Biol Med. 1990;9(1):19-21.

Cheng Z, Zhang W, Hou X, Wang B, Zhu Y, Zhang P, Zhao F, Chen D. Synthesis, Characterization, and Evaluation of Redox-Sensitive Chitosan Oligosaccharide Nanoparticles Coated with Phycocyanin for Drug Delivery. Nanoscale Res Lett.2019;14(1):389.

Chuengsamarn S, Rattanamongkolgul S, Luechapudiporn R, Phisalaphong C, Jirawatnotai S. Curcumin extract for prevention of type 2 diabetes. Diabetes Care. 2012;35(11):2121-2127.

Cirri M, Maestrini L, Maestrelli F, Mennini N, Mura P, Ghelardini C, Di Cesare Mannelli L. Design, characterization and in vivo evaluation of nanostructured

lipid carriers (NLC) as a new drug delivery system for hydrochlorothiazide oral administration in pediatric therapy. Drug Deliv. 2018;25(1):1910-1921.

Cushnie TP, Lamb AJ. Antimicrobial activity of flavonoids. Int J Antimicrob Agents.2005;26(5):343-356.

Das S, Ghosh S, De AK, Bera T. Oral delivery of ursolic acid-loaded nanostructured lipid carrier coated with chitosan oligosaccharides: Development, characterization, in vitro and in vivo assessment for the therapy of leishmaniasis. Int J Biol Macromol. 2017;102: 996-1008.

Das S, Roy P, Pal R, Auddy RG, Chakraborti AS, Mukherjee A. Engineered silybin nanoparticles educe efficient control in experimental diabetes. PLoS One. 2014;9(7):e101818.

DeFronzo RA, Bonadonna RC, Ferrannini E. Pathogenesis of NIDDM. A balanced overview. Diabetes Care. 1992;15(3):318-68S .Gothai, P .Ganesan, S.Y. Park, S .Fakurazi, D.K. Choi, P. Arulselvan, Natural phyro-bioactive compounds for the treatment of type-2 diabetes:inflammation as a target.Nutrients. 8(8) 2016 461.

Dinarvand R, Sepehri N, Manoochehri S, Rouhani H, Atyabi F. Polylactide-co-glycolide nanoparticles for controlled delivery of anticancer agents. Int J Nanomedicine. 2011;6:877-895.

Donath MY, Ehses JA. Type 1, type 1.5, and type 2 diabetes: NOD the diabetes we thought it was. Proc Natl Acad Sci U S A. 2006; 103(33):12217-8.

Dutta L, Mukherjee B, Chakraborty T, Das MK, Mondal L, Bhattacharya S, Gaonkar RH, Debnath MC. Lipid-based nanocarrier efficiently delivers highly water soluble drug across the blood-brain barrier into brain. Drug Deliv.2018;25(1):504-516.

Edwards RL, Luis PB, Varuzza PV, Joseph AI, Presley SH, Chaturvedi R, Schneider C. The anti-inflammatory activity of curcumin is mediated by its oxidative metabolites. J Biol Chem. 2017;292(52):21243-21252.

Fang YP, Lin YK, Su YH, Fang JY. Tryptanthrin-Loaded Nanoparticles for Delivery into Cultured Human Breast Cancer Cells, MCF7: the Effects of Solid Lipid/Liquid Lipid Ratios in the Inner Core. Chem Pharm Bull. 2011; 59(2): 266-271.

Gandhi SV, Mittal PS, Gaikwad AM. Development and validation of stability indicating RP-HPLC method for simultaneous estimation of beclomethasone dipropionate and salbutamol sulfate.Int J Pharm Pharm Sci 2015;7:252-7.

Ganesan P, Arulselvan P, Choi DK. Phytobioactive compound-based nanodelivery systems for the treatment of type 2 diabetes mellitus - current status. Int J Nanomedicine. 2017;12:1097-1111.

Genuth S, Alberti KG, Bennett P, Buse J, Defronzo R, Kahn R, Kitzmiller J, Knowler WC, Lebovitz H, Lernmark A, Nathan D, Palmer J, Rizza R, Saudek C, Shaw J, Steffes M, Stern M, Tuomilehto J, Zimmet P. Expert Committee on the Diagnosis and Classification of Diabetes Mellitus2, the Expert Committee on the Diagnosis and Classification of Diabetes Mellitus. Follow-up report on the diagnosis of diabetes mellitus. Diabetes Care.2003;26: 3160– 3167.

Gharib A, Faezizadeh Z, Mesbah-Namin SA, Saravani R. Preparation, characterization and in vitro efficacy of magnetic nanoliposomes containing the artemisinin and transferrin. Daru. 2014;22(1):44.

Ghasemiyeh P, Mohammadi-Samani S. Solid lipid nanoparticles and nanostructured lipid carriers as novel drug delivery systems: applications, advantages and disadvantages. Res Pharm Sci.2018;13(4):288-303.

Ghosh S, Das S, De AK, Bera T. Amphiotericin B-loaded mannose modified poly(D, lactide-co-glycolide) polymeric nanoparticles for the visceral leishmaniasis:in vitro and in vivo approaches.RSC. Adv. 2017;7: 29575-29590.

Ghosh S, Bhattacharyya S, Rashid K, Sil PC.Curcumin protects rat liver from streptozotocin-induced diabetic pathophysiology by counteracting reactive oxygenspecies and inhibiting the activation of p53 and MAPKsmediated stress response pathways, Toxicol Rep.2015; 2:365–376.

Giovannucci E, Harlan DM, Archer MC .Diabetes and cancer: a consensus report. Diabetes Care.2010; 33: 1674-1685.

Girija KS,Kasimala BB,Anna VR. A new high-performance liquid chromatography method for the separation and simultaneous quantification of eptifibatide and its impurities in pharmaceutical injection formulation. Int J App Pharm. 2021;13(2):165-172.

Goel A, Kunnumakkara AB, Aggarwal BB. Curcumin as "Curecumin": from kitchen to clinic. Biochem Pharmacol. 2008;75(4):787-809.

Gouda W, Hafiz NA, Mageed L.et al. Effects of nano-curcumin on gene expression of insulin and insulin receptor.Bull Natl Res Cent.2019; 43:128.

Grama CN, Suryanarayana P, Patil MA, Raghu G, Balakrishna N, Kumar MN, Reddy GB. Efficacy of biodegradable curcumin nanoparticles in delaying cataract in diabetic rat model. PLoS One. 2013;8(10):e78217.

Gupta SC, Kismali G, Aggarwal BB. Curcumin, a component of turmeric: from farm to pharmacy. Biofactors. 2013.;39(1):2-13.

Gupta SC, Patchva S, Aggarwal BB. Therapeutic roles of curcumin: lessons learned from clinical trials. AAPS J. 2013;15(1):195-218.

H .King, R.E. Aubert, W.H. Herman,Global burden of diabetes 1995-2025 :prevalence,numerical estimates, and projections, Diabetes Care. 1998; 21: 1414-1431.

Hossain MS, Urbi Z, Sule A, Hafizur Rahman KM. Andrographis paniculata (Burm. f.) Wall. ex Nees: a review of ethnobotany, phytochemistry, and pharmacology. Scientific World Journal. 2014;2014:274905.

Hotta N.A new perspective on the biguanide, metformin therapy in type 2 diabetes and lactic acidosis. J Diabetes Investig.2019; 10(4): 906–908.

Huang J, Huang K, Lan T, Xie X, Shen X, Liu P, Huang H. Curcumin ameliorates diabetic nephropathy by inhibiting the activation of the SphK1-S1P signaling pathway. Mol Cell Endocrinol. 2013;365(2):231-240.

Hussain SA, Ahmed ZA, Mahwi TO,Aziz TA.Effect of quercetin on postprandial glucose excursion after mono- and disaccharides challenge in normal and diabetic rats. J Diabetes Mellitus.2012;2: 82–87.

Hussein SA, Elhadary AEA, Abdullah, Elgzar YMr. Biochemical study on the protective effect of curcumin on thioacetamide -induced hepatotoxicity in rats. Benha Veterinary Medical Journal.2014. 27(1) :175-185.

Hussein AK, Walunj A, Kolsi L. Applications of nanotechnology to enhance the performance ofthe direct absorption solar collectors. Journal of Thermal Engineering. 2016; 2(1): 529-540.

Italia JL, Sharp A, Carter KC, Warn P, Kumar MN. Peroral amphotericin B polymer nanoparticles lead to comparable or superior in vivo antifungal activity to that of intravenous Ambisome or Fungizone. PLoS One. 2011;6(10):e25744.

Joshi MD, Prabhu RH, Patravale VB. Fabrication of Nanostructured Lipid Carriers (NLC)-Based Gels from Microemulsion Template for Delivery Through Skin. Methods Mol Biol. 2019;2000:279-292.

Joshi RP, Negi G, Kumar A, Pawar YB, Munjal B, Bansal AK, Sharma SS. SNEDDS curcumin formulation leads to enhanced protection from pain and functional deficits associated with diabetic neuropathy: an insight into its mechanism for neuroprotection. Nanomedicine. 2013; 9(6):776-785.

Kar N,Chakraborty S, De AK, Ghosh S, Bera T.Development and evaluation of a cedrol-loaded nanostructured lipid carrier system for in vitro and in vivo susceptibilities of wild and drug resistant Leishmania donovani amastigotes.European Journal of Pharmaceutical Sciences.2017;104 : 196–211.

Karuppusamy C, Palanivel V, Kalaiselvan, R.Evaluation of antidiabetic activity of miglitol nanoparticles in streptozotocin induced diabetic rats. International Journal of Research in Pharmaceutical Sciences.2017; 8(1):103-108.

Kaur G, Invally M, Chintamaneni M. Influence of piperine and quercetin on antidiabetic potential of curcumin.J Complement Integr Med. 2016;13(3):247-255.

Kaur S, Nautyal U, Singh R, Singh S, Devi A. Nanostructure Lipid Carrier (NLC): the new generation of lipid nanoparticles.Asian Pacific Journal Of Health Sciences.2015; 2(2):76-93.

Kelidari HR, Saeedi M, Hajheydari Z, Akbari J, Morteza-Semnani K, Akhtari J, Valizadeh H, Asare-Addo K, Nokhodchi A. Spironolactone loaded nanostructured lipid carrier gel for effective treatment of mild and moderate acne vulgaris: A randomized, double-blind, prospective trial. Colloids Surf B Biointerfaces.2016;146:47-53.

Kesarwani K, Gupta R, Mukerjee A. Bioavailability enhancers of herbal origin: an overview. Asian Pac J Trop Biomed.2013 ;3(4):253-66.

Kharroubi AT,Darwish HM. Diabetes mellitus: The epidemic of the century. World J Diabetes. 2015 ; 6(6): 850–867.

Koga AY,Carletto B, Lipinski LC,Klein T,Farago PV. Development and validation of a high-performance liquid chromatography method for the determination of 17-B estradiol in polymeric nanoparticles. Asian J Pharm Clin Res. 2021;14(5):112-116.

Komalasari T,Harimurti S. A Review on the Anti-diabetic Activity of Andrographis paniculata (Burm. f.) Nees based In-vivo Study.International Journal of Public Health Science.2015;4(4) : 256-263.

Koo OM, Rubinstein I, Onyuksel H. Role of nanotechnology in targeted drug delivery and imaging: a concise review. Nanomedicine. 2005;1(3):193-212.

Korake S, Pawar A, Surywanshi S, Bothiraja C, Pawar A. High-performance liquid chromatography for the simultaneous estimation of cefoperazone and sulbactam

in rat plasma and its importance in therapeutic drug monitoring. Int J Pharm Pharm Sci. 2020;12(10): 92-97.

Korany MA, Haggag RS, Ragab MAA , Elmallah OA. A validated stability-indicating HPLC method for simultaneous determination of silymarin and curcumin in various dosage forms. Arab J Chem. 2013; 10(2): S1711- 1725.

Kumar S, Dilbaghi N, Rani R, Bhanjana G,Umar A.Novel approaches for enhancement drug bioavailability.Rev Adv Sci Eng.2013; 2(2):133-154.

Kumar S,Shachi S, Prasad NK. Diabetes Mellitus and Allopathic Medication Increase the Risk of Cancer Malignancy, but no Side Effect Associated with the Use of Antidiabetic Herbal Medicine. Curre Res Diabetes & Obes J. 2020; 13(4): 555868.

Kurangi BK, Jalalpure SS. Review of selected herbal phytoconstituents for potential

Lehar J, Krueger AS, Avery W, Heilbut AM, Johansen LM, Price ER, Rickles RJ, Short GF 3rd, Staunton JE, Jin X, Lee MS, Zimmermann GR, Borisy AA. Synergistic drug combinations tend to improve therapeutically relevant selectivity. Nat Biotechnol.2009;27(7):659-66.

Levita J, Nawawi A, Mutalib A, Ibrahim S. Andrographolide: A Review of its Antiinflammatory Activity via Inhibition of NF-kappaB Activation from Computational Chemistry Aspects. Int J Pharmacol.2010; 6(5): 569-576.

Li H X, Zhang HL, Zhang N, Wang N, Yang Y, Zhang Z Z. Isolation of three curcuminoids for stability and simultaneous determination of only using one single standard substance in turmeric color principles by HPLC with a ternary gradient system. LWT - Food Sci Technol 2014; 57(1) : 446-51.

Li J, Luo L, Wang X, Liao B, Li G. Inhibition of NF-κB expression and allergen-induced airway inflammation in a mouse allergic asthma model by andrographolide. Cell Mol Immunol.2009; 6 (5) :381-385.

Li W, Fitzloff J F. Determination of andrographolide in commercial andrographis (Andrographis paniculata) products using HPLC with evaporative light scattering detection. J Liq Chromatogr Relat Technol. 2002; 25(9): 1335-43.

Liang E, Liu X, Du Z, Yang R, Zhao Y. Andrographolide Ameliorates Diabetic Cardiomyopathy in Mice by Blockage of Oxidative Damage and NF-κB-Mediated Inflammation. Oxidative Medicine and Cellular Longevity.2018, 9086747.

Lim SW, Jin JZ, Jin L, Jin J, Li C. Role of dipeptidyl peptidase-4 inhibitors in new-onset diabetes after transplantation. Korean J Intern Med.2015;30(6):759-770.

Lombardi Borgia S, Regehly M, Sivaramakrishnan R, Mehnert W, Korting HC, Danker K, Roder B, Kramer KD, Schafer-Korting M. Lipid nanoparticles for skin penetration enhancement-correlation to drug localization within the particle matrix as determined by fluorescence and parelectric spectroscopy.J Control Release.2005;110(1):151-63.

Lomlim L, Jirayupong N, Plubrukarn A. Heat accelerated degradation of solid-state andrographolide. Chem Pharm Bull. 2003; 51(4): 24-26.

M. Abdollahi, A. Hosseini. Streptozotocin. Encyclopedia of Toxicology.2014;402-404.

Ma Z, Shayeganpour A, Brocks DR, Lavasanifar A, Samuel J. High-performance liquid chromatography analysis of curcumin in rat plasma: application to the pharmacokinetics of polymeric micellar formulation of curcumin. Biomed Chromatogr.2007;21: 546–552.

Ma Z, Shayeganpour A, Brocks DR, Lavasanifar A, Samuel J. High-performance liquid chromatography analysis of curcumin in rat plasma: application to the pharmacokinetics of polymeric micellar formulation of curcumin. Biomed Chromatogr 2007;21(5): 546–552.

Maji R, Dey NS, Satapathy BS, Mukherjee B, Mondal S. Preparation and characterization of tamoxifen citrate loaded nanoparticles for breast cancer therapy. Int J Nanomedicine. 2014; 9: 3107–3118.

Martin A. Physical Pharmacy. 4th ed. Philadelphia, PA: Lippincott Williams & Wilkins;

Martin RC, Aiyer HS, Malik D, Li Y. Effect on pro-inflammatory and antioxidant genes and bioavailable distribution of whole turmeric vs curcumin: Similar root but different effects. Food Chem Toxicol. 2012;50(2):227-31.

Martin RC, Aiyer HS, Malik D, Li Y. Effect on pro-inflammatory and antioxidant genes and bioavailable distribution of whole turmeric vs curcumin: Similar root but different effects. Food Chem Toxicol. 2012;50(2):227-31.

Masarudin MJ, Cutts SM, Evison BJ, Phillips DR, Pigram PJ. Factors determining the stability, size distribution, and cellular accumulation of small, monodisperse chitosan nanoparticles as candidate vectors for anticancer drug delivery: application to the passive encapsulation of [(14)C]-doxorubicin. Nanotechnol Sci Appl. 2015; 8: 67–80.

Masarudin MJ, Cutts SM, Evison BJ, Phillips DR, Pigram PJ. Factors determining the stability, melanoma treatment. Indian J Health Sci Biomed Res.2018; 11(1): 3–11.

Mishra K, Dash AP, Dey N. Andrographolide: A Novel Antimalarial Diterpene Lactone Compound from Andrographis paniculata and Its Interaction with Curcumin and Artesunate. J Trop Med. 2011;579518;1-7.

Mishra K, Dash AP, Swain BK, Dey N. Anti-malarial activities of Andrographis paniculata and Hedyotis corymbosa extracts and their combination with curcumin. Malar J. 2009;8:26.

Mittal G, Carswell H, Brett R, Currie S, Kumar MN. Development and evaluation of polymer nanoparticles for oral delivery of estradiol to rat brain in a model of Alzheimer's pathology. J Control Release. 2011;150(2):220-228.

Mohseni R, ArabSadeghabadi Z, Ziamajidi N, Abbasalipourkabir R, RezaeiFarimani A. Oral Administration of Resveratrol-Loaded Solid Lipid Nanoparticle Improves Insulin Resistance Through Targeting Expression of SNARE Proteins in Adipose and Muscle Tissue in Rats with Type 2 Diabetes. Nanoscale Res Lett. 2019;14(1):227.

Monami M, Dicembrini I, Kundisova L, Zannoni S, Nreu B, Mannucci E. A meta-analysis of the hypoglycaemic risk in randomized controlled trials with sulphonylureas in patients with type 2 diabetes.Diabetes Obes Metab.2014; 16 : 833-840.

N. Shinde , A. S. Chauhan, S. K. Gupta, S. H. Bodakhe , D. P. Pandey , Antifertility studies of curcumin and andrographolide combination in female rats, Asian Pacific Journal of Reproduction. 2015; 4: 188-194.

Naazneen S, Sridevi A. Development of assay method and forced degradation study of valsartan and sacubitril by RP-HPLC in tablet formulation. Int J App Pharm.2017; 9(1): 9-15.

Nair KL, Thulasidasan AKT, Deepa G, Anto RJ,Kumar GSV. Purely aqueous PLGA nanoparticulate formulations of curcumin exhibit enhanced anticancer activity with dependence on the combination of the carrier.International Journal of Pharmaceutics.2012; 425 : 44–52.

Naseri N, Valizadeh H, Zakeri-Milani P. Solid Lipid Nanoparticles and Nanostructured Lipid Carriers: Structure, Preparation and Application. Adv Pharm Bull.2015;5(3):305-13.

Natarajan J, Karri V, De A. Nanostructured Lipid Carrier (NLC): A Promising Drug Delivery System. Glob J Nano. 2017; 1(5): 00120-00125.

Nathani R, Gahane LG, Ranganayakulu SV. Synthesis, applications and challenges of nanofluids:Review. IOSR Journal of Applied Physics. 2014; 21-28.

Nguyen MH, Yu H, Kiew TY, Hadinoto K. Cost-effective alternative to nano-encapsulation: Amorphous curcumin-chitosan nanoparticle complex exhibiting high payload and supersaturation generation. Eur J Pharm Biopharm.2015;96:1-10.

Nikalje AP. Nanotechnology and its Applications in Medicine. *Med chem*. 2015; 5: 081-089.

Nishiyama T, Mae T, Kishida H, Tsukagawa M, Mimaki Y, Kuroda M, Sashida Y, Takahashi K, Kawada T, Nakagawa K, Kitahara M. Curcuminoids and sesquiterpenoids in turmeric (Curcuma longa L.) suppress an increase in blood glucose level in type 2 diabetic KK-Ay mice. J Agric Food Chem. 2005 ;53(4):959-963.

Nuckols TK, Keeler E, Anderson LJ, Green J, Morton SC, Doyle BJ, Shetty K, Arifkhanova A, Booth M, Shanman R, Shekelle P. Economic Evaluation of

Quality Improvement Interventions Designed to Improve Glycemic Control in Diabetes: A Systematic Review and Weighted Regression Analysis. Diabetes Care. 2018;41(5):985-993.

Nugroho AE, Andrie M, Warditiani NK, Siswanto E, Pramono S, Lukitaningsih E. Antidiabetic and antihiperlipidemic effect of Andrographis paniculata (Burm. f.) Nees and andrographolide in high-fructose-fat-fed rats. Indian J Pharmacol.2012;44(3):377-381.

Nugroho AE, Lindawati NY, Herlyanti K, Widyastuti L, Pramono S. Anti-diabetic effect of a combination of andrographolide-enriched extract of Andrographis paniculata (Burm f.) Nees and asiaticoside-enriched extract of Centella asiatica L. in high fructose-fat fed rats. Indian J Exp Biol. 2013;51(12):1101-8.

Pahwa R, Kataria U, Rana AC, Rao R and Nanda S: Solid Dispersion Technology: Recent Advancements in the Delivery of Various Phytoconstituents. Int J Pharm Sci Res 2015; 6(2): 510-520.

Pardeike J, Hommoss A, Müller RH. Lipid nanoparticles (SLN, NLC) in cosmetic and pharmaceutical dermal products. Int J Pharm. 2009; 366:170-184.

Patarapanich C, Laungcholatan S , Mahaverawat N , Chaichantipayuth C, Pummangura S. HPLC determination of active diterpene lactones from Andrographis paniculata Nees planted in various seasons and regions in Thailand, Thai J . Pharm. Sci.2007; 31: 91-99.

Patra JK, Das G, Fraceto LF et al. Nano based drug delivery systems: recent developments and future prospects. J Nanobiotechnol.2018; 16:71.

Paul P, Sengupta S, Mukherjee B, Shaw TK, Gaonkar RH, Debnath MC. Chitosan-coated nanoparticles enhanced lung pharmacokinetic profile of voriconazole upon pulmonary delivery in mice. Nanomedicine (Lond). 2018;13(5):501-520.

Pearson ER, Flechtner I, Njolstad PR, et al. Switching from insulin to oral sulfonylureas in patients with diabetes due to Kir6.2 mutations. N Engl J Med. 2006; 355(5):467-477.

Phattanawasin P, Burana-osot J, Sotanaphun U, Kumsum A. Stability-indicating TLC-image analysis method for determination of andrographolide in bulk drug and A*ndrographis paniculata* formulations. Acta Chromatogr .2016; 28(4): 525–540.

Piazzini V, Micheli L, Luceri C, et al. Nanostructured lipid carriers for oral delivery of silymarin: Improving its absorption and in vivo efficacy in type 2 diabetes and metabolic syndrome model. International Journal of Pharmaceutics.2019;572:118838.

Piero MN, Nzaro GM, Njagi JM. Diabetes mellitus – a devastating metabolic disorder. Asian Journal of Biomedical and Pharmaceutical Sciences.2014;4(40):1-7.

Poolsup N, Suksomboon N, Kurnianta PDM, Deawjaroen K. Effects of curcumin on glycemic control and lipid profile in prediabetes and type 2 diabetes mellitus: A systematic review and meta-analysis. PLoS One. 2019;14(4):e0215840.

Prabaningdyah NK, Riyanto S, Rohman A, Siregar A. Application of HPLC and response surface methodology for simultaneous determination of curcumin and desmethoxy curcumin in Curcuma syrup formulation. J Appl Pharm Sci.2017; 7(12): 058-064.

Prasad S, Tyagi AK, Aggarwal BB. Recent developments in delivery, bioavailability, absorption and metabolism of curcumin: the golden pigment from golden spice. Cancer Res Treat. 2014;46(1):2-18.

Priyadarsini KI. The chemistry of curcumin: from extraction to therapeutic agent. Molecules. 2014;19(12):20091-112.

Qizhen D, Jerz G, Winterhalter P. Separation of andrographolide and neoandrographolide from the leaves of *Andrographis paniculata* using high-speed counter-current chromatography.J Chromatogr A. 2003 ;984(1):147-151.

Rani R, Dahiya S, Dhingra D, Dilbaghi N, Kaushik A, Kim KH, Kumar S. Antidiabetic activity enhancement in streptozotocin + nicotinamide-induced diabetic rats through combinational polymeric nanoformulation. Int J Nanomedicine.2019;14:4383-4395.

Rani R, Dahiya S, Dhingra D, Dilbaghi N, Kim KH, Kumar S. Evaluation of anti-diabetic activity of glycyrrhizin-loaded nanoparticles in nicotinamide-streptozotocin-induced diabetic rats. Eur J Pharm Sci.2017;106:220-230.

Rao NK. Anti-hyperglycemic and renal protective activities of A*ndrographis paniculata* roots chloroform extract. Iran J Pharmacol Ther. 2006; 5: 47-50.

Rao YK, Vimalamma G, Rao CV, Tzeng YM. Flavonoids and andrographolides from Andrographis paniculata. Phytochemistry.2004; 65: 2317–2321.

Reddy KR, Satyanarayana SV and Reddy VJ: Factorial design based optimization and in-vitro – ex-vivo evaluation of clobetasol loaded nano structured lipid carriers. Int J Pharm Sci & Res. 2019; 10(9):4374-83.

Rizos CV, Kei A, Elisaf MS. The current role of thiazolidinediones in diabetes management. Arch Toxicol. 2016;90(8):1861-81.

Rudra A, Deepa RM, Ghosh MK, Ghosh S, Mukherjee B. Doxorubicin-loaded phosphatidylethanolamine-conjugated nanoliposomes: in vitro characterization and their accumulation in liver, kidneys, and lungs in rats. Int J Nanomedicine. 2010; 5: 811–823.

Saini R, Saini S, Sharma S. Nanotechnology: the future medicine. J Cutan Aesthet Surg. 2010;

Salvi VR,Pawar PK.Nanostructured lipid carriers (NLC) system: A novel drug targeting carrier. Journal of Drug Delivery Science and Technology.2019;51:255-267.

Samuel D,Bharali D,Mousa SA.The role of nanotechnology in diabetes treatment:current and future perspectives. Int J Nanotechnol.2011;8:53-65.

Santos AC, Veiga FJ,Sequeira JAD,Fortuna A,Falcao A,Pereira I,Pattekari P,Fontes-Ribeiro C,Ribeiro AJ. First-time oral administration of resveratrol-loaded layer-by-layer nanoparticles to rats – a pharmacokinetics study Analyst, 2019.6;1-31.

Santoshkumar J,Manjunath S,Mariguddi DD, Kalashetty PG,Dass P, Manjunath C.Anti-diabetic effects of turmeric in alloxan induced diabetic rats. Journal of Evolution of Medical and Dental Sciences.2013; 2(11) ,1669-1679.

Schraufstatter E, Bernt H. Antibacterial action of curcumin and related compounds. Nature. 1949 Sep 10;164(4167):456.

Seo KI, Choi MS, Jung UJ, Kim HJ, Yeo J, Jeon SM, Lee MK. Effect of curcumin supplementation on blood glucose, plasma insulin, and glucose homeostasis

related enzyme activities in diabetic db/db mice. Mol Nutr Food Res. 2008 ;52(9):995-1004.

Sharma M, Sharma A, Tyagi S. Quantitative HPLC analysis of andrographolide in *Andrographis paniculata* at two different stages of the life cycle of a plant. Acta Chim Pharm Indica. 2012; 2(1): 1-7.

Sharma RA, Steward WP, Gescher AJ. Pharmacokinetics and pharmacodynamics of curcumin. Adv Exp Med Biol. 2007;595:453-470.

Sharma S, Kulkarni SK, Chopra K. Curcumin, the active principle of turmeric (*Curcuma longa*), ameliorates diabetic nephropathy in rats. Clin Exp Pharmacol Physiol. 2006 ;33(10):940-945.

Shi A, Li D, Wang L, Li B, Adhikari B. Preparation of starch-based nanoparticles through high-pressure homogenization and miniemulsion cross-linking: Influence of various process parameters on particle size and stability.Carbohydrate Polymers.2011;83(4):1604–1610.

Shi F, Wei Z, Zhao Y, Xu X. Nanostructured Lipid Carriers Loaded with Baicalin: An Efficient Carrier for Enhanced Antidiabetic Effects. Pharmacogn Mag.2016;12(47):198-202.

Shi G J, Zheng J, Wu J, Qiao HQ, Chang Q, Niu Y, Sun T, Li YX, Yu JQ. Beneficial effects of Lycium barbarum polysaccharide on spermatogenesis by improving antioxidant activity and inhibiting apoptosis in streptozotocin-induced diabetic male mice. Food Funct. 2017;8(3):1215-1226.

Shinde N, Chauhan AS, Gupta SK, Bodakhe SH, Pandey DP. Antifertility studies of curcumin and andrographolide combination in female rats. Asian Pac J Reprod.2015; 4(3): 188-194.

Shoskes D, Lapierre C, Cruz-Correa M, Muruve N, Rosario R, Fromkin B, Braun M, Copley J. Beneficial effects of the bioflavonoids curcumin and quercetin on early function in cadaveric renal transplantation: a randomized placebo controlled trial. Transplantation. 2005;80(11):1556-1559.

Shukla SK, Shukla SK, Govender PP.Giri NG, Biodegradable Polymeric nanostructures in therapeutic applications:Opportunities and challenges. RSC Adv.2016; 6(97): 94325-94351.

Singh A, Meena AK, Mishra S, Pant P, Padhi MM. Studies on standardization of *Andrographis paniculata* Nees and identification by HPTLC using andrographolide as a marker compound. Int J Pharm Pharm Sci 2012; 4: 197-200.

Singh CK, George J, Ahmad N. Resveratrol-based combinatorial strategies for cancer management. Ann N Y Acad Sci. 2013;1290(1):113-21.

Singh S, Pandey VK, Tewari RP, Agarwal V. Nanoparticle based drug delivery system:advantages and applications, Indian J Sci Technology.2011;4(3): 177-184.

Srimal RC, Dhawan BN. Pharmacology of diferuloyl methane (curcumin), a non-steroidal anti inflammatory agent. J Pharm Pharmacol.1973;25(6):447-52.

Stolf AM, Cardoso CC, Acco A. Effects of Silymarin on Diabetes Mellitus Complications: A Review. Phytother Res. 2017;31(3):366-374.

Sunder BS, Mittal AK. Bio-analytical method development and validation for simultaneous determination of ledipasvir and sofosbuvir drugs in human plasma by RP-HPLC method.Int J Curr Pharm Res. 2018;10(3):21-26.

Suneetha A, Manasa K. Development and validation of a visible spectrophotometric method for determination of andrographolide in Karmen plant extract. Asian J Pharm Ana .2014; 4(2): 85-88.

Syed HK, Liew KB, Loh GOK, Peh KK. Stability indicating HPLC–UV method for detection of curcumin in *Curcuma longa* extract and emulsion formulation. Food Chem.2015; 170: 321–326.

Thamlikitkul V, Dechatiwongse T, Theerapong S, Chantrakul C, Boonroj P, Punkrut W, Ekpalakorn W, Boontaeng N, Taechaiya S, Petcharoen S, et al. Efficacy of Andrographis paniculata, Nees for pharyngotonsillitis in adults. J Med Assoc Thai. 1991;74(10):437-442.

Tiyaboonchai W, Tungpradit W, Plianbangchang P. Formulation and characterization of curcuminoids loaded solid lipid nanoparticles. Int J Pharm. 2007;337:299-306.

Tomkin GH, Owens D. Diabetes and dyslipidemia: characterizing lipoprotein metabolism. Diabetes Metab Syndr Obes. 2017;10:333-343.

Trevor AJ, Katzung BG, Kruldering-Hall M: Katzung and Trevor's Pharmacology: Examination and board review, 11. Ed, Chapter 5, 2015; 169.

United States Pharmacopeia,NF-43,2020,Vol.1.

Uprit S, Kumar Sahu R, Roy A, Pare A. Preparation and characterization of minoxidil loaded nanostructured lipid carrier gel for effective treatment of alopecia. Saudi Pharm J. 2013;21(4):379-385.

Uttekar MM, Das T, Pawar RS, Bhandari B, Menon V, Nutan, Gupta SK, Bhat SV. Anti-HIV activity of semisynthetic derivatives of andrographolide and

computational study of HIV-1 gp120 protein binding. Eur J Med Chem. 2012;56:368-74.

Valeron PF , Pablos-Velasco PL. Limitations of insulin-dependent drugs in the treatment of type 2 diabetes mellitus. Med Clin (Barc).2013 ;2:20-25.

Validation of analytical Procedure: Text and Methodology. ICH. Q2(R1); 2005.

Van de Laar FA, Lucassen PL, Akkermans RP, van de Lisdonk EH, Rutten GE, van Weel C. Alpha-glucosidase inhibitors for patients with type 2 diabetes: results from a Cochrane systematic review and meta-analysis. Diabetes Care. 2005 ;28(1) :154-63.

Veld P I. Insulitis in human type 1 diabetes: the quest for an elusive lesion. Islets. 2011;3(4):131-138.

Verma VK, Zaman MK, Verma S, Verma SK, Sarwa KK. Role of semi-purified andrographolide from Andrographis paniculata extract as nano-phytovesicular carrier for enhancing oral absorption and hypoglycemic activity. Chinese Herbal Medicines.2019,12(2):142-155.

Wang AZ, Gu F, Zhang L, Chan JM, Radovic-Moreno A, Shaikh MR, Farokhzad OC. Biofunctionalized targeted nanoparticles for therapeutic applications. Expert Opin Biol Ther. 2008;8(8):1063-70.

Wichitnithad W, Jongaroonngamsang N, Pummangura S, Rojsitthisak P. A simple isocratic HPLC method for the simultaneous determination of curcuminoids in commercial turmeric extracts. Phytochem Anal. 2009; 20: 314– 319.

Woldu MA, Lenjisa JL . Int J Basic Clin Pharmacol. 2014; 3(2) :277-284.

Wolfgang S.Light Scattering from Polymer Solutions and Nanoparticle Dispersions.Berlin: Springer Berlin Hidelberg GmBH & Co. KG. 2007: 43–44.

Worasuttayangkurn L, Nakareangrit W, Kwangjai J, et al. Acute oral toxicity evaluation of *Andrographis paniculata*-standardized first true leaf ethanolic extract. Toxicol Rep. 2019;6:426-430.

Xu J, Li Z, Cao M, Zhang H, Sun J, Zhao J, Zhou Q, Wu Z, Yang L. Synergetic effect of *Andrographis paniculata* polysaccharide on diabetic nephropathy with andrographolide. Int J Biol Macromol.2012 ;51(5):738-742.

Xu T, Pan J, Zhao L. Simultaneous determination of four andrographolides in *Andrographis paniculata* Nees by silver ion reversed-phase high-performance liquid chromatography. J Chromatogr Sci. 2008; 46(8): 747-750.

Y .Lin, Z .Sun, Current views on Type 2 diabetes.J.Endocrinol.2010; 204 : 1-11.

Yang DK, Kang HS. Anti-Diabetic Effect of Cotreatment with Quercetin and Resveratrol in Streptozotocin-Induced Diabetic Rats. Biomol Ther . 2018; 26(2) :130-138.

Yao LH, Jiang YM, Shi J, Tomás-Barberán FA, Datta N, Singanusong R, Chen SS. Flavonoids in food and their health benefits. Plant Foods Hum Nutr. 2004; 59 :113-122.

Yu BC, Chang CK, Su CF, Cheng JT. Mediation of beta-endorphin in andrographolide-induced plasma glucose-lowering action in type I diabetes-like animals.Naunyn Schmiedebergs Arch Pharmacol. 2008; 377 :529-540.

Yuan H, Ma Q , Ye L, Piao G. The Traditional Medicine and Modern Medicine from Natural Products. Molecules. 2016; 21 :559.

Yuting C,Rongliang Z,Zhongjian J,Yong J.Flavonoids as superoxide scavengers and antioxidants. Free Radic Biol Med. 1990; 9(1) :19–21.

Zhang XF, Tan BK. Anti-diabetic property of ethanolic extract of Andrographis paniculata in streptozotocin-diabetic rats. Acta Pharmacol Sin. 2000; 21(12) :1157-64.

Zhao LR, Du YJ, Chen L, Liu ZG, Pan YH, Liu JF, Liu B. Quercetin protects against high glucose-induced damage in bone marrow-derived endothelial progenitor cells. Int J Mol Med. 2014; 34(4) :1025-31.

International Journal of Applied Pharmaceutics

ISSN- 0975-7058 Vol 13, Issue 5, 2021

Original Article

ANALYTICAL METHOD DEVELOPMENT, VALIDATION AND STABILITY STUDIES BY RP-HPLC METHOD FOR SIMULTANEOUS ESTIMATION OF ANDROGRAPHOLIDE AND CURCUMIN IN CO-ENCAPSULATED NANOSTRUCTURED LIPID CARRIER DRUG DELIVERY SYSTEM

ASIT KUMAR DE[a], TANMOY BERA[b*]

[a]Department of Chemistry, Jadavpur University, Kolkata 700032, West Bengal, India, [b]Laboratory of Nanomedicine, Division of Pharmaceutical Biotechnology, Department of Pharmaceutical Technology, Jadavpur University, Kolkata 700032, West Bengal, India
Email: proftanmoybera@gmail.com

Received: 25 May 2021, Revised and Accepted: 28 Jul 2021

ABSTRACT

Objective: The current study aims to boost the bioavailability criteria of two natural bioactive compounds, andrographolide and curcumin by their combination in nanostructured lipid carrier (NLC) and also to develop a straightforward reverse-phase high-performance liquid chromatography (RP-HPLC) method to validate, quantify of andrographolide and curcumin simultaneously in novel NLC formulation.

Methods: The reliable chromatographic separation was executed by using a column of Phenomenex octadecylsilane (C18) at 35 °C column oven temperature using a mobile phase of 0.02 M potassium dihydrogen orthophosphate (KH_2PO_4) salt solution of pH 3.0 as a buffer and acetonitrile in 50: 50 v/v fixed ratio and 1.5 ml/min flow rate of with 20 µl injection load. The detection was carried out at 240 nm isosbestic wavelength employing a photodiode array (PDA) detector.

Results: Andrographolide and curcumin were eluted at 2.4 and 4.9 min, respectively. Quantification and linearity were achieved for both drugs at the 10-140 µg/ml range. The method is specified as the presence of excipients utilized in the formulation failed to interfere with the estimation of andrographolide and curcumin. The developed method was successfully utilized to work out the drug loading efficiency and *in vitro* drug release study of those drugs in NLC formulation and also for the estimation of those drugs from rat plasma.

Conclusion: The developed high-performance liquid chromatography (HPLC) method may be utilized in the future estimation of andrographolide and curcumin simultaneously in NLC and other nanoformulations both *in vitro* and *in vivo*.

Keywords: Andrographolide, Curcumin, Nanoformulation, RP-HPLC method development, Forced degradation

DOI: https://dx.doi.org/10.22159/ijap.2021v13i5.42181. Journal homepage: https://innovareacademics.in/journals/index.php/ijap

INTRODUCTION

The bioactive compounds are gaining interest by their wide pharmacological actions like antimicrobial, antioxidants, anti-inflammatory and anticarcinogenic actions. Recently these natural compounds have been encouraged by their prospective health benefits [1-4]. These phytochemicals have important bioactivity but the main drawback related to them is their limited solubility and bioavailability [5]. To enhance the bioavailability of those compounds, the employment of nanoformulation is vital. The use of a modified drug delivery system enhanced the absorption of phytoconstituents in high blood level concentration and sometimes drug combinations result in synergistic effects [1].

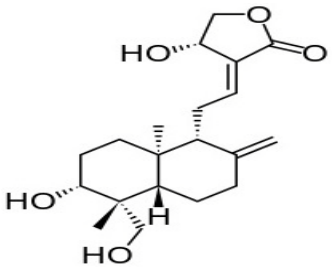

Fig. 1: Chemical structure of andrographolide

Andrographolide, a diterpenoid lactone is the major active constituent found in *Andrographis paniculata*. *Andrographis paniculata* is widely utilized in ayurvedic formulations [6]. Andrographolide has been isolated and purified in the crystalline form [7]. Andrographolide showed a wide spectrum of pharmacological activities like anti-inflammatory, neuroprotective, antioxidant, anticancer, antimicrobial and hepatoprotective. It is also applied in the treatment of acquired immunodeficiency syndrome (AIDS) and symptoms related to immune disorders [8]. Andrographolide showed other activities like liver protection, anti-diabetic [9] and anti-malarial [10]. The chemical structure of andrographolide is shown in fig. 1.

Curcumin is the principal active ingredient present within the rhizome of turmeric (*Curcuma longa*). It is incorporated in dietary supplements and cosmetic ingredients. It has also other pharmacological actions [11-13]. The chemical structure of curcumin is shown in fig. 2.

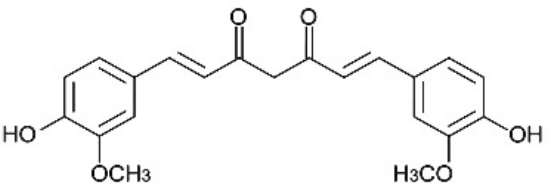

Fig. 2: Chemical structure of curcumin

Many studies were carried out to enhance the bioavailability of andrographolide and curcumin to increase their therapeutic responses [14, 15]. Antimalarial, antifertility activity of curcumin and andrographolide have shown a synergistic effect [16-18]. To overcome the bioavailability constraints of these drugs, we have incorporated andrographolide and curcumin into a nanostructured lipid carrier (NLC) system [19]. It has been demonstrated that the therapeutic activity of a drug can be correlated to its drug loading values [20]. With the increase of drug loading, the therapeutic potential also increases.

Global Journal of
Nanomedicine
ISSN: 2573-2374

Juniper Publishers
key to the Researchers

Research Article
Volume 3 Issue 2 - October 2017

Glob J Nanomed

Inhibitory Effect of Quercetin-Loaded Nanostructure Lipid Carrier on Compound 48/80-Induced Mast Cell Degranulation

Asit Kumar De, Rajkumar Shil, Santanu Ghosh, and Tanmoy Bera*

Division of Pharmaceutical Biotechnology, India

Submission: August 11, 2017; **Published:** October 25, 2017

***Corresponding author:** Tanmoy Bera, Division of Pharmaceutical Biotechnology, India, Tel: +919831470041, E-mail: proftanmoybera@gmail.com

Abstract

Quercetin is naturally occurring flavanoids, it is abundant in nature and the human beings are taken up it through their daily meals. The different pharmacological activity of quercetin has been evaluated since a long time. The scientific exploration of quercetin revealed that it is effective as anti-oxidant, anti-inflammatory agent; it can reduce the elevated levels of cholesterol, triglycerides, low-density-lipoproteins etc. However, solubility and bioavailability has been an issue for the quercetin. In this experimental work we not only evaluate the antihistaminic activity of quercetin but also developed a nano structure lipid carrier system for quercetin and explore its effectiveness as an antihistaminic agent.

It was found that the quercetin loaded nano structured lipid carrier system was successfully fabricated with adequate drug loading and entrapment efficiency. The intracellular uptake of formulated delivery system by isolated mice peritoneal mast cells has also been studied. The antihistaminic activity of quercetin and quercetin loaded lipid carrier system was compared against the standard antihistaminic agents like prednisolone, cromolyn sodium and it was found that the quercetin loaded lipid carrier system have showed superior activity than the free quercetin and the standard antihistaminic agents.

Keywords: Quercetin; NLC; Lipid based formulation; Compound 48/80; Mast cell; Antihistaminic

Abbreviations: Nano structured Lipid Carrier; qNLC: quercetin Loaded Nano Structured Lipid Carrier

Introduction

Allergic diseases and asthma have been prevalent since a long ago and still, now the incidence of these types of disease condition increased in such a manner that it has appeared as a major health concern. As per world health organization, more than 1.8lakhs of mortality is caused by asthma annually [1]. Ages are no bar for the occurrence of this type of disease; it may happen in any age group. The diseases like asthma and allergy are initiated by the process of inflammation. CD4+T helper cell responses are important for the initiation and propagation of the disease condition [2]. Interleukin-4, 5, 9 and 13 are the cytokines which are secreted by TH2 cells and they are the most important mediators of the process of inflammation. Mast-cell degranulation, increased IgE level is the characteristic phenomenon of asthma and allergy related diseases [3].

The treatment of this kind of disease condition falls into different categories like mast cell stabilizers, corticosteroids, antihistaminic agents. They may act by blocking the mediators responsible for inflammation or by preventing the process which initiates the process of inflammation. The present chemotherapy for this purpose is efficient however long term side effects still be a concern. Skin fragility, immunosuppressant is associated with the long term use of oral corticosteroids. It was also observed that the new generation antihistaminic agents are showed sedative effects [4,5]. Hence, there is always a need for a new antihistaminic agent which could effectively treat the disease condition as well as tolerable in patients in long term.

Searching for a new antihistaminic agent as well as a new drug delivery system for this type of diseases we have developed